Cross Linked Actin Networks (CLANs) in the Trabecular Meshwork Cells of the Outflow System, Their Nature and Functional Significance With Respect to Glaucoma

Thesis submitted in accordance with the requirements of the
University of Liverpool
For the degree of Doctor of Philosophy

By

Nichola Claire Wade

August 2010

0.1.1 Preface

This thesis is based on work conducted in the University of Liverpool, Ophthalmology Department between October 2004 and September 2008. The work was carried out under the supervision of Professor Ian Grierson and Doctor Luminita Paraoan.

0.1.2 Acknowledgements

The following work was undertaken with funding from the University of Liverpool Samuel Crossley Barnes Scholarship.

I wish to thank all those who have supported me throughout this work and those that gave unstintingly of their time, and those who have shared with me their knowledge and experience which allowed this project to be completed. In Particular:

Professor Ian Grierson; Dr. Luminita Paraoan; Professor Mike White; Dr. Dave Spiller; Mr. Daniel Brotchie, Dr. Lyndsay Davies; and Miss Donna Gray.

0.1.3 Abstract

A unique cytoskeletal feature of human trabecular meshwork cells in vitro and ex vivo is the presence of cross-linked actin networks (CLANs) that are abundant in a proportion of cells exposed to dexamethasone and also in cells from glaucoma patients. The aim of the work was to determine whether CLANs were present in the bovine trabecular meshwork and whether they were also induced by dexamethasone, and to determine if such structures were comparable to CLANs in human cells. Cultures of human and bovine cells and ex vivo dissections of bovine tissue were stained with phalloidin (F-actin) and propidium iodide (nuclei) and imaged by confocal microscopy, thereafter being subjected to image analysis. Other potential CLAN inducing agents were also tested and work was undertaken to examine whether or not it was possible to observe CLANs forming in living cells via transfection with a human β actin eGFP plasmid. Some CLAN-like structures were identified in ex vivo bovine tissue cultured with and without dexamethasone; however it was found that bovine cells in culture produced abundant CLANs when exposed to dexamethasone that was comparable to, if not better than the response from human cells. This work showed that CLANs are also stimulated via the application of bovine aqueous humor and TGFβ2, direct application of 5ng/ml TGFβ2 induces more CLANs than dexamethasone. This work demonstrates that bovine cells provide a suitable model for future investigations of CLAN formation and function where human cells and tissues are not available, and the bovine cells might be better in some respects for CLAN research.

The transfection experiments were successful, and this procedure enabled CLAN formation to be captured for the first time. We now have some insights into the physical formation of CLANs.

0.2 Tables

0.2.1 Table of Contents

0.2.2 List of Figures

0.2.3 List of Tables

1. Introduction

1.1 The Bovine Eye

1.1.1 Development and Anatomical Overview

The eye develops from several layers (the forebrain, mesenchyme and ectoderm) (Arey, 1965). Development is complex and passes through many stages, including the development of a preliminary optic vesicle, which develops into the so called optic cup before final maturation into a recognisable eye (Arey, 1965; Bron et al, 1997; Slatter, 2001a) (Fig 1). At birth, the eyeball measures approximately 16 to 17 mm in diameter, this size increases rapidly in the weeks following birth until it reaches the adult size after thirteen weeks (Leeson and Leeson, 1970).

The average diameter of the eye in a fully grown cow is 34 to 37 mm anterior-posterior, 37 to 42 mm vertically, and 38 to 43 mm transversely there is a small sex difference with the measurements being slightly bigger in the males than in the females (Prince et al, 1960).

The bovine eyeball is similar in many respects to the human eyeball; however there are some key differences such as size (the bovine eye is clearly larger) muscle insertion sites (the bovine has four, the human eye six), bovine eyes have a thicker cornea, and the bovine eye has a tapetum, which is not present in the human eye, the bovine eye also lacks a macula which is present in the human eye.

For dissection, the bovine eyeball may be orientated by the pupil anteriorly, and the optic nerve, which lies laterally beneath the posterior pole of the eye.

In an un-dilated state, the pupil is transversely ellipsoid – with the widest part of the ellipse indicating the outer edge of the eye; the pupil becomes rounded once in the dilated state however; and therefore if the specimen has a rounded pupil other

Figure 1: Diagram of the Bovine Eyeball

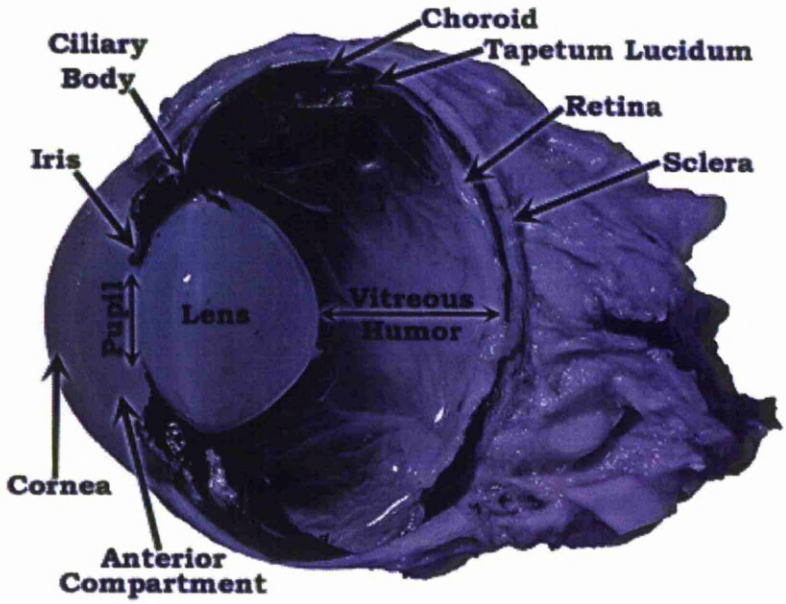

indicators such as the rectus muscle insertion points and the position of the optic nerve can be used to orientate the eye (Slatter, 2001b).

The major tunics (or layers) of the bovine eye are the same as those that are found in the human eye, namely; the fibrous tunic (comprising the tough white-coloured sclera and the transparent cornea, which merge at the point of the corneoscleral limbus) and the vascular tunic (which comprises the choroid, ciliary body and iris) (Slatter, 2001b).

The choroid in the cow is a highly vascular and pigmented tissue. Upon dissection of the eye, the vivid blue / green colour of the semi-circular *tapetum lucidium*, which lays both posteriorly and marginally above the optic disc, can be clearly seen. The function of this tissue is to reflect scattered light, which reportedly enhances night vision (Dellman and Brown, 1976; Dyce et al., 1987; Ollivier et al, 2004).

The ciliary body comprises the anterior part of the choroid. It is recognizable by the "ciliary crown" – a collection of vascular radial processes, from which zonular fibres extend toward the lens, where they connect to the lens' elastic capsule. The ciliary processes are the sight of aqueous humor production, as in the human eye (Hogan et al.1971, Budras and Habel, 2004). The ciliary ring (*orbiculus ciliaris*) is a structure that contains extremely small ciliary folds and lies posterior to the ciliary processes (Hogan et al.1971). The iris lies between the ciliary body and the pupil. It is usually a dark coloured tissue in the cow, due to the heavily pigmented posterior epithelium (*pars iridica retinae*). As in the human eye, the iris acts as a diaphragm that controls the amount of light that can enter the eye.

There are small, dark projections on the superior and inferior edges of the pupil. These are vascular appendages (the *granular iridica*) that are covered by a layer of retinal pigment epithelium, and it is this that imparts colour to this tissue (Hogan et al, 1971, Garner and Klintworth, 1998). The retina lines the entire vascular layer inside

the eye. The optical part of the retina (the part involved with sight) is the major component of this tissue, and covers the inner eye from the optic disc to the *ora serrata* near the ciliary body. The retina has an inner nerve containing layer (that contains the vision producing cells) and an outer layer which is pigmented (except for the section that lies over the *tapetum)* (Bron et al, 1997; Slatter, 2001b; Budras and Habel, 2004). The "blind" (non vision producing) part of the retina lines the iris and ciliary body. The iridial section is pigmented in its inner layer, while the outer layer is pigmented in the ciliary section. The nerve fibres of the retina exit the eye via the *area cribosa* after which they form the optic nerve (Hogan et al, 1971; Garner and Klintworth, 1998; Slatter, 2001b; Budras and Habel, 2004).

The anterior chamber (the area between the posterior of the cornea and the pupil) and posterior chamber (the area between the lens and the rear of the pupil) are in direct communication via the pupil. Aqueous humor once formed, flows from the posterior chamber, through the pupil to the anterior chamber angle. The anterior segment of the bovine eye is an asymmetric structure. The anterior-posterior extension of the outflow region is much wider in the superior and inferior quadrants than in the nasal and temporal. The differences in size appear to be in the region directly adjacent to the aqueous plexus (Flugel et al, 1991; Bron et al, 1997).

Within the irideo-corneal anterior chamber angle, the iris is attached to the scleral ring via delicate radial trabeculae. Between these trabeculae lie the spaces of Fontana, through which aqueous humor drains before it enters the venous plexus and exits the eye (Bron et al, 1997; Slatter, 2001b; Budras and Habel, 2004).

1.1.2 The Bovine Outflow system

The bovine outflow system has been an important tissue in eye / glaucoma research ever since it was first used by Barany to investigate the influence of hyaluronidase on outflow resistance (Barany and Scotchbrook, 1954). The large size of the bovine meshwork allowed it to be used for classical biochemical investigations including the characterization of its metabolic enzymes (Anderson et al, 1980). The ease of dissection (when compared to the much smaller human tissue) and the large size of the bovine meshwork attracted Grierson et al, (1985) to use it for cell culture. The bovine meshwork cells were found to be hardy and had a pronounced growth potential. Their phenotype was found to be very similar to the human trabecular meshwork (HTM) equivalent in culture (Grierson et al, 1985; Grierson et al, 1986; Crean et al, 1986).

Bovine meshwork cells and ex vivo organ cultures of trabecular meshwork tissue, have been used for a wide range of investigations including those that have involved the bovine meshwork cell cytoskeleton (Grierson et al, 1986; Grierson and Hogg, 1995; Tian et al, 2000) and cell contraction (Wiederholt et al, 1995; Thieme et al, 1999; Rosenthal et al, 2005) with respect to trabecular meshwork outflow. In vivo, the anatomy of the bovine meshwork is somewhat different from the human trabecular meshwork, and has a reticular organisation rather than a true trabecular organization (Flugel et al, 1991).

One finding of particular interest to this work was that of Gerometta et al, 2004, who found that all bovine eyes tested (n = 12) exhibited "a robust steroid response" (a rise in intraocular pressure (IOP) following the topical administration of glucocorticoid (prednisolone-acetate, in this case.) To date, there has been no satisfactory conclusion

as to why this phenomenon occurs so uniformly in cattle, however, this finding further supports the usefulness of the bovine eye, and its outflow system in glaucoma and outflow research.

1.2 The Human Eye and Outflow System

1.2.1 An Overview of Anatomy and Physiology

The human eye is a highly sophisticated organ of photoreception that allows light from the environment to be converted to electrical signals (via the rod and cone cells of the retina and the optic nerve) that are transmitted to the visual cortex of the brain where they are processed to produce vision. All of the other parts of the eye are present to support the function of vision, either directly (cornea, pupil, lens) or indirectly by nourishing or supporting the primary vision structures (ciliary body and aqueous outflow tissues) (Bron et al, 1997; Snell and Lemp, 1998).

The eyes develop from the mesoderm (lens) and ectoderm (retina and cornea) germ cell layers. The first stage of development (embryogenesis) is complete at 3 weeks gestation when the optic sulcui appear on either side of the cranial end of the neural fold. The second stage of development (or organogenesis - when the primary organ rudiments are present) is completed by the 8^{th} week of gestation. The third and final stage is differentiation; during which the organs proper are formed. This stage usually begins around the 12th week of gestation and extends up to birth (Hogan et al, 1971; Barishak 1992; Snell and Lemp 1998).

During differentiation, the retina, optic nerve, vitreous, lens, and the structures of the chamber angle are developed. The macula continues differentiation after birth and is

Figure 2: Diagram of the Human Eye

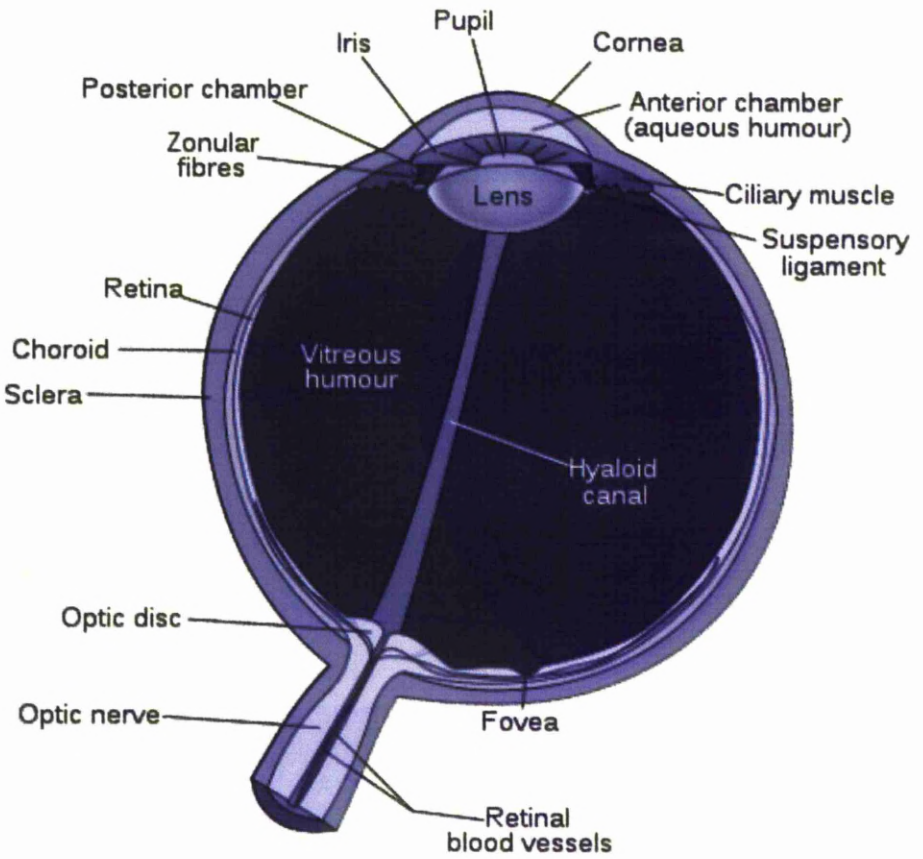

fully formed after 45 months. The adult eye measures approximately 2.5 cm in diameter, a size that is normally reached at approximately 2 years of age (Barishak 1992).

The eyeball is formed from three layers (or tunics) the fibrous, uveal and neural layers. The outermost (external) layer is the fibrous layer; it is so called because it is composed of a tough protective fibrous coat that protects the more delicate internal layers. This layer also helps to maintain the shape of the globe (crucial for proper vision) and allows for extraocular muscle insertion and eye movement without deformation of the globe (Hogan et al, 1971; Bron et al, 1997; Tortora et al, 2009) (Fig 2).

The sclera forms the major part of the outer coat of the eye. It runs from the corneoscleral junction anteriorly to the point of optic nerve insertion posteriorly. It is composed of very dense, irregular and overlapping type I and III collagen fibres, and is largely avascular and acellular and is well hydrated. It is these factors that combine to give the sclera its white colour. The arrangement of the collagen fibres also imparts rigidity to the eye which prevents any expansion from increased intraocular pressure (IOP) and also resists external compression. The sclera merges with the cornea at the corneoscleral junction (or limbus) (Snell and Lemp, 1998).

The cornea is composed of 5 layers. Externally is a layer of stratified squamous epithelium which has numerous microvilli and ridges on the outermost layer. There is a glycocalyx coat which helps to stabilise the tear film that protects this layer. The air-tissue interface and the tear film are responsible for most of the refractive power of the cornea. This layer is followed by the anterior limiting lamina (Bowman's layer), an avascular hypocellular stroma, the posterior limiting membrane (Descemet's

membrane) and a layer of non-replicating endothelial cells on the innermost surface (Tortora et al, 2009; Snell and Lemp, 1998).

Light entering the eye is refracted by the curvature of the cornea. Corneal transparency is vital for vision and is maintained by the active transport of water from the stroma to the aqueous humor (Bron et al, 1997; Tortora et al, 2009).

The collagen (type I, III and V) bundles in the cornea are arranged regularly in thick, flattened lamellae-like structures. This arrangement of collagen, its dehydration (relative to the cornea) and its avascular nature ensure it is a transparent structure that allows light to enter the eye through its thinnest central point (approximately 0.5mm) (Hogan et al, 1971; Tortora et al, 2009).

The uveal tract is composed of the choroid posteriorly and the ciliary body and iris anteriorly. The choroid is the vascular coat of the eye positioned between the sclera and the innermost retina, which runs in one continuous layer from the optic nerve through to the pupil (Hogan et al, 1971; Bron et al, 1997; Tortora et al, 2009).

This pigmented vascular loose connective tissue consists of 5 distinct layers. Beneath the retina lies Bruch`s membrane. This is followed by a rich capillary bed called the choriocapillaris, then Haler's layer (which contains the large vessels), Sattler's layer (medium sized vessels) and finally the suprachoroid (Snell and Lemp, 1998; Tortora et al, 2009).

The iris is a contractile circular diaphragm like structure that separates the anterior and posterior chambers of the eye. It is attached by its root at the iridocorneal angle where it merges with the ciliary body and the trabecular meshwork. The iris is composed of 4 layers, the anterior border, a stroma of loose connective tissue which

contains collagen fibres, fibroblasts and melanocytes (the melanocytes impart colour to the iris), the dilator pupillae muscle, and the posterior pigmented epithelium. The muscle layer of the iris allows it to constrict or dilate the pupil in response to light levels (Hogan et al, 1971; Snell and Lemp, 1998; Tortora et al, 2009).

The ciliary body forms a 5mm ring that extends from the scleral spur (below the cornea at the corneoscleral junction) to the ora serrata posteriorly. The ciliary body is roughly triangular in cross section, and is divided into two regions, the pars plicata anteriorly and the pars plana which merges into the neuroretina posteriorly. The suspensory ligaments which hold the lens in place are attached to the ciliary muscle anteriorly (Hogan et al, 1971; Bron et al, 1997; Snell and Lemp, 1998; Tortora et al, 2009).

The third layer is the neuroretina. The neuroretina is composed of two main layers, the inner stratified layer of neural cells and an outer epithelial monolayer called the retinal pigment epithelium (RPE). The RPE is responsible for the maintenance and homeostasis of the neural layer. These cells utilise vitamin A to synthesise photoreceptor pigments, and phagocytose degenerated outer segments. They also transport nutrients, metabolites and water. Loss of these cells results in loss of photoreceptor cells (specialised neurons, the rods and cones) and eventually loss of vision (Hogan et al, 1971; Bron et al, 1997; Tortora et al, 2009).

Once light is focussed onto the neuroretina, it causes polarisation of the photoreceptor cells. This light is then converted into electrical signals which are relayed to the brain via the ganglion cells. Cone cells are responsible for colour vision and are found in highest concentration in the macula, which is the area that produces central vision.

Rods are important in peripheral vision and during low light levels and for night vision (Bron et al, 1997; Hogan et al, 1971; Tortora et al, 2009).

Other intraocular structures further improve the transmission of light through the eye to the neuroretina. The pupil reduces light scatter inside the eye and controls the amount of light that can enter the eye by increasing or reducing its diameter. The lens further focuses light onto the retina. The lens does not have the refractive power of the cornea, but it has the ability to change shape via its suspensory ligaments and the ciliary muscle so that it can focus light from near or far objects. Ciliary muscle relaxation causes tension in the lens zonules, stretching the lens capsule which results in a decrease in the convexity of the anterior surface of the lens and allows distance vision. The opposite situation (contraction of the ciliary muscle and an increase in the convexity of the anterior surface of the lens) allows focus for near objects. The ability of the lens and ciliary muscle to change from near to distance vision is called accommodation. The ability of the lens to accommodate near and far focus decreases with age (Hogan et al, 1971; Bron et al, 1997; Tortora et al, 2009).

Aside from the structures directly involved in vision, there are other components in the eye that have a supportive role. The vitreous humor is a transparent, clear viscoelastic gel that fills the posterior chamber between the lens and the neuroretina. It has a refractive index of 1.33 and its viscosity is 2 to 4 times that of water. It is mostly acellular, except for occasional hyalocytes (which are phenotypically similar to macrophages) that remove debris. It is also avascular and unlike the aqueous humor is not replenished. The vitreous is mostly (>98%) composed of water with salts, carbohydrates, type II collagen fibres and hyaluronic acid making up the remainder. The collagen fibres are 8-12nm in diameter, and they trap hyaluronic acid molecules.

The vitreous is held in place by attachment at three sites, around the anterior border of the retina, at the macula, and at the optic nerve. The origin of the vitreous has not as yet been firmly established. Theories of its origin include secretion by the hyalocytes, ciliary epithelium, or the hyaloid vessels present during foetal development (Berman and Voaden, 1970; Hogan et al, 1971; Tortora et al, 2009).

Aside from its role in lens accommodation, the ciliary body is also responsible for the production of the aqueous humor. The aqueous and its flow through the tissues of the outflow system are a major component of this work and will be discussed in detail in subsequent sections.

1.2.2 The Trabecular Meshwork

From approximately the seventh week gestation fibrils of mesoderm in the early internal cornoesclera forms parallel bundles which are the precursors to the corneoscleral meshwork. Schlemm's canal is present by twelve weeks on the venous side of the newly formed vascular channels in the associated mesoderm. The anterior chamber angle also begins to form at this time as the neuroectoderm grows forward to form the beginnings of the epithelial layers of the iris (Hogan et al, 1971; Bron et al, 1997; Snell and Lemp, 1998).

The limbus of the eye undergoes much change and differentiation between the third and fifth month gestation. Following further growth, the corneoscleral meshwork separates from the surface of the developing iris. There is progressive migration of Schlemm's canal in the direction of the anterior chamber as the chamber angle deepens and grows wider. Growth and differentiation then slows so that the other regions of the TM are not developed until the seventh or eighth month of foetal life (Berman and Voaden, 1970, Tortora et al, 2009).

In the fully developed eye, the trabecular meshwork and related structures of the outflow pathways are embedded within the internal scleral sulcus, a circular groove on the inner aspect of the sclera in region of the corneoscleral limbus (Tam, 2009). The scleral sulcus extends from the edge of Descemet's membrane as far as the scleral spur, which is a wedge-shaped circular ridge that protrudes from Schlemm's canal (a circular collecting channel into which fluid drains after it filters through the trabecular meshwork) (Bron et al, 1997; Snell and Lemp, 1998; Tortora et al, 2009).

The trabecular meshwork itself has three distinct regions; the uveal meshwork, the corneoscleral meshwork and the juxta-cannilicular meshwork (or JCT) (Hogan et al, 1971; Bron et al, 1997) (Fig. 3).

The uveal meshwork extends from the iris root and ciliary body to Schwalbe's line. It is the inner most section of the TM, and is the first region through which the aqueous humor must pass after entering the chamber angle. The TM arrangement in this area is best described as "loose". The tissue here is composed of between one and three beams, which have relatively large spaces between them (25-75μm). These beams are covered by TM cells, which extend processes to each other to form a loosely organised, open net-like structure. These beams or lamellae have a core of densely packed connective tissue, which contains collagen (mainly type I and III (Marshall et al, 1991) dispersed with elastic fibres (Bron et al, 1997).

The corneoscleral meshwork comprises between 8 – 15 trabecular beams (Tamm, 2009). The cells that cover these beams are flat, and rest upon a basal lamina. The

beams attach to one another in several layers and form a porous filter-like structure, with the elliptical pores becoming smaller, and beams becoming closer together deeper into the tissue (Pores are generally within 5-50 microns in diameter). It is the structure in this region that contributes to outflow resistance (Llobert et al, 2003).

The JCT (which is the exterior portion of the TM that lies directly adjacent to Schlemm's canal) is the smallest part of the TM with a thickness of between 2–20 mm. There are no trabecular lamellae in this area. This region consists of loosely arranged connective tissue with 2-5 layers of cells throughout it that are embedded in the extracellular matrix (Tamm, 2009). Anteriorly, the trabecular beams are attached near Schwalbe's line and then extend posteriorly to the ciliary body and iris root. Aqueous humor passes from the JCT region into the episcleral veins or into Schlemm's via transcellular pores and via giant vacuoles (discussed later).

Schlemm's canal is shorter in diameter than the TM. The filtering portion of the TM (that through which aqueous passes) can be differentiated from a non-filtering region which has no Schlemm's canal adjacent to it and so is not able to allow aqueous to pass through it.

Those cells of the non-filtering portion of the TM differ in structure from those of the filtering TM (Raviola, 1982). There is some evidence that points to this region as an area where stem cell/progenitor cells exist. It is thought that these cells are capable of repopulating the filtering part of the TM after significant cell loss (Kelley et al, 2009).

The cells in this region form long processes which attach them to the extracellular matrix (ECM), as well as to each other and to the cells that line Schlemm's canal. The spaces between these cells are filled with ECM which is proteoglycan and hyaluronin rich. Another structural element of the JCT is a network of elastic fibres that run at a tangent to the endothelial cell layer of Schlemm's canal; and show some similarity to the collagenous beams of the corneoscleral meshwork, in that they have electron dense cores (Rohen et al, 1981). It is thought that these fibres act as mechanical tethers that ensure contact is maintained between the JCT and the endothelial cell layer of Schlemm's canal (Gasiorowski and Russel, 2009). The JCT also includes non-structural components such as myocilin, which associates with the ECM in this region, although the biological effect of this association is as yet unclear (Tamm, 2008). The formation and degradation of the ECM is driven by local growth factors such as TGFβ2, which act in both an autocrine and a paracrine way (Fuchshofer and Tamm, 2009). Additionally, other exogenous factors such as glucocorticoids (Clark and Wordinger, 2009) can also affect JCT-ECM turnover. This is interesting because it has been found (Tektas and lutjen-Drecoll, 2009) that a characteristic structural change in the eyes of patients with POAG and steroid-induced glaucoma is an increase in fibrillar ECM in the JCT, and this may contribute to the increased outflow resistance associated with these pathologies. More recently, Tektas et al (2010) have identified the same anomaly in the outflow pathways in the bovine eye, following treatment with prednisolone for 4 weeks. It would appear then that the accumulation of ECM plaques in the outflow system and increased outflow resistance (raised IOP) are intimately linked, even in the bovine model.

Figure 3: The Three Regions of the Trabecular Meshwork

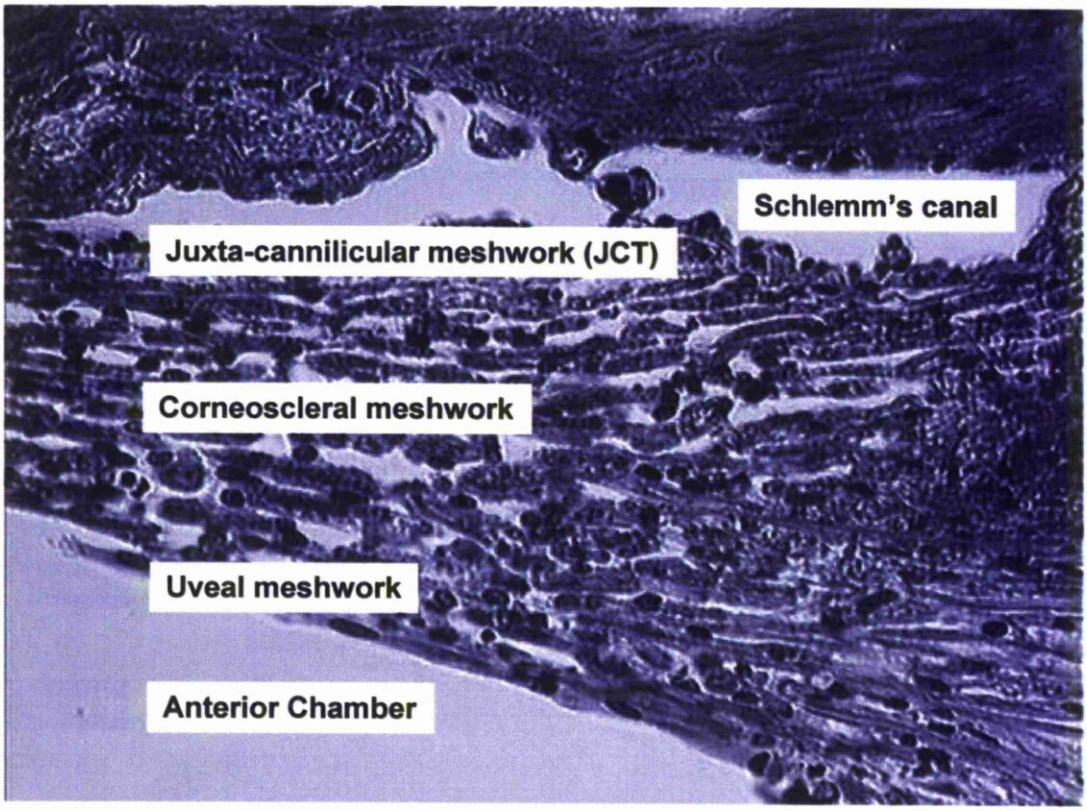

H & E stain on a wax section of human trabecular meshwork tissue. The three regions of the meshwork are labelled.

While not part of the trabecular meshwork, Schlemm's canal is so intimately linked to the trabecular meshwork and the outflow of aqueous humor, that it necessitates mention here (Hogan et al, 1971; Bron et al, 1997).

Schlemm's canal is an endothelial lined channel that is on average, 190-370 microns in diameter. The external endothelial cell layer of Schlemm's canal is flush with the most interior portion of the TM-JCT region of the trabecular meshwork. Although these two structures abut each other, there is no continuous contact between them. These cells lie on an incomplete basal lamina, and are not supported by ECM in all areas. Some regions are in direct contact with the extracellular spaces of the JCT. In these areas the pressure of the aqueous humour pushing against the basal aspects of these cells causes the formation of giant vacuoles (Johnstone and Grunt, 1973; Grierson and Lee, 1975 and 1977) which allow the passage of (relatively) large volumes of aqueous through the cells of the endothelium to Schlemm's canal. The formation of these vacuoles is thought to be pressure dependent, and their numbers has been shown to diminish within three minutes of the IOP being reduced to zero (Brilakis and Johnston, 2001). These structures are reported to form preferentially near to collector channels (Parc et al, 2000) and their numbers and size are reported to diminish with increasing age (Boldea et al, 2001). In addition to this intracellular route, there is also a paracellular route that aqueous humor may take to enter Schlemm's canal. Although of similar size to intracellular pores, the paracellular pores appear less commonly (Ethier et al, 1998) and according to Bill and Svedburgh (1972) these structures only account for approximately 10% of total outflow (resistance) in the eye.

Aqueous humor once drained into Schlemm's canal, enters the collector channels and aqueous villus to connect with the main circulatory system via the episcleral and conjunctival veins (Bron et al, 1997). There is also drainage of aqueous through the interstitial spaces in, where it flows via the ciliary muscle into both the supraciliary and supra-choroidal spaces, from where it may pass through the sclera (via spaces between the collagen fibrils within the sclera, and also through the loose connective tissues along the nerves and blood vessels that pierce the sclera. This was called uveo-scleral outflow by Anders Bill (1977).

1.2.3 Trabecular meshwork cells

Trabecular Meshwork (TM) cells (in vivo) differ in shape and size depending on which area of the TM they are in. The cells of the uveal meshwork are irregular, with an almost stellate arrangement and long processes. The cells in the corneoscleral region are flattened, and adhere to the trabecular beams in this region. The cells of the JCT area are, as briefly mentioned above, somewhat smaller than the cells of the other regions. They are embedded in an extra-cellular matrix and extend processes through this to remain in contact with each other. The cells of the trabecular meshwork rarely replicate (Polansky et al, 1979). They are supplied with nutrients via the aqueous humour, as it passes through.

Aside from their structural role, TM cells carry out numerous functions in vivo, including phagocytosis of cellular debris and pigment that may enter the TM (Wordinger and Clark, 1999) and turnover of the ECM (Yue, 1996). There is a decline in trabecular cell numbers with increasing age, so much so that by the age of 80, there is a reduction in TM cell numbers of almost 50% (Grierson and Hogg, 1995).

It has been reported that absolute TM cell numbers can differ per fellow eye, as well as between different people (Tcshumper and Johnson, 1990), and that this difference may be more marked in people with POAG (Grierson and Hogg; 1995).

Human trabecular meshwork culture was first described by Polansky in 1979. Since that time it has been used extensively to determine the biological and molecular properties of this cell type. One of the earliest reported in vitro glaucoma models used human TM cells treated with glucocorticoids (see 1.4.5). Glucocorticoids, (especially the more potent variants such as dexamethasone), can increase intraocular pressure, and this finding was then transferred to cell culture in order to examine glaucoma-like changes in human TM cells (Polansky et al, 2000). In addition to cytoskeletal changes (discussed later in section 1.5.4) treatment with glucocorticoids is known to induce other changes that are associated with glaucoma such as a down-regulation of ECM remodelling proteins (matrix metalloproteases or MMP's) which causes decreased outflow in vivo (Ehrich et al, 2005).

In vitro, TM cells have an irregular spread shape in sparse early cultures, and later become elongated and regular in mature confluent culture. Nuclei are approximately centralised, and numerous nucleoli may be present.

Early passage cells may contain pigment, but this is lost after 2 or 3 passages so that the cytoplasm is usually clear. It has been reported that TM cells cultured in aqueous humor differ from those grown in traditional cell culture media with replacement nutrients (Fautsch et al 2005) and that these differences extend from the physical (cell shape) to the molecular (altered protein expression).

The lens and cornea are of necessity transparent structures. They are entirely avascular, and therefore rely solely on a constantly renewed supply of nutrients in addition to gas exchange from the aqueous humor. In the same way, the constantly replenished aqueous removes waste products from the metabolism of these cells.

There are numerous salts and ions in the aqueous humor as well as a number of vitamins and enzymes and immune proteins. The aqueous contains over a 40-fold

TM cell lines are numerous and variable in their characteristics (growth rate, response to different treatments, etc) and immortalised cells will continue to far higher passage numbers than cells from non-immortalised primary cell cultures. For the purposes of this work the immortalised TM3 and TM5 cell lines were selected as these have been in common use in our laboratory, and are known to be stable in their doubling time. TM3 cells originally came from an elderly donor with POAG, and so are used as a glaucomatous cell line, while TM5 cells came from a healthy young adult with no known eye disease, and so serve as "normal" trabecular cells. We also experimented with other cell lines during this work (kind gifts from Alcon, Fort Worth, Texas) however, we found that for our purposes the TM3 and TM5 cell lines proved to be most useful and so these were used preferentially.

1.3 The Aqueous Humor

1.3.1 Function and Composition

The functions of the aqueous humor are: to provide nutrients and oxygen to the avascular lens and cornea; to remove metabolic waste; to enhance the diopteric power of the lens and to provide the IOP, which maintains the proper shape of the eye and its internal structures and allows for accurate vision. In addition, the presence of relatively high concentrations of immuno-globulins, might suggest an immune role.

The lens and cornea are of necessity transparent structures. They are entirely avascular, and therefore rely solely on a constantly renewed supply of nutrients in addition to gas exchange from the aqueous humor. In the same way, the constantly replenished aqueous removes waste products from the metabolism of these cells.

There are numerous salts and ions in the aqueous humor as well as a number of vitamins and enzymes and immune proteins. The aqueous contains over a 40-fold

increase in the plasma concentration of ascorbate (Krupin and Civan, 1996) which is comparable to the level found in cerebrospinal fluid (Rice, 2000). It has been suggested that the ascorbate may be modulating ion channel activity, in addition to neutralising reactive oxygen species (Nelson et al, 2007).

Bovine aqueous composition has been researched and it has been determined that the composition alters with increasing time post mortem, specifically the levels of carbohydrate decreases, while the levels of amino acids generally increase (except for Leucine, Arginine and Tyrosine, which decrease) (Ismail et al, 1977).

1.3.2 Formation

The ciliary body consists of two sections; the anterior pars plicata and the posterior pars plana. The anterior section is composed of (approximately) 70 radially arranged ciliary processes that project into the posterior chamber (Hogan et al, 1971; Kanski and McAllister, 1989).

Each process has a layer of pigment which is continuous with the retinal pigment epithelium and a non-pigmented layer which is continuous with the neuroretina. The centre of each process contains a capillary bed (Kanski and McAllister 1989).

The aqueous is formed via two processes; active secretion and passive secretion. The active secretion of the aqueous humor is driven (primarily) by vectorial ion trunsport (predominantly chloride ions) across the ciliary epithelium from ciliary stroma out into the posterior chamber, which results in the generation of an osmotic gradient that in turn drives water movement (Do et al, 2006). Aqueous secretion is diminished by factors that inhibit metabolism (such as hypoxia or hypothermia) but it is independent of the IOP level (Hogan et al; 1971; Kanski and McAllister, 1989; To, et al 2002).

The remaining 20% of aqueous is produced via passive processes such as diffusion and ultra-filtration. These processes are entirely dependant on the blood pressure in the capillaries, the plasma oncotic pressure, and the IOP. At higher IOP, the rate of aqueous secretion via the passive routes will be diminished (Kanski and McAllister, 1989). The normal rate of aqueous humor production in humans is reported to be 2-3μl per minute (Hogan et al, 1971; Kanski and McAllister, 1989; Bron et al, 1997).

1.3.3 Flow and Outflow

The great majority of outflow occurs via the conventional pathway (the trabecular meshwork, Schlemm's canal and the episcleral venous route). Aqueous flows from its point of formation in the posterior chamber, around the lens and through the pupil into the anterior chamber. Once in this chamber the fluid enters the chamber angle where it will flow through the three regions of the trabecular meshwork (Fig 4) (the inner-most uveal meshwork with its large pores, the large middle section of the corneoscleral meshwork with its highly organised beams and smaller intra-trabecular spaces, and finally the outermost JCT region with its extra-cellular matrix) before entering Schlemm's canal and flowing into the episcleral veins.

A minor amount (in adults) of outflow occurs through the unconventional (or uveoscleral) outflow route, which is open at the chamber angle, at the region of the anterior insertion of the ciliary muscle (Lutjen-Drecoll and Rohen, 1984; Tamm, 2009). Flow through the uveoscleral route is pressure independent (does not alter with increasing IOP), and is determined by bulk flow (Bill, 1965; Penderson and Toris, 1987).

At the time of writing, there appears to be no data for outflow rates in the bovine eye in vivo (whether by conventional or unconventional routes), however in artificially,

perfused bovine eyes, aqueous forms at a rate of 2.7±0.5µl per minute (Shahidullah, et al 2003). In non-human primates where this has been studied in more detail, it has been found that as much as 40–60% of aqueous drainage occurs through the uveoscleral route (Bill, 1971). Other animals have varying degrees of uveoscleral outflow including; cat (3%), rabbit (3-8%), dog (15%) and cynomolgus monkey (55%) (Alm, 2009).

Figure 4: Aqueous Flow through the Posterior and Anterior Chamber

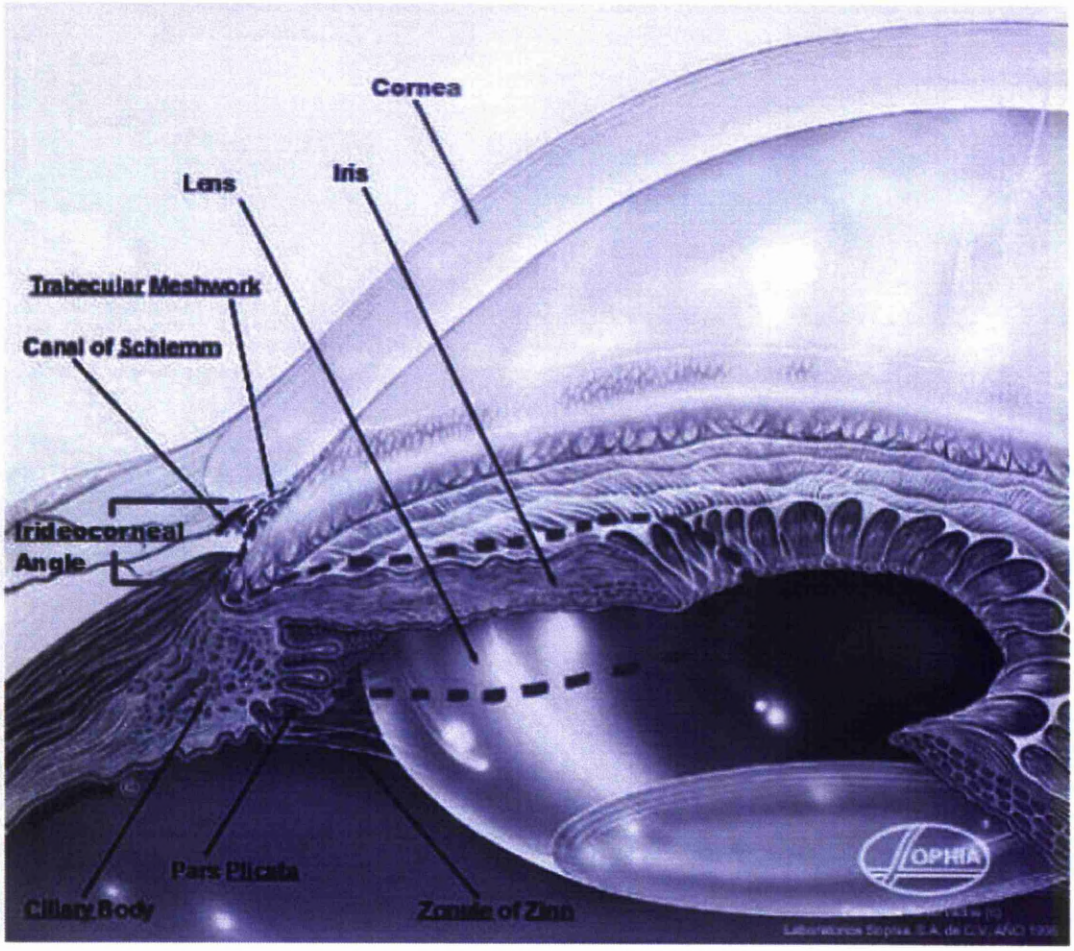

The amount of uveoscleral outflow appears to reduce with age. The mechanism behind this may be an increase in the connective tissue within the spaces of the ciliary muscle, especially within the reticular ciliary muscle, which faces the anterior chamber (Tamm, 1992) who reported that the connective tissue in this area increased from approximately 25% in the eyes of people aged 30 – 40 years to more than 50% in people over 60.

The rate of flow may be determined by the following factors:

- The rate of aqueous secretion,
- The resistance to outflow,
- The pressure within the episcleral veins.

These factors can be combined and expressed using a derivation of the Goldman equation:

$$P_o = (F/C) + P_e$$

Which may also be expressed as $\mathbf{F = C\ (P_o - P_e)}$.

Where by:

P_o = The IOP in mmHg

F = The rate of formation in µl/min, per mmHg

C = The Outflow facility in µl/min, per mmHg and

P_e = The episcleral venous pressure in mmHg.

The rate of flow alters daily in response to the circadian rhythm (Liu, 1998). However the variation is small enough that this change does not inadvertently affect vision (Morton Grunt 1951; Asejczyk Widlieka and Pierscionek, 2007).

1.4 The Glaucomas

1.4.1 Background

The glaucomas are a group of heterogeneous disorders that are together one of the most frequent causes of blindness in the world (Quigley, 1996). Although there are several different classifications of glaucoma, their final common pathway is an excavative atrophy of the optic nerve leading to progressive visual field defects and finally, total blindness (Funk, 2009). Raised intraocular pressure (IOP) is a significant risk factor for developing glaucoma, however while one person may develop nerve damage at a relatively low pressure, another person may have high eye pressure for years and never develop optic nerve damage. Loss of vision normally occurs very gradually over a prolonged period of time, and is often only recognized when the disease is quite advanced. Once lost, this damaged visual field can never be recovered. Worldwide, glaucoma is responsible for 12.3% of total world blindness, and is the second leading cause of vision loss after cataract (Resnikoff et al, 2002). Glaucoma affects 1:200 people aged fifty or less, and 1:10 over the age of eighty. If the condition is detected early enough it is possible to arrest the development (or at least slow the progression of vision loss) via pharmacological or surgical intervention (Foster and Resnikoff, 2005).

Symptoms

There are not any symptoms in the early stages of the disease in the most common type of glaucoma in the UK, primary open angle glaucoma (POAG). Often a preliminary diagnosis will be made during a routine sight test if tonometry is performed. The diagnosis of glaucoma will be made on the basis of a raised

intraocular pressure, peripheral visual field defects and optic nerve head appearunce (the presence of cupping). However, given that it is possible for there to be a high IOP with no optic nerve head cupping, or for there to be a normal pressure with optic nerve head cupping and vision loss (in normal tension glaucoma) a better definition of glaucoma might be; An optic neuropathy associated with visual field loss and / or changes in IOP (Kanski and McAllister, 1989).

Another glaucoma is angle closure glaucoma, the symptoms of which are dramatic and can include pain in or behind the eye ball, red eye, and a headache with nausea and vomiting and visual disturbances.

1.4.2 Risk Factors

The major risk factor for most glaucomas is increased intraocular pressure. Intraocular pressure is a function of the rate of production of aqueous humor by the ciliary processes in the ciliary body; and the resistance to its drainage from the eye through the trabecular meshwork (TM). The major risk factors are discussed below.

Intraocular Pressure

A generally accepted normal mean eye pressure value is 16 mmHg. The normal pressure range is from 10 to 21 mmHg. The eye pressure has a non-gaussian distribution with a skew towards higher pressures (meaning in many people a pressure above the 21 mmHg level is normal). As stated above, some eyes will undergo extensive glaucoma damage even when their pressure is in the 'normal' range, while others suffer no damage with pressure well above 21 mmHg. Despite this, a value of 21-22 mmHg has been widely accepted as a good way to determine 'normal' eye pressure from a pressure level which should be viewed with suspicion for glaucoma.

The normal distribution of eye pressure in POAG patients was analysed in the Baltimore Eye Survey (Tielsch et al, 1994). They found that the likelihood that an eye with glaucoma will have a pressure of more than 22 mmHg was almost 9 times more than the likelihood of it having a pressure of less than 21 mmHg and so this pressure is a useful, if imperfect aid in clinical diagnosis and provides a basis of proof for IOP lowering in the treatment of primary open angle glaucoma.

The Early Manifest Glaucoma (Leske et al, 2004) Trial showed that immediately treating people who have early stage glaucoma can delay the progression of the disease and vision loss. In this trial, 49% of patients had progression of visual field defects if the eye pressure was not lowered, but fewer than 30% had glaucoma progression when the eye pressure was immediately lowered to the benchmark normal eye pressure of 15.5 mmHg. There is some evidence, that a raised systolic blood pressure (BP) will cause an increase in the IOP, and that treatment with systemic anti-hypertensives may also reduce IOP (Leske and Podgor, 1983; Klein et al, 1981; Wilson et al 1987). However, this increase is only small; a 10mmHg increase in systolic BP will cause on average, an increase of 0.24 mmHg, while a 10mmHg rise in diastolic BP can cause a 0.40 mmHg increase in IOP, which would probably not significantly contribute to the pathology of glaucoma (Bonomi et al, 2000).

Aging

Everyone over the age 60 has an increased risk for glaucoma. This age limit is decreased to 40 years in the black population (Wilson et al, 1987). Age is the key risk factor for the development of primary open angle glaucoma, along with elevated intra ocular pressure.

Ethnicity

In a study funded by the National Eye Institute, researchers at the Johns Hopkins University reported that glaucoma is three to four times more likely to occur in Black people than in White people. In addition, glaucoma is six times more likely to cause blindness in Black people than in White people (Wilson et al, 1987).

Central Corneal Thickness

The National Eye Institute supported Ocular Hypertension treatment study has identified corneal thickness as a strong risk factor for developing glaucoma. Patients with corneal thickness of < 555 microns have a three fold greater risk of developing glaucoma, compared with those who have a cornea > 588 microns thick (Brandt et al, 2001; Dimasi, et al 2009). In another study funded by the National Eye Institute (The Advanced Glaucoma Intervention Study; AGIS), researchers found that black and white patients with advanced glaucoma respond differently to two surgical treatments for the disease. Black people (on average) have thinner corneas than white people (by about 23 microns) and they suggest that this may well be the factor that puts blacks at a higher risk for glaucoma progression.

Iridial Thickness

A recent study (Wang et al, 2009) found a correlation between the thickness of the iris, and the occurrence of angle closure glaucoma, where a thicker iris confers a greater risk of developing POAG.

Myopia

Myopic patients have a 2 to 3-fold increase in the risk of developing glaucoma compared with those who are not myopic. This association is weak for eyes with low

myopia, but is stronger for eyes with moderate-to-high myopia (Perkins and Phelps, 1982; Mitchell et al, 1999; Lee et al, 2008).

Diabetes

Numerous studies support a weak link between diabetes and glaucoma. This association is supported by the odds ratio (a number that shows the strength of association between two variables, which can vary from 0 to infinity). If the odds ratio is one or less, there is no association. If it is greater than 1, there is a link – the link is stronger with increasing number). For glaucoma and diabetes, there have been odds ratios in different studies ranging from 1.1 to 3.1 and so although it is linked; there is not a strong association (Ellis et al, 2000; Mitchell et al, 1997; Dielemans et al, 1995; Klein et al, 1994).

Family History

Glaucoma has a tendency to run in families. The Baltimore Eye Study found that the risk of developing glaucoma was approximately 3.7 fold higher for people that had a sibling with glaucoma. In another study (the Rotterdam Eye Study) it was found that the risk of having glaucoma was 9.2 fold for individuals who had a close relative with glaucoma (Wolfs et al, 1998; Tielsch et al, 1994; Okamoto et al, 2005).

Although it is clear that genetics plays an important role in POAG, specifics about the inheritance remain unclear. No single mode of inheritance can adequately describe glaucoma as a whole. Glaucoma development would seem to depend not on a single gene, but upon several genes and (in all probability on) some environmental factors too. There is however a minor percentage of glaucoma's (3% of POAG cases) that are caused by a defect in a single gene. One such gene is the Myocilin (MYOC) gene. This gene (also known as TIGR or GLC1A) was at first identified (Stone et al; 1997)

as a protein that was induced by glucocorticoid in cultured human trabecular meshwork cells. MYOC is responsible for the generation of autosomal dominant juvenile glaucoma and also for a subset of adult-onset POAG. Myocilin is a glycoprotein that is normally secreted from the trabecular meshwork cells into the aqueous humor. It has been shown that disease-causing mutations in the MYOC gene prevent myocilin from being secreted from trabecular meshwork cells, and mutant myocilin is not found to be present in the aqueous humor. These genetic forms of glaucoma are associated with high IOP and often require surgery to gain disease control (Allingham et al, 2009). Exactly what role myocilin plays in the development of GLC1A glaucoma (and in steroid-induced glaucoma) is as yet unknown.

Table 1: Known POAG gene loci

CANDIDATE GENE	POAG SUBTYPE	LOCUS NAME	LOCATION
MYOC	JOAG / AO	GLC1A	1q23-q24
	AO	GLC1B	2cen-q13
	EIOP		2p12
	JOAG / AO	GLC1H	2p16.3-p15
	AO	GLC1L	3p22-p21
	AO	GLC1C	3q21-q24
WDR36	AO	GLC1G	5q22.1
	JOAG	GLC1M	5q22.1-q32
	AO	GLC1F	7q35-q36
	AO	GLC1D	8q23
	JOAG	GLC1J	9q22
OPTN	AO / NTG	GLC1E	10p13
	AO	GLC1I	15q11-q13
	JOAG	GLC1N	15q22-q24
	EIOP		19p13.2
	JOAG	GLC1K	20p12

Key: JOAG – Juvenile open angle glaucoma; AO – Adult onset glaucoma; EIOP – Elevated intra pressure; NTG – Normal tension glaucoma (adapted from Allingham et al, 2009).

1.4.3 Classifications of Glaucoma

As described earlier, aqueous humor flows from the ciliary processes into the posterior chamber. It then flows through the pupil of the iris into the anterior chamber. From here the aqueous humor drains through the trabecular meshwork and Schlemm's canal into scleral plexuses and the general blood circulation. In a glaucomatous eye, there is some imbalance to this normal production, flow and outflow of aqueous humor.

There are numerous separate classifications of glaucoma (Foster et al, 2002) but almost all glaucomas can be broadly classified as either primary or secondary in origin. In primary glaucomas the elevated IOP is not associated with any other ocular disease, whereas secondary glaucomas are associated with other ocular (or non ocular) disease that alters aqeuous outflow, raising IOP as a result (Resnikoff et al, 2004). The major classifications and some of the of most commonly occuring forms of glaucoma are listed below.

Primary Glaucomas

Primary Open-Angle Glaucoma

This is the most prevalent of all the glaucoma types and affects 1:200 of the adult population aged over 40 years. Also called chronic simple glaucoma (CSG) this disease can be characterised by the following conditions being present:

An IOP of >21 mmHg

An open angle that appears normal

Optic nerve head cupping

Visual field defects

Not all these conditions need to be present for the diagnosis to be made. The lack of other symptoms with this disease often means that significant damage (vision loss) will have already occurred by the time the individual becomes symptomatic. The increased IOP in this case is caused by an increased resistance to outflow within the trabecular meshwork. The aetiology of this increased resistance has yet to be fully understood.

POAG is inheritable, there is approximately a 10% risk that a sibling of an affected person will also be affected, and around a 4% chance that their children will be affected (Resnikoff et al, 2004).

Normal or low Tension Glaucoma

People with this classification of glaucoma have IOP within the normal range and will (usually) have open chamber angles. This glaucoma has many features in common with POAG and although it occurs worldwide, it is particularly prevalent in Japan. In the United States, 15 – 25% of people with open angle glaucoma will have a normal IOP. It usually affects adults over 60 years old, and is more common in women than in men (Werner, 1996; Abedin et al, 1982).

Chronic Angle-Closure Glaucoma

The cause of this glaucoma type is the blockage (or covering) of the chamber angle and trabecular meshwork by the iris. This may occur intermittently, or persistantly but it occurs quite slowly and is usually asymptomatic because of this slow onset. If left unchecked this disease can progress to acute angle closure, and can cause vision loss in the same manner as POAG. This is uncommon in whites, and is more common in people of asian origin (Mapstone, 1977; Ritch, 1994; Sihota et al, 2004)

Acute Angle-Closure Glaucoma

Rapid angle closure results in a sudden rise in IOP and immediate treatment is required to avoid damage to the optic nerve and vision. This glaucoma is more prevalent than open angle glaucoma in Asia due to the narrower chamber angles in the asian / oriental race, but it accounts for less than 10% of all glaucomas in the united states. This form of glaucoma occurs in women three times more commonly than it does in men, there is an increasing risk with age (Epstein, 1997; Shields, 1998)

Developmental Glaucomas

Primary Congenital Glaucoma

The aetiology of this is the improper development of the trabecular meshwork. Present at birth, this condition is usually detected soon after, but may not be diagnosed until sometime later in infancy. Approximately 75% of all cases of primary congenital glaucoma occur bilaterally, and it occurs more frequently in boys than in girls (65:35%). This condition affects less than 0.05% of all ophthalmic patients in the United States (Gupta et al, 2007; Edward et al, 2008).

Infantile (Juvenile) Glaucoma

Juvenile glaucoma is a relatively rare; early-onset open-angle glaucoma (JOAG) that is most often found to be associated with strong myopia. There is a genetic disposition to this condition which shows an autosomal dominant transmission (Melamed and Ashkenazi, 1994; Wiggs et al, 1995).

Secondary Glaucomas

Pseudo-Exfoliation Glaucoma

Pseudo-exfoliation syndrome is a common ocular manifestation of a systemic disease, which is known to cause disease primarily in the eye. The exact aetiology of this condition remains unknown. The glaucoma that occurs with this syndrome is similar to POAG, but can be distinguished by the abnormal deposits of grunular material on

the lens and throughout the anterior chamber as well as in the trabecular meshwork (Forsius, 1979; Roth and Epstein, 1980; Ritch, 1984).

Traumatic Glaucoma

Traumatic glaucoma refers to a group of post-traumatic ocular disorders (which may have different underlying mechanisms) that lead to the common outcome of elevated intraocular pressure (IOP) and increased risk of optic neuropathy and vision loss.

Angle-recession glaucoma is classified as a type of traumatic secondary open-angle glaucoma. This condition may be under diagnosed because the onset is often delayed; and because a history of eye injury may be some time previous. Angle recession, with or without glaucoma, is a common consequence of blunt ocular trauma (Shields, 1998).

Neovascular Glaucoma (NVG)

This form of glaucoma was first documented in 1871, historically this condition has been referred to as hemorrhagic glaucoma, thrombotic glaucoma, congestive glaucoma or diabetic hemorrhagic glaucoma. Regardless of the underlying condition, retinal ischemia followed by a subsequent release of angiogenesis factors, cause NVG. The angiogenesis factors cause new blood vessels to grow from pre-existing blood vessels. NVG can cause glaucoma via secondary open-angle or secondary closed-angle processes. The growth of a fibro-vascular layer over the trabecular meshwork in the chamber angle, results in obstruction and a rise in IOP. NVG is a particularly damaging glaucoma, and delayed diagnosis and treatment can result in complete loss of vision or loss of the entire eye (Epstein et al, 1997; Tripathi et al, 1998).

1.4.4 Corticosteroid induced glaucoma

Steroid-induced glaucoma is a form of open-angle glaucoma that is usually associated with topical steroid use in the eye, but it can also develop with inhaled, oral, or intravenous steroid. Medications that are prescribed for a wide variety of non ocular conditions (e.g. depression, allergies, and neurological diseases) can produce pupillary dilation and so trigger an attack of acute angle-closure glaucoma in eyes that have narrow angles (Epstein, 1997; Rhee et al, 2006).

The normal population can be divided into 3 groups with respect to their response to (ocular) steroid treatment. Strong "steroid responders" will show a marked increase in IOP (>30 mmHg) after receiving a course of ocular steroid. "Moderate responders" will show an increase of between 22 – 30 mmHg, and poor or "weak responders" will show little or no response. Steroid-induced IOP elevation generally occurs within a few weeks of starting steroid treatment. In most cases, the IOP lowers spontaneously to the baseline within a few weeks (or months) upon stopping the steroid (Becker, 1965; Armaly, 1965; Clark et al, 1995). Some factors that may put an individual at increased risk for developing an increased IOP after taking steroid include pre-existing primary open-angle glaucoma, strong myopia, diabetes mellitus, and history of connective tissue disease (especially rheumatoid arthritis) and a family history of glaucoma (Doughty, 2001). It has been suggested that there is a link between the genes that determine whether or not a person will develop POAG and those that determine the response to steroid. People with a severe myopia and diabetics both

Table 2: Similarities in the features of POAG and steroid induced glaucoma.

SIMILARITIES BETWEEN POAG AND STEROID INDUCED GLAUCOMA		
DISEASE	POAG	STEROID INDUCED GLAUCOMA
OPEN ANGLE	YES	YES
ELEVATED OUTFLOW RESISTANCE	YES	YES
REVERSIBLITY OF IOP INCREASE	POSSIBLE	YES
GENETIC COMPONENT	YES	YES
OPTIC NERVE HEAD DAMAGE	YES	YES
INCREASED ECM	YES	YES
ALTERED TM MORPHOLOGY	YES	YES

Table demonstrating that there are many similarities between primary open angle glaucoma and steroid induced glaucoma. Steroid induced IOP rise is (usually) quickly reversible upon withdrawal of the stimulus. POAG is treatable but not always so easily and withdrawal of medication would likely lead to the IOP rise recurring.

It is known that glucocorticoid can induce the MYOC gene selectively in TM cells, and in addition a number of other genes are also upregulated including a serine protease inhibitor (alpha1-antichymotrypsin), a neuro-protective factor (pigment epithelium-derived factor) an anti-angiogenesis factor (cornea-derived transcript 6) and a prostaglandin synthase (prostaglandin D(2) synthase) (Lo et al, 2003).

1.4.5 Glucocorticoids

Background and Synthesis

Glucocorticoids (GC) are a class of steroid hormones. They are similar to the sex steroids and the mineralocorticoids but can be identified by their ability to bind to the glucocorticoid receptor (GR).

In vivo, GCs are synthesized by the adrenal cortical cells (within the adrenal cortex) of the adrenal glands. These cells contain large lipid droplets that are comprised of cholesterol and other steroid hormone precursor molecules necessary for steroidogenesis. The GCs produced by adrenal cortical cells are synthesized from cholesterol by specific enzyme catalysed reactions that involve the shuttling of precursor molecules between the endoplasmic reticulum and the mitochondria. Specifically, GCs are synthesized from progesterone by stepwise hydroxylation of C17, C-21 and C-11 (Stryer, 1995). All steroid hormones once synthesized are secreted directly from the cell. There is little or no storage of GCs therefore continued synthesis and secretion is necessary to maintain normal plasma levels.

In humans, the predominant GC is Cortisol (Fig 5). Cortisol is secreted basally but its plasma concentration fluctuates diurnally in response to light levels detected by the

Figure 5: Comparison of the Molecular Structures of Cortisol and Dexamethasone

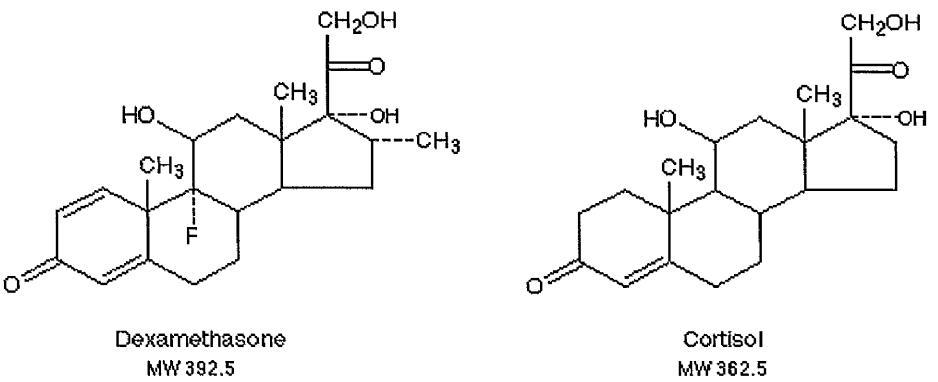

The synthetic steroid Dexamethasone is very similar to Cortisol, but it has three differences; an additional double bond in the "A" ring, an additional 9-alpha-fluoro group and 16-alpha-methyl group.

These changes make Dexamethasone far more potent than Cortisol, and it has a greater binding efficiency for the glucocorticoid receptor than Cortisol (its binding efficiency is 25 – 80 times that of Cortisol (Liapi and Chrousos 1992).

suprachiasmatic nuclei in hypothalamus via the retina. It is also released during the stress response when its function is to modulate stress and return homeostasis.

Deposition and Metabolism

Following its release into the blood stream Cortisol is bound mostly to plasma albumin. Cortisol is lipophillic and diffuses directly across the plasma membrane into the cell where it binds to the ligand binding site on the cytosolic Glucocorticoid receptor (GR). Coded for on chromosome 5 (5q 31) and found in almost every cell in the body, the GR is a ligand activated receptor which is normally held inactive by the association of several proteins including Hsp (heat shock protein) 70, Hsp 90 and the protein FKBP52. Upon binding GC, there is a conformational change in the receptor which unmasks proteins that causes one of two reactions to occur. It will either trunslocate to the nucleus of the cell where the active GR will bind to a glucocorticoid response element (GRE) located in the promoter region of numerous genes, or it will remain in the cytoplasm where it can complex with other transcription factors such as NF-kB and AP-1 (which are themselves able to transactivate numerous genes) preventing them from activating their target genes by transrepression. The effects of GC binding to the GRE are many, however one of the major effects of GC`s is their potent immuno-suppressive and anti inflammatory actions. GC`s can inhibit both cell mediated and humoral immunity (Zurier et al 1973) by suppressing genes that code for cytokines such as the interleukins (particularly IL2) and interferon's. GC`s also reduce macrophage sensitivity to lymphokines, retard epithelial growth and decrease post inflammatory neovascularization and reduce the permeability of inflamed capillaries. The effect of each particular GC is determined by its potency. The most potent synthetic GC is Dex, which has at least 20 fold the potency of hydrocortisone,

Figure 6: Glucocorticoid and Glucocorticoid Receptor

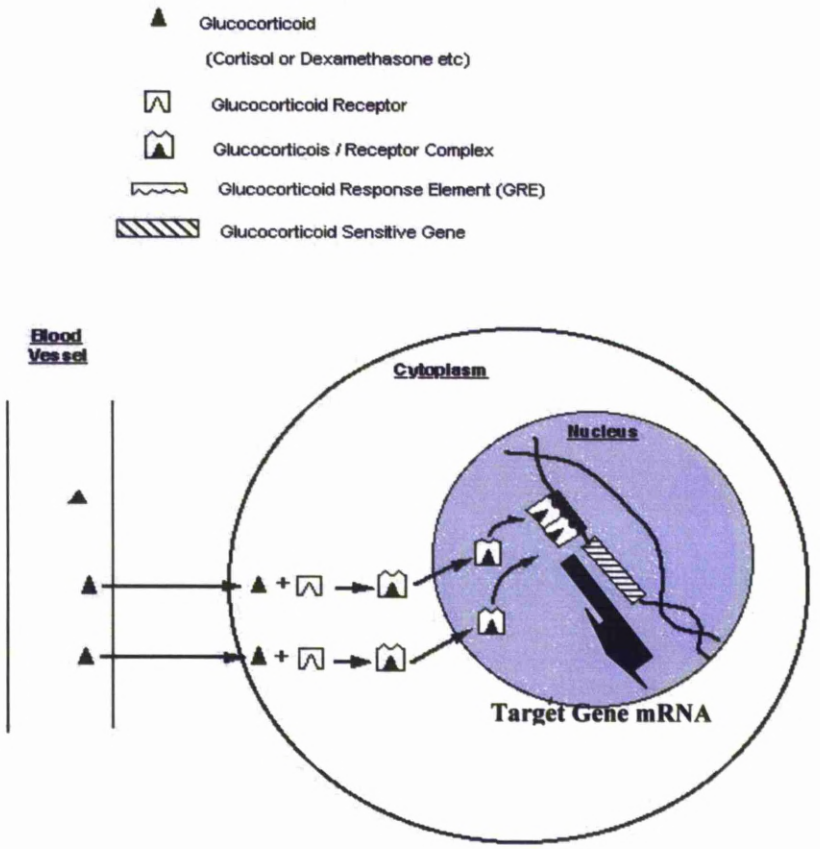

Diagrammatic illustration of the movement of glucocorticoid (GC) the blood stream to the target gene GRE. GC passes through the cell membrane by diffusion. Once inside the cytosolic it encounters a GC-receptor to which it binds. The binding causes a conformational change in the shape of the receptor which then unmasks motifs that cause it to be translocated to the nucleus. The glucocorticoid binds glucocorticoid response elements which are present in many genes (hence the wide ranging effects of glucocorticoids. The glucocorticoid receptor is recycled and used again. Research has shown that the GC-receptor complex is active within minutes of GC administration) (Croxtall et al, 2000).

and approximately 5 to 7 fold more potency than prednisolone (Kersey and Broadway 2006).

Dexamethasone ($C_{22}H_{28}FO_5$)

Synthetic GC's have were first synthesized in the 1950's. There is now at least 50 in common use. They have a number of uses including medical diagnosis of e.g. Cushing's disease (via the Dexamethasone suppression test) medical treatments (replacement of endogenous GC following adrenalectomy (Thompson 2007), treatment of autoimmune diseases e.g. SLE, allergic disease e.g. dermatitis, asthma, eczema and in inflammatory diseases such as arthritis. They are also used post trunsplant to try to prevent organ / tissue rejection.

One of the most potent synthetic GC's in common use is dexamethasone (Dex) (Fig. 5). It is used in at least 120 preparations (http://www.drugbank.ca) for treating a wide range of diseases including inflammatory diseases (e.g. rheumatoid arthritis), endocrine diseases (e.g. Cushing's syndrome), it is also used as an adjunct therapy in the treatments of cancer and during surgery such as wisdom teeth extraction, and during premature births where it aids maturation of the foetus's lungs. It is also used to prevent the onset and counteract the cerebral oedema that occurs with altitude sickness (www.nhs.co.uk).

An oral dose of dexamethasone is around 90% absorbed and peak plasma concentrations are reached between 1 to 2 hours later. Approximately 70% of circulating dexamethasone is bound to plasma protein, mostly albumin. This figure remains unchanged even if the dose of dexamethasone is increased. The plasma half life of dexamethasone has been shown to be 3.6 ± 0.9 hours. Following an oral dose, tissue distribution studies in animals have shown a high uptake of dexamethasone by

the liver, kidneys and adrenal glands. In man over 60% of circulating steroid are excreted in urine within 24 hours, largely as unconjugated steroid.

Ophthalmologic uses of Dexamethasone

In the eye dexamethasone is usually given to reduce redness, inflammation and swelling. The most commonly used method of administration is eye drops, and it has been shown that steroid is measurable in the aqueous humor 15 – 30 minutes following the application of a single drop to the cornea (Watson et al, 1988).

Local administration to the eye is preferable to systemic routes due to lessened side effects. Additionally an oral dose of approximately 500mg would be required to reach an aqueous humor concentration equivalent to that achieved with one drop of Dex administered to the eye itself (Irving et al, 1960).

When applied topically to the eye, dexamethasone is absorbed into the cornea, aqueous, iris, choroid, ciliary body and retina. The glucocorticoid receptor (GR) is expressed in the trabecular meshwork, and here glucocorticoid (GC) binding (especially dexamethasone) inhibits phospholipase A2, which in turn prevents the generation of molecules that mediate inflammation such as prostaglandins.

There are a number of side effects associated with prolonged dexamethasone use in the eye including corneal thinning which may lead to a possible perforation, sub capsular cataracts, optic nerve head damage and visual field disturbances.

Approximately one third of the general population are steroid responders, and these people will have a marked increase in the intraocular pressure (IOP) following exposure to dexamethasone. The risk of increased IOP is more marked in people who take anticholinergenics in addition to dexamethasone, especially atropine and in those

people who are predisposed to acute angle closure. The efficacy of dexamethasone is reduced by phenytoin, phenobarbitone, ephedrine and rifampicin.

1.4.6 Pharmacological Treatments for Glaucoma

Glaucoma treatment is designed to reduce the intraocular pressure (IOP) by reducing the production, or increasing the outflow of aqueous humor. Depending on the type of glaucoma, medications, surgery or a combination of both are used. Intraocular pressure can usually be lowered using different medications in eye drop, oral, or injectable forms (at least in the early stages of the disease).

Prostanoids (Latanoprost, bimatoprost, travoprost and unoprostone)

It is generally accepted that these medicines lower IOP by increasing outflow through the unconventional pathway (Bito, 1997) although there are some studies which suggest that outflow via the conventional pathway is also increased (Ziai et al, 1993; Brubaker et al, 2001). In either situation, aqueous inflow is not affected (Linden and Alm, 1999). Other studies have found that prostaglandins have a direct effect on specific ciliary muscle prostanoid receptors. The prostanoid receptors are not only in the ciliary muscle, but are widely distributed in the eye (which explains why prostaglandins have numerous effects within the eye). Activation of these receptors stimulates several linked responses, including cAMP formation; and the induction of c-Fos and c-Jun (Schachtschabel et al, 2000). These signals lead to increased biosynthesis of matrix metalloproteinases, which are a family of neutral proteinases that can cleave proteinaceous extracellular matrix molecules. These matrix metalloproteinases can initiate the alteration of collagen in the ciliary muscle, causing

an increase in the spaces along the ciliary muscle fibres, which in turn reduces the hydraulic resistance within the uveoscleral outflow (unconventional) pathway (Schachtschabel et al, 2000).

Miotics (Pilocarpine and Carbachol)

These drugs work by either direct or indirect mechanisms. Direct acting agents stimulate the parasympathetic muscarinic receptors, resulting in contraction of the longitudinal muscle of the ciliary body (which are attached to the scleral spur) causing them to pull on the trabecular meshwork; opening the pores and increasing aqueous outflow. Indirect agents work by inactivating acetylcholinesterases. Some agents may bind reversibly, others bind permanently. The result of inactivating this enzyme is an increased concentration of acetylcholine available to bind the muscarinic receptors, which again results in the contraction of the longitudinal muscles of the ciliary body and increased trabecular outflow facility (Grierson et al, 1979; Zimmerman and Kooner, 2001).

Adrenergics (Apraclonidine, brimonidine, dipivefrin)

Adrenergics include the non-selective alpha-1 and alpha-2 adrenergic medicines (adrenalin and dipivefrin) and the selective alpha-2 adrenergic medicines (apraclonidine and brimonidine).

Adrenalin (and noradrenalin) as a non-selective agent will bind to both classes of alpha and beta adrenergic receptors in the ciliary body. Upon binding to beta receptors, this agent will induce an increase in aqueous flow. This counterintuitive effect however is counteracted by the main activity of this agent on the alpha-2 receptors in the ciliary boy, which cause vasoconstriction and a decrease in aqueous production.

Additionally, adrenalin has been shown to act on beta-2 receptors in the trabecular meshwork and in the uveoscleral pathway where it increases outflow facility by increasing cAMP (Boger, 1983). The selective agent brimonidine has two mechanisms of action. It both decreases aqueous humor production, and increases outflow via the uveoscleral route (Gupta, 2004).

Beta-Blockers

Beta adrenoreceptors have been categorised into three subclasses (beta-1, beta-2 and beta-3). The beta-1 receptor is located primarily in the heart. Stimulation of this receptor increases heart rate, cardiac contractility and atrioventricular conduction. The beta-2 receptor is found primarily in the bronchial muscle, blood vessels and in the uterus. Agents (antagonists) that block these receptors have the opposite effect. The beta-3 receptor is involved in the mediation of lipolysis. Different beta blockers have different affinities for the different receptors. Levobetaxol has a high affinity for the beta-1 adrenoreceptor, while Levobunolol has a higher affinity for the beta-2 adrenoreceptor (Phan et al, 1991; Sharif and Xu, 2004).

The beta-blocker class of drugs are antagonists and act as competitive inhibitors at the beta-adrenoreceptor site. They are classified as selective or non-selective, based on their affinity to the beta-1 and beta-2 receptors. Selective antagonists inhibit only one receptor, while non-selective antagonists inhibit both beta-1 and beta-2 receptors (Zimmerman, 1993).

Ocular beta-blockers decrease IOP by decreasing the formation of aqueous humor. These medicines are able to decrease aqueous formation by up to 50% (Yablonski et al, 1978; Neufeld et al, 1983; Gaul et al, 1983).

Despite the prolonged use of these medicines, the exact mechanism of action that results in a lowering of the IOP has yet to be fully elucidated.

Normally, when a beta-adrenergic agonist binds to its receptor, this will result in the activation of a regulatory G protein. This stimulates membrane bound adenyl cyclase catalysing the conversion of ATP to cAMP. In this model for the mechanism of actions of ocular beta-blockers, intracellular cAMP acts as a second messenger that ultimately stimulates production of aqueous humor from the ciliary processes.

It has been demonstrated that Timolol and other beta-blockers can inhibit cAMP production in the ciliary body. However, a direct relationship between the inhibition of cAMP and a decrease in IOP is not supported in all studies. One study in particular found no correlation between a reduction in cAMP and a reduction in IOP (Schmitt et al, 1981; Caproli et al, 1984). These observations in the ciliary body suggest that the IOP lowering effect of ocular beta-blockers may not be mediated directly through the competitive inhibition of receptors.

An alternative mechanism suggested by Polansky et al, 1992; is that there is endogenous adrenergic tone controlling tonic stimulation to produce aqueous. They suggest that beta-blockers exert their effect by interfering with this tonic stimulation.

Carbonic Anhydrase Inhibitors (Acetazolamide brinzolamide dorzolamide methazolamide)

This class of medicines may be given orally or topically. They affect a decrease in IOP by inhibiting aqueous production. They achieve this action by non-competitive, reversible binding to the carbonic anhydrase enzyme. The inhibition of this enzyme results in a reduced flow of sodium and fluid into the posterior chamber, from the ciliary processes. This process is highly dependant on the transport of sodium by the

Na+-K+-ATPase which in turn is dependant on the formation of bicarbonate. Carbonic anhydrase is responsible for much of the bicarbonate production, and so by inhibiting this, it is possible to reduce the rate of aqueous humor production (Gupta, 2004).

Hyperosmotics (Mannitol glycerin isosorbide)

Hyperosmotics are used in the treatment of acute angle-closure glaucoma. The effects last only 6-8 hours, so they are not for long-term use. They are commonly used as an emergency treatment for (e.g.) angle closure glaucoma, prior to surgery, and with other acute IOP elevations. These drugs are (often) sugar-based medications or other compounds which when given intravenously, or orally result in an increase in plasma osmolality, which has the effect of drawing water from the eye (especially the vitreous) into the plasma, thereby lowering the IOP (Zimmerman and Kooner, 2001).

1.5 The Cytoskeleton

1.5.1 An Overview of the structural elements of the cytoskeleton

The cytoskeleton is a complex network of numerous interconnected protein filaments that extend throughout the cell and together form a supporting scaffold-like structure that extends from just below the surface of the plasma membrane to the nucleus in all eukaryotic cells.

The three major components of the cytoskeleton are microtubules, microfilaments and intermediate filaments which are held together by a number of accessory proteins.

Each of these major components has a distinct size, structure and distribution pattern within the cell and they are all formed by the polymerisation of different protein monomers. These three filaments are widely conserved proteins but are unique to eukaryotic cells, no such structures are found in prokaryotic cells. The absence of these structures may suggest that the cytoskeleton played a crucial role in the evolution of eukaryotic cells (Becker and Deamer 1991).

The major role of the cytoskeleton is to support the plasma membrane thereby maintaining the correct cell shape. This in turn allows for the proper organisation of intracellular organelles, intracellular trunsport, and other key cell functions such as motility (Lazarides and Revel 1979) and division (Fletcher and Mullins, 2010).

Microtubules

The microtubules are the largest of the cytoskeleton components with a diameter of approximately 25 nm. They can be broadly classified into two groups which differ in their degree of structural stability. One group is highly organised and stable and form structures associated with movement such as cilia (the axonemal microtubules). The

other group is composed of a less organised, more dynamic structure found in the cytoplasm and can be termed cytoplasmic microtubules (Brinkley 1985, Allen 1987). Microtubules radiate outwards from a microtubule organising centre near the nucleus and extend in a lace-like pattern throughout the cell. Examples of these organising centres are the centrosomes and the poles of the mitotic spindle (Brinkley 1985).

The cytoplasmic microtubules perform a variety of functions within the cell. They maintain cell structure and shape; they confer polarity and determine the distribution of the other key cytoskeleton components such as the endoplasmic reticulum and the Golgi apparatus (Chrétien et al, 1995). Although all the components of the cytoskeleton have some role in maintaining cell architecture, microtubules appear to be of the greatest importance in this regard. Their radiating network of fibres from the nucleus guide vesicles and other organelles within and throughout the cytoplasm towards the plasma membrane (Lazarides 1980) (Fig 7).

Figure 7: Components of the Cytoskeleton

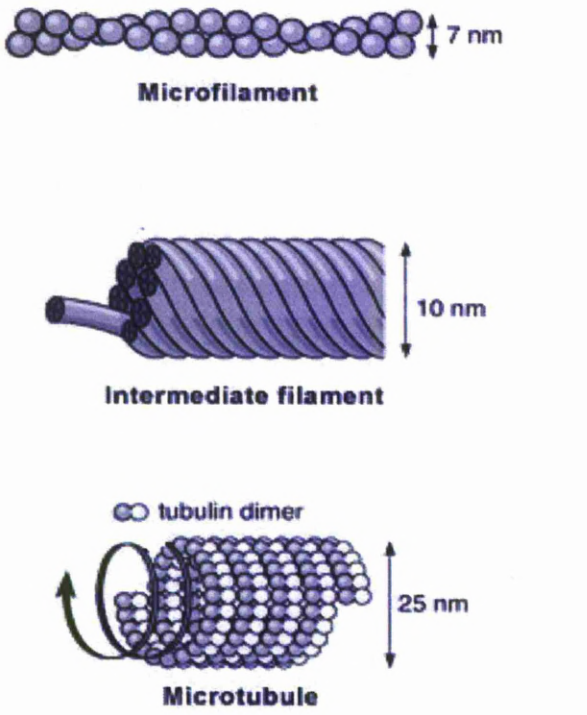

Diagrammatic representation of the constituent parts of the cytoskeleton. The insoluble polymers of all three components are composed of many smaller sub-units which assemble and disassemble constantly according to need at the time. Dexamethasone causes a shift in the equilibrium of the actin pool causing an increase in the G to F actin ratio i.e. it increases the amount of F actin with out increasing the over all actin content of the cell by increasing polymerization and decreasing de-polymerization (Koukouritaki et al, 1996),

Structure

The microtubules are straight, hollow cylindrical tubes with an overall diameter of 25nm and an inner lumen diameter of approximately 15nm (Chretien et al, 1995). The length of these tubules can vary greatly from 200nm up to 25μm in some nerve cell axons. The microtubule is composed of longitudinal arrays of protofilaments arranged side by side around the hollow central lumen. Each protofilaments is a linear polymer of tubulin molecules. Tubulin is a dimeric protein composed of two similar but separate subunits called α and β tubulin which are linked together covalently. Each of these peptides has a diameter of 5nm and a molecular weight of about 50,000 (Wade and Hyman 1997; Downing and Nogales 1998). Bound to the αβ dimer are two molecules of GTP. These high energy molecules are not necessary for the polymerisation of these monomers into the microtubule polymer as polymerisation can occur even if the GTP is replaced by a nonhydrolysable analogue. The Hydrolysis of GTP appears to change the affinity of the microtubule end for incoming dimers and may play a role in polarity during formation.

All of the tubulin dimers within a protofilaments are orientated in the same direction, meaning that all the α subunits face one direction while all the β subunits face the other. This orientation of the dimers confers a polarity to the microtubule which has important implications for the formation of the microtubules within a cell. One end (the plus end) of the growing microtubule will grow faster than the other (the minus end) (Kozielski et al 1999). The plus end is orientated away from the nucleus ensuring that microtubule growth occurs in an outward direction.

Polymerisation

Microtubules form via the reversible polymerisation of tubulin dimers. The α and β subunits are synthesised separately which then associate to form the dimeric tubulin

molecules. As the dimers polymerise they form rings as an intermediate step before uncoiling to form the protofilaments which associate side by side into sheets. As the sheet grows to contain 13 protofilaments it folds over to form the cylindrical shape of a recognisable microtubule (Chrétien et al. 1995). The microtubule then elongates as required by the addition of dimers.

Intermediate Filaments

Intermediate filaments range in diameter from 8 – 12 nm. Most studies into these cells have been done in various animal cells where these filaments occur singly or in bundles playing a structural or tension bearing role in regions of the cell that are subjected to mechanical stress (Lazarides 1980). These cytoskeletal components may be important in maintaining the position of the nucleus by forming a ring around the perimeter that extends both into the cytoplasm and into the nuclear pores, where it may connect to the nuclear lamina filaments which are similar in function to the cytoplasmic intermediate filaments. The intermediate filaments are the least soluble and most stable of the three major cytoskeletal components and because of this it has been suggested that the intermediate filaments serve as a scaffold for the entire cytoskeleton.

The intermediate filaments differ in composition from tissue to tissue, according to the cell type in which they are found (Table 3) (Lazarides 1980).

As all intermediate filaments are products of related genes, they all share some common features even if they do differ considerably in their size and chemical properties (Parry and Steinert 1999). Intermediate filaments are fibrous, unlike the other two cytoskeletal components which are globular. They all contain a central rod-like domain which is between 310 and 315 amino acids in length. This central region

consists of four separate coiled helices interspersed by three short linking regions. On either side of the central domain lay the N and C-terminal domains that can differ in size and function – it is these that give the intermediate filaments their functional diversity (Steinert et al, 1985; Steinert and Roop 1988).

The basic structural component of the intermediate filament is the protofilaments. These are formed by the lateral alignment of two dimers which forms a tetrameric protofilament. These protofilaments then associate by overlapping end to end to form a filamentous structure. When fully assembled the intermediate filament is described as being 8 protofilaments thick (Steinert, Jones et al. 1984) (Fig 7).

Table 3: Major Types of Intermediate Filaments and their component proteins

Tissue	IF Protein	Molecular weight K
Epithelial	*Keratin acidic / basic*	*44-60 / 50 - 70*
Mesenchymal	*Vimentin*	*53*
Muscle	*Desmin*	*52*
Glial	*GFAP (Glial Fibrillary Acidic Protein)*	*51*
Neuronal	*NF Protein (neurofilament)*	*60/100/130*

Microfilaments

The third class of cytoskeletal components are the actin microfilaments. These filaments were studied intensively during this work and so will be described in much greater detail in the next section.

1.5.2 Actin

Microfilaments are the smallest of the cytoskeletal filaments with a diameter of around 7nm. Microfilaments are commonly thought of as being associated with contraction in muscle cells, however microfilaments occur in almost all other eukaryotic cells and are also involved in cell movement (amoeboid movement, locomotion in cultured cells and cytoplasmic streaming), the maintenance of cell architecture and structure, and in processes such as the formation of cleavage furrows that divide the cytoplasm during mitosis (Becker and Deamer 1991).

Most animal cells have a network of microfilaments and associated proteins just below the surface of the cell membrane which is properly called the cell cortex. This cortex confers structural rigidity to the cell surface and is also involved in other processes such as shape change and cell movement.

Structure

The microfilaments are polymers of a protein called actin. Actin is a ubiquitous protein found in nearly all eukaryotic cells including those of plants, algae and fungi. It is the single most abundant protein in most cells and can comprise more than 5 - 10% of total cellular protein (Becker and Deamer 1991).

Actin is synthesised as a monomer called globular (G) actin. G actin is a single polypeptide chain containing 375 amino acids and has a molecular weight of 42KDa.

Each molecule of G actin has a molecule of ATP or ADP bound to it non-covalently, between the two domains in the folded G actin monomer.

G actin monomers can polymerise reversibly to form a long strand of filamentous (F) actin, once the concentration of G actin reaches a critical concentration. This concentration value for the polymerisation of F actin from G-ATP actin is 20 fold lower than for G-ADP actin.

During polymerisation, each new monomer is attached to the next with a rotation of 166 degrees and each G actin monomer is in contact with four other monomers in the strand. This gives the appearance of an intertwined double stranded filament although it is in fact only a single stranded coiled structure.

Stress fibres

The stress fibres are composed of bundles of between 10-30 F actin filaments (Cramer et al, 1997). These bundles are held together by the actin cross-linking protein alpha(α) actinin (Lazarides and Burridge, 1975). Other actin cross-linking proteins such as filamin and fascin have also been detected in these fibres (Adams, 1995; Chen et al, 1999). Alpha-actinin is located irregularly along the fibre length and alternates with bands containing non-muscle myosin (Weber and Groeschel- Stewart, 1974) and tropomyosin (Lazarides, 1975). The bands of α-actinin in stress fibres can be seen as electron-dense striations (Langanger et al, 1984; Langanger et al, 1986). Actin filaments have inherent polarity, each having a plus (or barbed) end and a minus (or pointed) end.

Analysis of the polarity of actin filaments in stress fibres has shown that the sarcomeric model (which is based on the contraction apparatus in skeletal muscle cells) does not really explain the complexity of contraction in these structures

satisfactorily. In a muscle sarcomere, each block of actin filaments must have the opposite polarity to its preceding block to allow sliding contraction to occur. The myosin motors move towards the barbed ends of the actin filaments and the gap between each block of actin filaments decreases.

Analysis of non-muscle cells has shown that actin filaments in many stress fibres show an alternating polarity while in other stress fibres, actin filament polarity is uniform. In yet other stress fibres the actin filaments in a bundle can show an apparently rundom orientation (Cramer et al, 1997).

In motile cells, the majority of stress fibres show a single overall polarity, meaning that at the end of each filament, the polarity is uniform with all barbed ends pointing outwards. However, the distribution of filament polarities may be varied at the centre of the fibre (Cramer et al, 1997) (Fig 7).

1.5.3 Actin in the cells of the outflow system

The actinomyosin system is composed of actin microfilaments and numerous microfilament associated proteins. It is a feature of almost all cells, and is particularly important in the trabecular meshwork cells of the outflow system. There are many microfilament based structures throughout the cells of the trabecular meshwork. These include focal adhesions, cell–cell junctions, and stress fibres (Geiger et al. 1995). Filamentous actin is the major component of microfilaments, but other actin-associated proteins modulate its organization. The microfilaments are involved in a range of cellular processes from cell adhesion and motility to organelle traffic and adhesion-mediated signal transduction. The dynamics of the actinomyosin system therefore plays an important role in maintaining the cell shape, cell volume, cell contractility, and in the adhesion between neighbouring trabecular cells and between

these cells and the extra-cellular matrix. Changes in the trabecular meshwork cell microfilaments can affect the trabecular meshwork outflow resistance by altering (e.g.) the dimensions and / or the direction of the outflow pathways. Such changes can be modulated directly by cytoskeletal disrupting agents such as Latrunculin A (Epstein et al 1999) or indirectly by the inhibition of specific proteins or cellular contractility via administration of protein kinase inhibitors such as the serine–threonine kinase inhibitor H-7 (Bershadsky et al, 1996). It has been reported that H-7 when administered intracamerally or topically to living monkey eyes, doubles the normal aqueous outflow facility and decreases the intra ocular pressure (Tian et al. 1998, 2004). Morphological studies in live monkey eyes indicated that the H-7 induced increase in aqueous outflow facility is associated with cellular relaxation and with drainage surface expansion in the trabecular meshwork and within Schlemm's canal, and is also accompanied by loss of extra cellular matrix (Sabanay et al, 2000, 2004).

The Rho kinase inhibitor Y-27632 causes reversible changes in cell shape and a decrease in the number of actin stress fibres seen, as well as a decrease in the number of focal adhesions, in human trabecular meshwork cells (Rao et al, 2001). In isolated bovine meshwork strips, Y-27632 completely blocks calcium-independent phorbol myristate acetate or endothelin-1-induced contraction (Thieme et al. 2000; Renieri et al. 2008). Rho kinase inhibitors, such as Y27632, Y-39983, HA-1077, H-1152 and INS117548, increase outflow facility and often decrease IOP in living rabbit eyes, enucleated porcine eyes and in living monkeys in a manner that is similar to that seen with H-7 (Honjo et al, 2001a, 2001b; Rao et al. 2008).

Additionally, trabecular meshwork cells are contractile – this contraction is associated with increased aqueous drainage while the converse is also true (Weiderholt et al, 1994).

All these results show that chemical or drug induced alterations of the actin in the trabecular meshwork cells of the outflow system can cause changes in outflow facility and intra ocular pressure, and outlines the importance of the actin cytoskeleton in the proper maintenance of eye physiology.

1.5.4 Cross-Linked Actin Networks (CLANs)

As stated above, there are normally two common patterns of F-actin seen within cells; either there is a diffuse arrangement of F-actin or there are stress fibres. A far less common actin arrangement is a dome-like configuration of F actin comprised of polygonal units which inter-connect to form a network (Lazarides, 1975; Gordon and Bushnell, 1979; Ireland and Voon, 1981). These polygons form very early culture in a variety of cell types and seem to be transient structures that are no longer present to any great extent when the cultured cells become well established (Lazarides, 1976).

The functional significance of the polygonal networks, or for that matter their mechanism of formation, remains obscure. Atomic force measurements indicate that these structures impart increased rigidity to the cell (Meller and Theiss, 2006) and there have also been suggestions that such a geodesic arrangement made up of polygonal networks of actin may impart structural stability in line with "tensegrity" theory (Ingber, 1998).

Other polygonal actin structures are induced in confluent, cultured human TM cells following exposure to glucocorticoids, the most effective of which is dexamethasone (Clark et al, 1994). Clark called these structures cross-linked actin networks (or CLANs) and noted that these structures formed in confluent TM cultures. Unlike the previously mentioned polygonal networks, these structures seemed to be reasonably persistent; and were specific to TM cells as CLANs were not induced in a range of

other ocular cell types following exposure to dexamethasone (Clark et al, 1994). CLANs were also abundant in the TM cells ex vivo outflow tissue perfused with dexamethasone, and these tissue-associated structures were found to be identical to the cell culture equivalent (Clark et al, 2005). The suggestion that geodesic cross-linking arrangements may make the TM cells (and therefore the tissue) "stiffer" (or at least, less elastic) and therefore more resistant to aqueous outflow is a credible hypothesis (Tan et al, 2006) for future evaluation.

Apart from reorganising the cytoskeleton within some TM cells, glucocorticoids have affects on many other TM cell activities (Wordinger and Clark, 1999) that include extracellular matrix production (Wilson et al, 1993) and matrix metalloprotease activity (Snyder et al, 1993). In addition, some biological mechanisms of glucocorticoid modulation of TM cell function are probably actin associated; including functional effects on DNA endoreplication (Tripathi et al, 1989), inhibition of cell proliferation (Clark and Wordinger, 2009), inhibition of cell migration (Clark et al, 1994), alteration of TM cell volume (Clark et al, 1994) and a reduction in phagocytic ability (Matsumoto and Johnson, 1997). It has been established that a proportion of patients on corticosteroid treatment are at risk of developing a form of glaucoma called corticosteroid glaucoma (refer to chapter 1.3.3) that has many features in common with primary open angle glaucoma (Goldmann, 1962; Spaeth et al, 1977).

CLANs are not just associated with glucocorticoid exposure. They appear to be abundant in TM cultures derived from donor patients that had POAG (Clark et al, 1995a). CLAN-like structures have been observed in the (JCT) tissues of the glaucomatous outflow system (Read et al, 2006), and abundant CLANs were observed in the TM of both POAG patients and elderly human eyes (Hoare et al,

2009). It remains to be determined whether or not CLANs have a central role in key architectural and functional events in the TM tissue that are associated with diseases like POAG. Little is known about the nature, formation, associations and functions of these distinctive F-actin arrangements.

To date virtually all attempts to identify and study CLANs have been restricted to human cells in vitro and ex vivo (Clark et al, 1994; Clark et al, 1995b; Clark et al, 2005; Read et al, 2006; Filla et al, 2006). Given the low availability of human tissue for use in research, it was thought desirable to determine if the cells and trabecular meshwork tissue of another species was suitable for the furtherance of CLAN and glucocorticoid research.

My Supervisor (Prof. Ian Grierson) has a long history of the use of bovine eyes and tissues, and so it was he whom suggested that we first examine CLAN formation in this species. The rationale for this, apart for a sound familiarity, was that the bovine eyes are readily obtainable in large quantities. The eyes themselves are large (compared to human eyes) and the dissection and removal of the meshwork is easier to accomplish, even without a dissecting microscope. Additionally, the bovine meshwork cells are hardy cells and are relatively easy to grow up from primary cultures. It was decided that other species would be examined if we were unsuccessful in generating CLANs in bovine cells. The rabbit (Knepper et al, 1985) pig (McMenamin and Steptoe, 1991) and rat (McMenamin and al-Shakarchi, 1989) outflow systems have been thoroughly researched previously and rabbits are thought to respond to dexamethasone treatment with elevated IOP, the same has recently been shown to be the same in sheep treated with dexamethasone (Gerometta et al, 2010).

Figure 8: Examples of CLANs in dexamethasone treated bovine meshwork cells

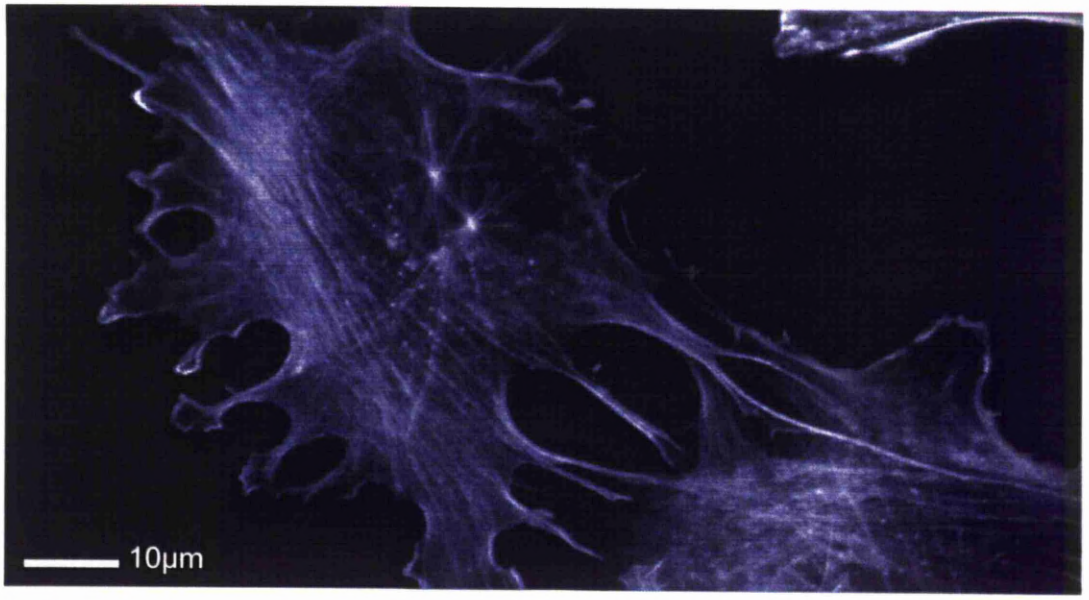

Bovine meshwork cells treated with dexamethasone for 72 hours (phalloidin / actin image). The central cell contains a large (double) starburst-like CLAN. In addition this cell also contains numerous stress fibres, and is well spread. The cell toward the bottom right of the image contains "speckling" which is atypical for these cells unless they have been treated with dexamethasone.

Figure 9: Examples of CLANs in dexamethasone treated bovine meshwork cells

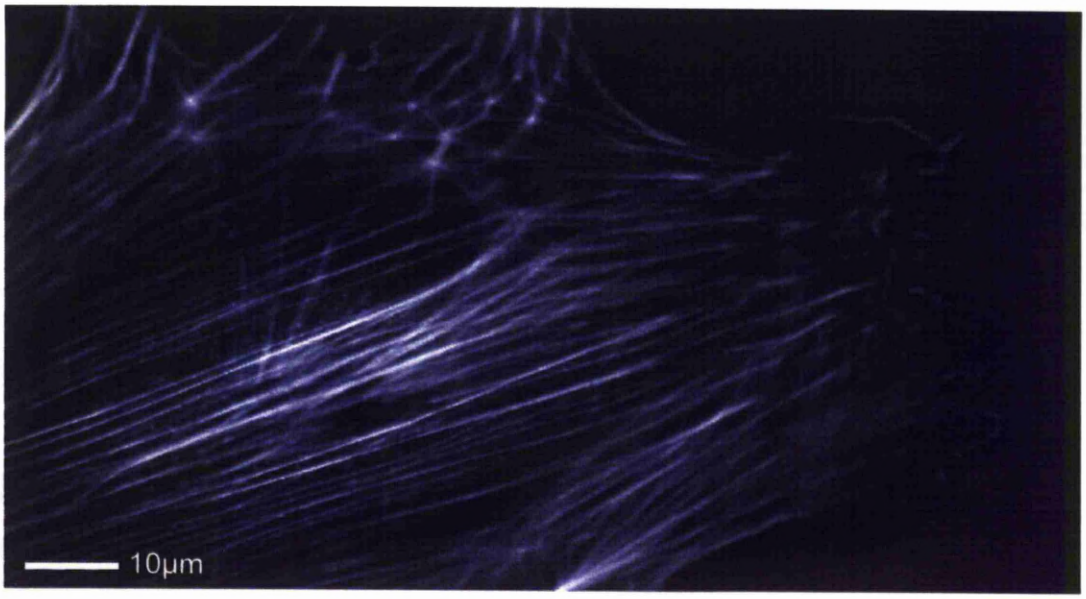

Bovine meshwork cell treated with dexamethasone for 72 hours. This image shows the abundant stress fibres present in these cells, additionally there is a CLAN area at the top of the image / cell, which contains a highly geodesic structure that spreads out into a basket-like CLAN arrangement toward the edge of the cell.

Figure 10: Examples of CLANs in dexamethasone treated bovine meshwork cells

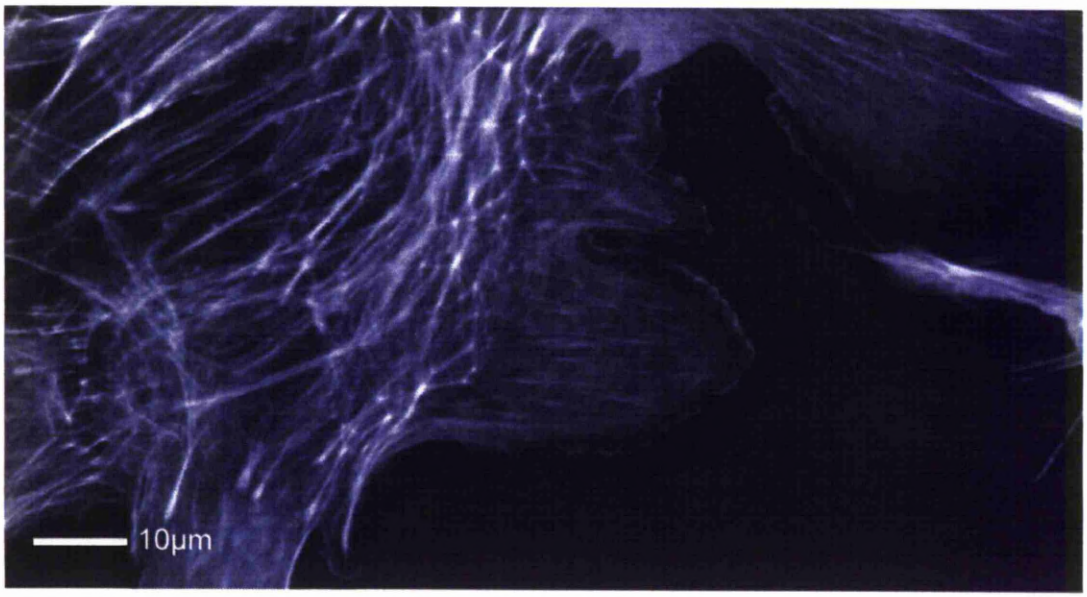

Bovine meshwork cells treated with dexamethasone for 72 hours. This cell contains a very large (in excess of 40 "hubs") basket-like CLAN arrangement. Of interest in this image is the various sizes of the hubs which range from very visible (centre of image) to very fine (lower left of image above the scale bar). The cell with the large CLAN in it shows little in the way of stress fibres, unlike some of the other cells around it.

1.5.5 Actin Associated Proteins

There are many families of proteins which can specifically bind to, and cause changes in / effect, the actin component of the cytoskeleton. Some of these must be important in the formation of CLANs, but as yet, this area of research remains unexplored. There are several families of proteins which can be classified as follows:

According to affinity for specific filaments

Actin-associated (e.g. myosin)

Microtubule-associated (e.g. Tau protein)

Intermediate Filament-associated

According to the binding site affinity

End binding proteins (nucleation, capping, Arp2/3, gelsolin)

Side binding proteins (tropomyosin)

According to primary function

Cross-linkers

- Gel formation (filamin, spectrin)
- Bundling (alpha-actinin, fimbrin, villin)

Polymerization effects

Induce depolymerization (gelsolin)

Stabilizing (profilin, tropomyosin)

Motor proteins

Myosins (actin based)

Kinesin

DNA / RNA based

Motor proteins move or slide along cytoskeletal fibres, myosin on microfilaments and kinesin and dynein on the microtubules using energy from ATP hydrolysis.

Mechano-sensing the extracellular environment

Cells, including trabecular meshwork cells, are capable of sensing external mechanical stimuli (such as contraction / stretch or fluid shear within the trabecular meshwork) and translating them into biochemical signals. This ability allows cells to adapt to their physical surroundings by remodelling their cytoskeleton in response to different stresses by activating various signalling pathways and in some cases by changing their gene expression (Vogel and Sheetz, 2006). This "sensing" usually involves two separate processes; mechano-sensing (recognising a change in the external environment or a change on pressure / force on the cell surface) and mechano-transduction. In these processes, stretch, pressure (deformation) or other forces need to be transmitted from the outside environment to the proteins (and organelles) within the cell so that they might adapt accordingly. The actin cytoskeleton composed of actin filaments, possibly myosin motors, and certainly actin cross linking proteins plays a critical role in force propagation (signal transduction)

through the plasma membrane, in response to external stimuli. For a mechano-transduction system to function it requires minimally, at least one sensor and one transducer (Wang et al, 2009). Such sensors are usually located within the cell membrane, where they sense the mechanical stimuli (such as force, pressure or changes in flow speed across / over the membrane) and then transmit the mechanical stimuli to the inside of cell (Vogel and Sheetz, 2006). Ion channels, Integrins, protein kinases, G proteins, intercellular junction proteins, focal adhesion proteins and numerous other membrane-associated signal-transduction molecules are capable of sensing mechanical stimuli (Ingber, 2006; Vogel and Sheetz, 2006; Wang et al, 2009). This stimulus is passed to a transducer (usually bound to the inside of the cell membrane or free within the cytoplasm) which then converts the original mechanical signal into a chemical or biological signal. Physiological examples of mechano-sensation could include hearing (Fettiplace and Hackney, 2006), blood pressure regulation (Chien, 2007), and bone remodelling (Robling et al, 2006). It is probable that trabecular meshwork cells in vivo (and vitro) also possess this ability, as they have been reported to rearrange their cytoskeletons (form CLANs) after being subjected to mechanical stretch, and fibroblasts have been shown to rearrange their cytoskeletons into a geodesic arrangement in response to a zero gravity environment (Ingber 1998).

Mechano-Sensors and the Actin Cytoskeleton

The mechanical properties of the actin network, and its ability to sense deformations or stretch, depend on its morphology, and / or on its microstructures, such as; filament length, filament and bundle diameter, and the heterogenicity / homogeneity of the fibres within each bundle (Sato et al, 1992). It is also dependant upon the binding

strength between the actin filaments, different cross-linking proteins and on the motor activities of that cell (Ingber, 2006; Vogel and Sheetz, 2006; Wang et al, 2009).

The major protein of the actin cytoskeleton is as previously discussed monomeric globular "G" actin, which is found in all eukaryotic cells. Each monomer is organized into four sub domains, which surround a central cleft which binds ATP and magnesium ions. The end of G-actin adjacent to the bottom of this cleft is termed the "plus" end and the opposite end, the "minus" end. Within F (filamentous) actin, the plus end of one G-actin monomer is connected to the minus end of the next G-actin monomer (Janmey et al, 1990). This polarity is continued higher up at the level of the microfilaments, and these also have well-defined plus (positive) and minus (negative) ends. The 8-nm wide F-actin filament is a left-handed helix which has 13 G-actin monomers per repeat and a repeat length of 37 nm (Janmey et al, 1990). Actin microfilaments have a right-handed helical structure with two F-actin strands twisted around each other. Each G-actin monomer is rotated 166° in respect to its two nearest monomers on the opposite side of the strand (Holmes et al, 1990). Within each strand, sub-domains 2 and 4 bond to sub-domains 1 and 3 in the next monomer of the strand, and each monomer binds to the other strand via a hydrophobic plug which links the two strands together.

Actin Cross-Linking Proteins (ACLPs) can organize actin filaments into structures such as bundles or meshwork's, depending on their molecular structures, kinetic properties, and concentration (Revenu et al, 2004). "Bundle forming" ACLPs include fascin, villin, fimbrin, plastin, and dynacortin. Examples of "meshwork" forming ACLPs are filamin, Arp2/3, gelsolin and ERM (ezrin, radixin, and moesin) proteins (Pollard, 2007). Most of these proteins have additional functions within the cell (e.g.

Arp2/3 also nucleates (or is the focus for) actin assembly in the cytoplasm, while ERMs allow actin filaments and actin meshwork's or bundles to bind to the cell membrane (Pollard, 2007). Some ACLPs, particularly α-actinin and dynacortin, can form either bundles or meshworks depending on their concentration in the cell and on the ratio of F actin to ACLPs (Girard et al, 2004). Some ACLPs (particularly villin, espin, forked, fimbrin and fascin), are monomeric and contain minimally two actin-binding motifs, allowing them to crosslink as monomers. In contrast, ACLPs, such as filamin A, α-actinin and dynacortin, are dimeric proteins. Filamin A, cortexillin, and most dynacortin form parallel dimers while α-actinin forms anti-parallel dimers. Different ABDs generally associate with different areas of the actin monomer and each binds with different affinity (Forgacs, 1995).

To cross-link or bundle two actin filaments, the ACLP must have a minimum of two actin-binding domains associated with each subunit, through which the ACLP is in contact with the actin filament(s). This occurs by either dimerising a monomer with one actin binding domain (ABD) or by having two (or more) ABDs within a single monomer (Tseng et al, 2005). The strength of the actin interactions and the conformational arrangement of the actin network (whether it be a meshwork or bundle) varies with different ABDs, and with the different conformations of ABDs within each ACLP (Tseng et al, 2005). For example, ABDs could be closely linked via "short" spacers such as fimbrin, which would result in a tightly packed actin bundle, or the spacer might be elongated as it is in α-actinin and spectrin, which form loose networks by comparison to the previously mentioned ABD (Bañuelos et al, 1998).

The presence of myosin-II can alter the character of the actin network. Following mechanical stimuli, the actomyosin system commences a continuous remodelling of its microstructure (assembly/disassembly of actin filaments and myosin II thick

filaments in addition to the bundling/unbundling of actin filaments by ACLPs). During remodelling, the whole network is more or less out of mechanical equilibrium, which leads to transient behaviours within the network (Mizuno et al, 2007; Wilhelm, 2008). This transient loss of equilibrium is probably the cause of the temporary geodesic cytoskeletal structures seen in settling cells and in cardiac fibroblasts (Entcheva and Bien, 2009). It has not been researched, but it is possible that the "hub" sites with CLANs correlate to the position of focal adhesions. It is speculative, but further possible that the change from stress fibres to CLANs is initiated via the mechano-sensing focal adhesions within trabecular meshwork cells.

Focal Adhesions as Mechano-sensors in the Actin Cytoskeleton

Focal adhesions and their use in mechano-sensing the external environment of the cell are important in many cellular processes such has cell growth, differentiation and motility. Focal adhesions are "mechanical links" between the cytoskeleton and the exterior of the cell and or the extracellular matrix (ECM). Focal adhesions are large molecular complexes that are formed from a large number of different proteins, including several integrins and actin binding proteins such as talin, vinculin, paxillin, (Zamir and Geiger, 2001; Geiger et al, 2009). Within focal adhesions, integrins form hetero-dimers, with α and β subunits (non-covalently bound together) each with an extracellular domain, a transmembrane helix, and a short cytoplasmic tail (Puklin-Faucher and Sheetz, 2009). The cytoplasmic "tail" of the β-integrin binds to the talin (actin binding protein) "head" domain. Talin may then anchor directly to actin or via a secondary actin binding protein such as vinculin (Puklin-Faucher and Sheetz, 2009). Focal adhesions can be in a stationary position within the plasma membrane (possibly temporarily located in "membrane stable" lipid rafts) or mobile, while undergoing a

continual exchange of components with the cytoplasm. Focal adhesions tend to accumulate in areas with increased local force (Tan et al, 2003) and tend to be orientated toward the direction of the applied force (Riveline et al, 2001).

Focal adhesion formation is initiated after the activation of integrins. Inactive integrins have a "bent" shape whereas the active forms have an "extended" or straightened morphology (Hynes, 2002). Integrins may be activated either by their "head" end binding to the ECM (referred to as outside-in signalling) or by the "tail" binding to talin (inside-out signalling) (Hynes, 2002). The next mechano-sensitive protein within the focal adhesion is talin. Talin is a large protein consisting of an N-terminal "head" region and a long "rod" region. Close to talin's amino-terminal is a FERM (band 4.1, ezrin, radixin, moesin) domain, via which talin binds to several molecules including integrin(s), focal adhesion kinases and other receptors (Tadokoro et al, 2003). Talin-binding to the integrin β tail disrupts an intra-cellular "salt" bridge between the α and β integrin subunits, which increases the integrins binding affinity for the extracellular matrix (Tadokoro et al, 2003). Talin binds vinculin, and has eleven vinculin binding sites in its rod region. Vinculin is a 116kDa actin-binding protein, which is the main link between the core focal adhesion proteins to the actin component of the cytoskeleton (Tamada et al, 2004; Giannone and Sheetz, 2006).

Mechanically induced focal adhesions cause activation and recruitment of many downstream kinases (Brakebusch and Fässler, 2003), some of these kinases may affect actin remodelling by regulating small GTPases and other actin binding proteins. Focal adhesion kinase binds to integrin, talin and paxillin, which further enhances focal adhesion kinase activities, which then initiates stress fibre formation. Integrin-linked kinase binds to the tails of the β integrin subunits, paxillin and phospholipids, which induces the phosphorylation of several protein kinases that are up-stream of

actin polymerization. Integrin –linked kinase also initiates the formation of a complex which then recruits F-actin localisation to the focal adhesion sites (Huveneers and Danen, 2009).

2.0 Materials and Methodology

2.1 Focus

The primary question we needed to answer was whether or not CLANs were present within the trabecular meshwork cells of another species (initially bovine) and also to determine whether CLANs – if present – were able to be induced at an experimentally useful level.

Once we had answered the first question, subsequent research was to be directed towards trying to further our understanding of CLANs – specifically how they form and if they form in response to other stimuli – and additionally, if possible, to determine why they form at all and what the consequences of their formation might be. Given that these structures are microscopic, work undertaken utilised bovine tissue explants, and primary cell cultures derived from these. Bovine eyes used in this work were purchased from Hewitt's (Yew Tree House, Church Lane, Huxley, Chester, Cheshire CH3 9BH).

Light / fluorescent and confocal microscopy was undertaken for the majority of the work within our own facilities, with the exception of work that involved transfection with β actin eGFP constructs, which was carried out using Professor Mike Whites live imagine confocal microscopy facilities (University of Liverpool). The human β actin eGFP construct was a kind gift from the laboratories of Professor Ballestrem and Professor Imhof (Department of Pathology, Centre Medical Universitaire, Geneva, Switzerland).

2.2 Bovine Eye Dissection

Bovine eyes were collected from a local abattoir and transported back to our laboratories within three hours of the animal's death. The globes were cleaned of excess tissue, and were then soaked in an antibiotic solution prior to dissection.

Each globe was cut in half, and the lens was removed from the anterior segment in a sterile hood. This segment was then further dissected into quadrunts, and each quadrunt was positioned with the cornea facing down. A small section of each quadrunt was taken prior to meshwork extraction (to allow examination of chamber angle) and after extraction (to determine if the meshwork was fully removed). The iris was then reflected (pulled backwards along itself) carefully, so as not to tear the meshwork, resulting in the full chamber angle being exposed.

The bovine trabecular meshwork is heavily pigmented, and is easy to identify and relatively easy to dissect – even without a dissecting microscope, and removing the meshwork is easier in the bovine eye than in the human eye, but good quality, ultra fine forceps are required for successful extraction, during which the meshwork is carefully held at one end and then pulled out by gently pulling the tissue back on itself. Strips of meshwork served as explants for primary culture, they were also used for whole meshwork tissue culture work.

2.3 Primary Cell & Tissue Culture and Routine Actin Visualisation

Cells for experimentation were grown up in ventilated tissue culture flasks, however cells to be used for experimental runs were grown in lab-tek (Nunc) culture systems – which are glass (or plastic) slides on which various numbers of growing chambers are secured. These chambers may be filled with 0.2 to 0.8ml of culture medium – or test reagent, and have a lid to prevent contamination and slow evaporation. After required

experimentation time has elapsed, the cells can be washed, fixed and stained within the chamber. The wells are then removed and the cells can be cover slipped in the usual manner.

For tissue culture, meshwork strips were removed and carefully placed into each well of a 6 well plate which already contained 2ml of warmed Dulbecco's modified eagles medium (DMEM) fortified with 10% foetal calf serum (FCS), 2mM glutamine, 100U/ml penicillin, 100μg/ml streptomycin and fungizone (2.5 μg/ml amphotericin) (All from Life Technologies, Scotland). These were incubated under standard conditions (37°C, 5% CO_2) for a period of days with media carefully replaced every day. All strips were carefully monitored under the microscope for any sign of infection, any showing even possible infection were immediately discarded.

After desired experimental time, tissue strips were washed in three changes of phosphate buffered saline (PBS). They were then fixed by agitating them in 10% formalin for 5 minutes before being stored in a fridge (4C) for 12 hours before they were again washed in three changes of PBS before they were re-stored or used.

For primary cell culture, strips were removed and carefully placed into the bottom of a 25cm^2 ventilated tissue culture flasks. It was important to ensure that the tissue strip adhered to the bottom of the flask (and did not float) otherwise the cells would not migrate out of it.

A small quantity (5ml) of 37°C DMEM (fortified as described above) was carefully (so as not to disturb the strip) pipetted into the flask. The strips were then incubated for several days (all strips were again subjected to daily examination so that any strips with signs of infection were discarded) and media was changed daily.

After sufficient cells had moved from the tissue onto the bottom of the flask, the strip was removed, the media was changed, and the cells were cultured until confluence. After this was achieved, the cells were trypsinized and split in a 1:4 ratio into larger $75cm^2$ flasks. These cells were again grown up to confluence after which they were split into four further flasks and grown up. At confluence half of the flasks were trypsinized (0.25% trypsin and 0.02% EDTA) and spun down before freezing in a 10% dimethyl sulphoxide (DMSO) 90% culture medium suspension. The cells in the remaining flasks were split and grown further. These cells have many melanin grunules in their cytoplasm early in culture. These diminish with each passage however, and have usually disappeared entirely by the 3^{rd} or 4^{th} passage (Grierson, et al. 1985).

To visualise the actin once these cells were fixed, they were subjected to Phalloidin (Wulfe et al, 1979) and Propidium Iodide staining. Phalloidin is a phallotoxin derived from the poisonous death cap (amanita phalloides) mushroom; it binds selectively to F actin (Low and Weiland, 1974; Wulf et al, 1979). Phalloidin binds at the junction of the two actin subunits, as this area is not usually associated with any actin binding proteins most of the F actin in cells is available for phalloidin labelling (Barden et al, 1987; Faulstich et al, 1993). In living cells, this binding is irreversible, and prevents actin depolymerising, which can lead to cell (and organism) death.

Phalloidin bound to a fluorescent conjugate has been used by numerous researchers to demonstrate actin in formalin fixed tissue. The majority of the experiments undertaken in this thesis utilised Alexa Fluor 488-Phalloidin (Invitrogen). This Conjugate binds to actin as previously mentioned, it is excited by light with a wavelength of 495nm (blue light) under the fluorescent microscope and it emits "green" light at a wavelength of approximately 519nm.

Propidium Iodide is a non specific (in that it stains both RNA and DNA) intercalating nucleic acid stain. It is excited with light with a wavelength of 488nm, it emits red light that can be detected at 562-588nm.

Because of the differences in the excitation / emission spectrum of Alexa-488 phalloidin and Propidium Iodide, it is possible to combine both of these stains on one slide so that it is possible to capture and image of the actin and the nucleus of the same cell (albeit by taking and combining two images).

Phalloidin & Propidium Iodide staining protocol

Cells were washed in three changes of PBS. They were then stained with a solution of Alexa-488 Phalloidin (20-25µl/ml) in PBS with 0.1% Tween-20 for 45-60 minutes (cells) or overnight (minimally 12 hours) for whole meshwork strips. After this the cells/tissues were again washed in 3 changes of PBS and then stained with a Propidium Iodide/PBS solution (5µl/ml) for 5 – 10 minutes (cells) or up to 1 hour (meshwork strips). After the allotted time, the cells/tissue were washed in 3 changes of PBS and then mounted using a fluorescent mounting media (DAKO cytomation, UK). Cells were kept covered during staining to limit exposure to light as light fades the fluorescent stain, as did exposure to the excitation lights during microscopy.

Microscopy

Routine qualitative evaluation was performed by conventional fluorescence microscopy using a Nikon Optiphot microscope. More detailed analysis on fixed phalloidin stained cells was carried out using a MRC-600 confocal laser scanning microscopy imaging system (Bio-Rad UK). Confocal imaging of cells transfected

with our human β-actin eGFP was carried out using a Zeiss Axiovert confocal microscope.

2.4 Human Cell Lines

Two transformed cell lines (TM3 and TM5) kindly provided by Alcon Laboratories, Fort Worth, TX (Pang et al, 1984) were used during this work. The TM3 cells were derived from a 72 year old donor who had medically controlled POAG at the time of death. The TM5 cells were derived from an 18 year old donor who had no recorded history of eye disease. The transformation of these cells has been described by Pang et al (1984). Various other non transformed human lines were also examined early in this work.

2.5 Dexamethasone (DEX) Treatment

During the initial dose / response studies cells were allowed to become confluent. The controls were then treated with vehicle (0.1% ethanol) while the experimental groups were exposed to 10^{-9}M, 10^{-8}M or 10^{-7}M DEX for up to 10 days, with medium changes every other day. Time response investigations continued DEX treatment up to day 14. All experiments were repeated minimally three times, and all experimental runs were performed in low serum conditions (0.5%) or with no serum present.

All cells used for experimental runs were less than 8^{th} passage, except for the cells used in the experiments that examined CLAN formation in multiple passage cells (25^{th} passage in this case). This work confirmed earlier work by (Grierson et al, 1985) who found that these cells had diminished growth, but that indicators of senility (cytoplasmic vacuolation, multiple nuclei) were not commonly observed.

Previous work (Clark et al, 1994) has shown that a concentration of 10^{-7}M DEX is optimal for CLAN formation in a wide range of human cell lines.

To generate the correct concentration of DEX for these experiments DEX was purchased (Sigma-Aldrich) in powdered form. The required amount was dissolved in pure ethanol to create a 1mM solution. A quantity of this was then further diluted in cell culture media to achieve the desired working concentration.

2.6 Aqueous Humor Experiments

Aqueous humor was extracted from freshly obtained eyes in the manner described by (Hogg et al, 1995). The eyes used for aqueous extraction were different to those used for other experiments, as removal of aqueous can cause the chamber angle to collapse. Using a dissecting microscope 500 to 800µl of aqueous was removed using a 1ml syringe and a short 25 gauge needle. The aqueous was discarded if the anterior chamber deformed during extraction or if the aqueous was discoloured. Care was also taken to position the needle with the bevel upwards, well clear of the iris to avoid touching it and contaminating the sample.

After collection the aqueous was either used immediately, or was stored at -80C until required. Comparisons were made between fresh and frozen aqueous with regard to their respective CLAN inducing abilities.

For time course and concentration experiments the aqueous humor was diluted in DMEM alone or in DMEM plus FCS. The bovine cells were exposed to neat (unaltered, undiluted natural aqueous) aqueous or dilutions of aqueous for up to 1 week. The appearance of the cells during aqueous treatment was carefully monitored for any signs of degeneration and any sign of apoptosis was noted.

A number of preliminary studies were undertaken to try to determine what constituent(s) of aqueous might be responsible for the generation of CLANs.

Pooled aqueous was heat denatured at 80C for 10 minutes. Other aliquots of aqueous were subjected to pH change by the addition of either 0.1M NaOH or HCl to alter the pH of the aqueous to either pH 3 or 11. This alteration was maintained for no longer than 45 minutes, as described previously (Joseph et al, 1989) and was neutralised by the addition of acid / alkali.

Further samples of aqueous humor were subjected to ultrafiltration. As there was no data or identified causal constituent two very broad filters were used. Aqueous samples were placed in either a 5,000 or a 30,000 Dalton (molecular weight cut off) ultra filter centrifugal tube (Amicon US). Aqueous was loaded into the top chamber of these tubes. The top was screwed on, and the tube was then spun at approximately 1,200 rpm. Centrifugal force pulls the aqueous through the filter. Any constituents larger than the filter size are prevented from passing through the filter into the bottom collecting chamber and are caught within the pores of the filter.

2.7 TGFβ2 Treatment

Previous studies have shown that there is an up regulation of endogenous TGFβ2 in the eyes of POAG patients (Min et al, 2006; Stephan et al, 2008). We wished to examine the effect of TGFβ2 on our bovine and human CLAN producing cells, and to determine its effect on CLANs (if any).

Cells were seeded and grown to confluence as for other experimental conditions, and at the start of the experimental run the desired concentration of TGFβ2 (Sigma) 1, 5 or 10ng/ml was added to the culture media. The initial experiments run for three days

as I have good information regarding the levels of CLANs induced at this time with and without a number of inducing agents.

Once the optimum concentration of TGFβ2 had been established a longer run was set up to determine what level of CLAN expression would be reached over time.

2.8 Experiments to Determine the Level of Apoptosis in Dexamethasone Treated Cells

Bovine meshwork cells were grown for 3 days in the presence of 10^{-7}M dexamethasone. After this time the media was changed to one without dexamethasone, but with 5µl per ml propidium iodide. The cells were allowed to incubate in this media at room temperature before they were washed and fixed using 10% neutral buffered formaldehyde. The cells were then stained with phalloidin in the usual manner and were allowed to dry over night in the refrigerator before they were imaged the following day.

Images were collected using blue light (phalloidin image) and then green light (propidium iodide image). As the propidium iodide was added to the cells while they were still alive, only cells whose nuclei were compromised would take up the stain (healthy cells exclude propidium iodide). By this method it was hoped that it would be possible to identify CLANs and be able to tell if they were associated with apoptotic nuclei (or not).

2.9 Experiments in living Cells

As previously stated, all work on CLANs to date has been undertaken retrospectively, that is to say that cells are examined after they have been treated and fixed. CLANs are dynamic structures; and the ability to observe them form in living cells would be

useful and tell us much about CLAN formation, however first it was necessary to determine if it was possible to image CLANs forming in living meshwork cells. To this end, staining of the actin in these cells using a human β actin construct (a kind gift from the laboratories of B. Imhof, Geneva) was undertaken (fig: 11).

The visualisation of CLANs in living cells had up to the start of this work, not been achieved by any research group. It is a difficult procedure because of the unpredictability of CLAN formation in any given cell. The following outlines my attempts to do so.

Figure 11: Human β Actin-eGFP Plasmid Map

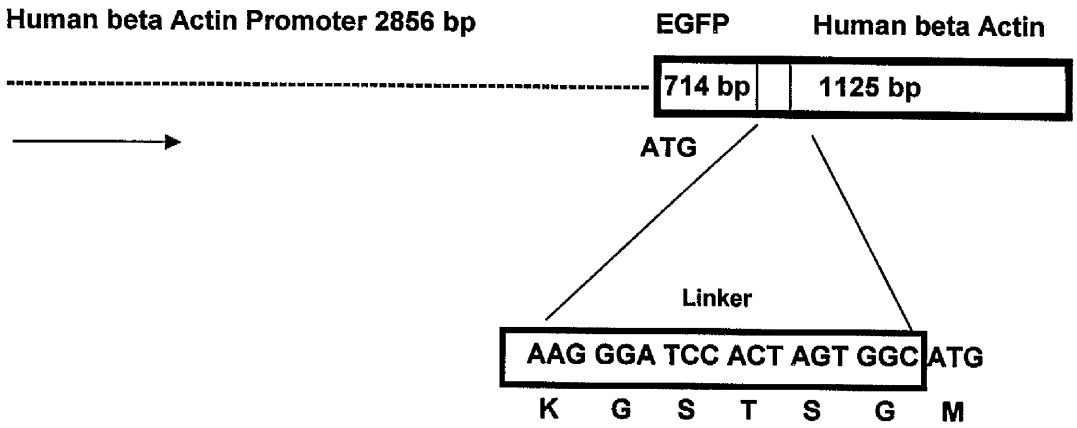

Simplified diagrammatic representation of the Human beta-Actin eGFP plasmid used during the live cell imaging work.

2.9.1 Transfection of Competent Bacterial Cells

Competent *E.Coli* (DH5α) bacteria were taken from our laboratories frozen stock. To create a single colony of competent cells for use in transfection, a single streak from this stock was scraped across the surface of an agar plate using a previously flamed inoculation loop. The plate(s) were then incubated over night at 37°C before being examined the next day for colonies.

A single colony was picked (using a sterile yellow pipette tip) and agitated into 10ml of LB medium in a universal container. This was again allowed to grow in the incubator over night until a large quantity of competent bacteria was obtained. The following day these cells were span down and were re suspended for use or for freezing. 50µl aliquot of these cells was added to a 1.5ml tube on ice. 20 – 30ng of plasmid DNA was added to this tube gently, the tube being gently flicked to mix the contents. These cells were then placed on ice for 30 minutes before being heat shocked in a water bath set to approximately 42°C for 90 seconds prior to being returned to ice for a further 2 minutes. Following this 350µl of SOC medium was added to the tube(s) using best practice aseptic technique, after which the media was incubated for a further 90 minutes with agitation.

The bacteria were then streaked out onto LB plates containing appropriate antibiotics and were again incubated over night. Bacteria that had not taken up the plasmid, (which conferred antibiotic resistance to the antibiotic in the plate media) were dead. Bacteria that had taken up the plasmid had grown into colonies. It was these colonies that could be picked for further work.

For the next stage I utilised a Qiagen mini-plasmid prep kit. The procedure followed was as outlined in the handbook. Following this procedure I was left with an amount

of pure plasmid DNA which was eluted into 50µl of distilled H_20. Each sample was examined spectroscopically so that the quantity of DNA (µg/ml or ng/µl) could be determined. For this plasmid, 2 minipreps were selected.

1) mean absorbance = 0.02: (50 x mean absorbance (A_{260}) x 100 = 100µg/ml)
2) mean absorbance = 0.03: (50 x mean absorbance (A_{260}) x 100 = 150µg/ml)

The plasmid mini-prep was then subjected to restriction endonuclease digestion and agarose gel electrophoresis and full sequencing.

2.9.2 Restriction Enzyme Digest and Agarose Gel Electrophoresis

The human β actin e-GFP plasmid contained 9,200bp (of which the human β actin ORF comprised 1,200bp, and the eGFP ORF comprised 500bp). It also contained three restriction nuclease cutting sites for EcoR1, BamH1 and HINDIII.

Samples were prepared as follows:

Sample 1	**A**	**B**	**C**
Plasmid (µl)	10	10	10
Buffer (µl)	2	2	2
Enzyme(s) (µl)	2(EcoR1)	2(EcoR1+BamHI)	2(EcoR1+HINDIII)
Water (µl)	6	4	4
Total Volume	20	20	20

Sample 2	**A**	**B**	**C**
Plasmid (µl)	6.7	6.7	6.7
Buffer (µl)	2	2	2
Enzyme(s) (µl)	2(EcoR1)	2(EcoR1+BamHI)	2(EcoR1+HINDIII)

Water (µl)	9.3	7.3	7.3
Total Volume	20	20	20

The above samples were prepared in small PCR tubes. Samples were heated in the PCR machine to 37°C for 90 minutes. After this time the temperature was increased to 65C for 10 minutes before they were transferred to a 1.5ml eppendorf tube after which 0.1 volume of sodium acetate pH 5.2 (2µl) and 2 x Volume of 95% alcohol (samples are now 22 µl = 44 µl) were added and mixed in by gently flicking the tube, then quickly spinning the tubes in a centrifuge before allowing them to stand at room temperature for 1 hour. Following the allotted time, 100µl of 70% alcohol was added to each tube and each tube was again flicked before they were spun at 13,000 rcf for 15 minutes. Once a pellet was formed the alcohol was carefully pipetted off, and the tubes were allowed to air dry. Once the tubes appeared dry, 20µl of distilled water was added to each tube – fluid was gently pipetted in and tubes were pulsed in a centrifuge – the opposite way to the previous spin, to re suspend the pellet. Tubes were then stored at -20°C over night.

The three digests of this plasmid were run on a 0.8% Agarose electrophoresis gel

That was made up by adding 0.8g of agarose to 100ml of 0.5% TBE. The solution was then mixed by swirling before it was heated in a microwave for 3 minutes. 2µl of ethidium bromide was then added and it was swirled again to mix. This solution was then poured into a pre-prepared mould and allowed to set (30 minutes).

All samples to be run on the gel had 5µl of bromophenol blue loading buffer added to them. The markers were prepared by taking the required volume of marker (1µl) and adding 9µl of water and 5µl of loading buffer. For this work a 100bp and 1kb marker was chosen to be run at the same time as the markers. The samples were run at 120 volts until the markers could be seen to be two/thirds of the length of the gel.

Given the map that came with the plasmid, we were expecting to find the following Bands on the gel:

1) EcoR1 only – 1 band expected on the gel at 9,200
2) EcoR1 + BamHI – 1 band expected on the gel at 1,200 + another at 8,000
3) EcoR1 + HINDIII – 1 band expected on the gel at 1,700 + another at 7,500

The gel is shown in Fig.12.

0.8% Agarose gel of human beta Actin-gfp

- Lane 1 100 bp Marker
- Lane 2 ECORI-expect 1 band / 9,200 bp
- Lane 3 EcoRI + BamHI expect 2 bands 1,200/800 bp
- Lane 4 EcoRI + HINDIII expect 2 Bands 1,700 + 750
- Lane 5 ECORI-expect 1 band 9/200 bp
- Lane 6 ECORI + BamHI/2 bands 1,200bp + 8,000 bp
- Lane 7 ECORI + Hind III / 2 bands 1,700 + 7,500 bp
- Lane 8 1kb DNA Marker

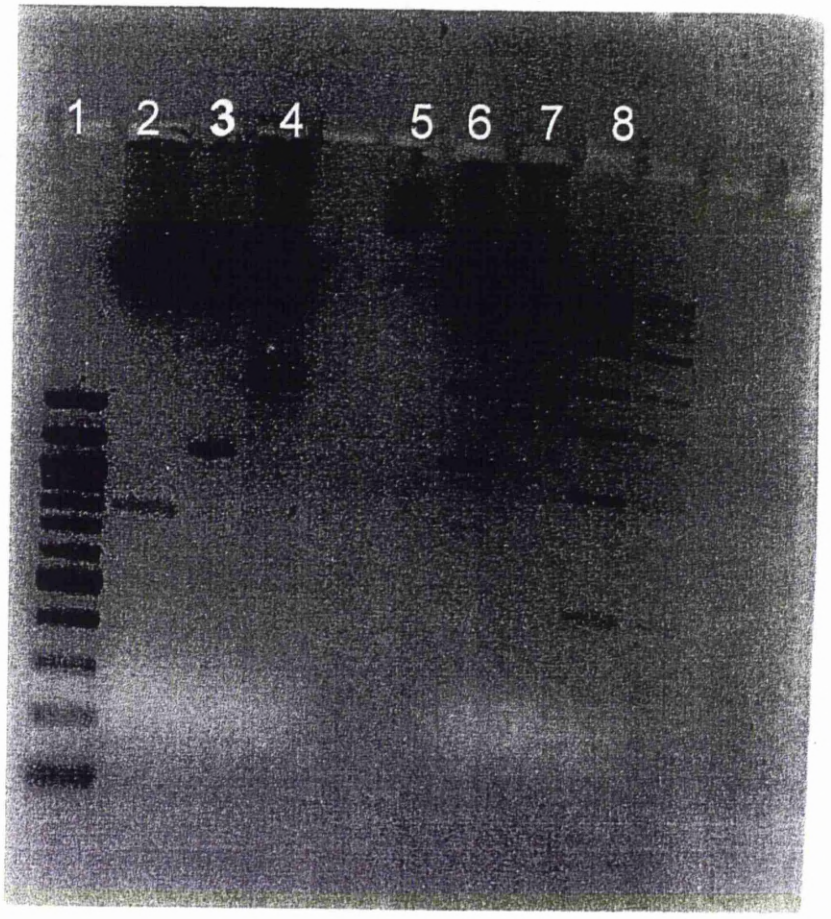

Figure 12: Restriction Enzyme Digest of the human-β Actin-eGFP Plasmid

Nikki Wade 14/07/2006

2.9.3 Plasmid Sequencing

To further substantiate the results from the gel, it was decided that the plasmid should be genomically sequenced. Primers were designed and purchased from (MWG, UK). The 3 Primers were as follows:

1) F1 – C C A G C C A T G T A C G T T
2) R1 – A A C G T A C A T G G C T G G
3) R2 – G C G G C G A T A T C A T C A T

The F1 (Forward – 5` to 3`) Primer motif would allow the plasmid to be sequenced from the start of the eGFP sequence moving into the actin sequence. R1/2 (Reverse – 3` to 5`) Primers were designed to allow sequencing from the end of the actin sequence back through toward the eGFP sequence.

Plasmid and primers were sent to Geneservice (Nottingham, UK) for sequencing.

The sequencing confirmed that we did have the full eGFP and actin sequences. The Actin primer had the full length human promoter. These sequences were compared to the bovine sequences. We found that the (amino acid) sequence homology was 100%.

Bovine beta actin amino acid sequence:

>P60712-1 (uniprot identifier)

MDDDIAALVVDNGSGMCKAGFAGDDAPRAVFPSIVGRPRHQGVMVGMGQK

DSYVGDEAQSKRGILTLKYPIEHGIVTNWDDMEKIWHHTFYNELRVAPEEHP

VLLTEAPLNPKANREKMTQIMFETFNTPAMYVAIQAVLSLYASGRTTGIVMD

SGDGVTHTVPIYEGYALPHAILRLDLAGRDLTDYLMKILTERGYSFTTTAEREI

VRDIKEKLCYVALDFEQEMATAASSSSLEKSYELPDGQVITIGNERFRCPEALF

QPSFLGMESCGIHETTFNSIMKCDVDIRKDLYANTVLSGGTTMYPGIADRMQ

KEITALAPSTMKIKIIAPPERKYSVWIGGSILASLSTFQQMWISKQEYDESGPSI

VHRKCF

Human beta actin amino acid sequence:

>P60709-1(uniprot identifier)

MDDDIAALVVDNGSGMCKAGFAGDDAPRAVFPSIVGRPRHQGVMVGMGQK

DSYVGDEAQSKRGILTLKYPIEHGIVTNWDDMEKIWHHTFYNELRVAPEEHP

VLLTEAPLNPKANREKMTQIMFETFNTPAMYVAIQAVLSLYASGRTTGIVMD

SGDGVTHTVPIYEGYALPHAILRLDLAGRDLTDYLMKILTERGYSFTTTAEREI

VRDIKEKLCYVALDFEQEMATAASSSSLEKSYELPDGQVITIGNERFRCPEALF

QPSFLGMESCGIHETTFNSIMKCDVDIRKDLYANTVLSGGTTMYPGIADRMQ

KEITALAPSTMKIKIIAPPERKYSVWIGGSILASLSTFQQMWISKQEYDESGPSI

VHRKCF

Sequence Comparison Using ClustalW

```
P60712-1    MDDDIAALVVDNGSGMCKAGFAGDDAPRAVFPSIVGRPRHQGVMVGMGQKDSYVGDEAQS
60

P60709-1    MDDDIAALVVDNGSGMCKAGFAGDDAPRAVFPSIVGRPRHQGVMVGMGQKDSYVGDEAQS
60

            ************************************************************

P60712-1    KRGILTLKYPIEHGIVTNWDDMEKIWHHTFYNELRVAPEEHPVLLTEAPLNPKANREKMT
120

P60709-1    KRGILTLKYPIEHGIVTNWDDMEKIWHHTFYNELRVAPEEHPVLLTEAPLNPKANREKMT
120

            ************************************************************

P60712-1    QIMFETFNTPAMYVAIQAVLSLYASGRTTGIVMDSGDGVTHTVPIYEGYALPHAILRLDL
180

P60709-1    QIMFETFNTPAMYVAIQAVLSLYASGRTTGIVMDSGDGVTHTVPIYEGYALPHAILRLDL
180

            ************************************************************

P60712-1    AGRDLTDYLMKILTERGYSFTTTAEREIVRDIKEKLCYVALDFEQEMATAASSSSLEKSY
240
```

```
P60709-1    AGRDLTDYLMKILTERGYSFTTTAEREIVRDIKEKLCYVALDFEQEMATAASSSSLEKSY
240

            ************************************************************

P60712-1    ELPDGQVITIGNERFRCPEALFQPSFLGMESCGIHETTFNSIMKCDVDIRKDLYANTVLS
300

P60709-1    ELPDGQVITIGNERFRCPEALFQPSFLGMESCGIHETTFNSIMKCDVDIRKDLYANTVLS
300

            ************************************************************

P60712-1    GGTTMYPGIADRMQKEITALAPSTMKIKIIAPPERKYSVWIGGSILASLSTFQQMWISKQ
360

P60709-1    GGTTMYPGIADRMQKEITALAPSTMKIKIIAPPERKYSVWIGGSILASLSTFQQMWISKQ
360

            ************************************************************

P60712-1    EYDESGPSIVHRKCF  375

P60709-1    EYDESGPSIVHRKCF  375

            ***************
```

2.9.4 Plasmid Maxi-prep

After sequencing confirmed that the plasmid did in fact contain the correct sequences, a maxi prep was made. A flask containing 200ml of LB broth (previously autoclaved) containing antibiotic had a picked colony added to it and was shaken (gently) over night at 37°C. The following day, the suspension was centrifuged to pellet the bacteria. A Qiagen maxi prep kit was then used to produce a larger volume of plasmid DNA in the following way.

Buffer P1 (10ml) was added to the pellet to re-suspend it. To this, 10ml of buffer P2 was added. This was gently mixed and allowed to incubate for 5 minutes at room temperature. Ice cold buffer P3 (again, 10ml) was added, the tubes were mixed by gentle inversion, and then placed on ice for 20 minutes.

After allotted time the solution was again spun to form a pellet. During the spin the Qiagen 500 column was primed by the addition of 10ml of QBT buffer, which was allowed to run through. After the centrifugal run had finished, the supernatant was

removed and added to a 50ml falcon tube. The supernatant was then run through the column, followed by 30ml of buffer QC.

DNA was then eluted from the tube by the addition of 2 x 5ml of buffer QF. The eluate was caught in a clean plastic centrifuge tube. DNA was precipitated by the addition of 7ml of 4C isopropanol. This was then span, the supernatant removed and 5ml of 70% alcohol was added before the sample was again spun, the alcohol removed and the sample allowed to air dry. Once dry, the pellet was re suspended in 500µl of distilled water. DNA was quantified and calculated to be 20ng/µl.

2.9.5 Transfection Protocol

For transfection into human cells the transfection reagent Fugene 6 (Roche) was selected. The first trials of transfection were carried out using Hela cells – because of their fast doubling time, and previous experience with these cells and fugene 6, which also has a high transfection efficiency rate and is reported to have been successfully in over 600 cell types (data sheet). The protocol followed was that recommended within the reagent data sheet.

Two days before transfection cells were selected and transferred into an Iwaki plate (a small dish that has a clear central region suitable for imaging through using an inverted microscope).

For optimisation of the level of fugene 6: DNA, three small sterile tubes were taken and labelled with 3:1, 3:6 and 6:1 and 97µl of serum/additive free media was added to the first two tubes and 94µl was added to the last tube. Taking extreme caution to not touch the plastic of the tubes, 3µl of Fugene were added directly into the media in the first two tubes while 6µl were added to the last tube. All tubes were then gently flicked to encourage mixing of the contents, and were left to stand at room

temperature for 5 minutes after which appropriate quantities of plasmid DNA were added (1μg, 2μg and 6μg). The tubes were again gently flicked and left to stand at room temperature for 30 minutes (data sheet recommends 5 to 45 minutes).

The fugene/DNA solution was added to the cells in the Iwaki plates "dropwise" as carefully as possible dispersed over the entire plate. The plates were then incubated over night or up to 48 hours depending on the transfection efficiency in each cell line.

2.9.6 Image Collection and Analysis

Images were collected on a Zeiss Axiovert fluorescent confocal microscope. The entire dish was observed and cells that showed clear bright stress fibre staining were marked for tracking over time by clicking on the centre of each cell (the co-ordinates of which were then remembered by the imaging program).

There was a balance between the number of cells (fields of view) that could be followed and the elapsed time between each image. The program worked by moving from one cell to the next in the order in which they were selected. If too many cells were selected the time between images would be longer and it was felt important images could be missed (it being that no data exists that details the length of time it takes for the stress fibre pattern to dissolve and the CLAN organisation to appear).

The single images were concatenated into a movie for each field of view at the end of the imaging run. Each movie was then carefully examined and pertinent data were extracted.

As the equipment used for this work was borrowed, and given that each run would last minimally 12 hours, I was limited in the number of times we could run these experiments. I managed however to undertake sufficient runs for some very interesting preliminary conclusions to be made.

3.0 Results

3.1 Initial Investigations into the CLAN forming potential of Bovine Meshwork Cells

3.1.1 CLAN Incidence and Morphology

Description of CLANs and qualitative results

Initial studies proved that dexamethasone did consistently induce CLANs in bovine meshwork cells from confluent cultures after several days' dexamethasone exposure (Fig 17).

For the work within this thesis, stringent CLAN identification and counting techniques were developed. To be included as a CLAN a structure had to have (minimally) 5 "hubs" and 3 triangulated arrangements of actin "spokes" (Fig 13).

This rigorous definition was adopted so that structures that were not CLANs would not be included in the counts (type 1 error). There were many more small structures present in the cells and tissues that did not meet these criteria and so the CLAN counts and numbers given here are very likely to be low estimates of CLAN numbers in the bovine meshwork cell population.

In well spread cultures of bovine (and human) meshwork cells, from sparse culture to confluence, the predominant F-actin arrangement was an abundance of stress fibres along the long axis of the cell. These varied in size from 10 to 30μm, and had a thickness of 0.2 to 1μm.

Polygonal actin structures were also a common finding in the meshwork cells in both untreated and treated cells. There was no discernable difference in the types, numbers or architectural arrangements between both species studied. However, in the absence of dexamethasone, but in the presence of serum, bovine meshwork cells produced many more CLANs than human cells did.

The "hubs" of these structures were usually stained more brightly than the spokes, and were therefore easier to identify and image (Fig 15).

There was considerable heterogenicity in the size and over all shape of these structures, but the polygonal structure remained a common feature of even the largest CLAN in both human and bovine cells. A CLAN was considered to be large if it contained 20 or more hubs. Large CLANs were far more common after treatment with dexamethasone, whereas only small CLANs were found in untreated cells. In treated cells large CLANs in adjacent cells sometimes appeared to connect to each other (in that it was difficult to tell where one ended and another began). There was no disturbance in the geodesic arrangement where these CLANs in adjacent cells appeared to be joined together (Fig 15).

Figure 13: Different Types of CLANs in Bovine Meshwork Cells Treated with Dexamethasone

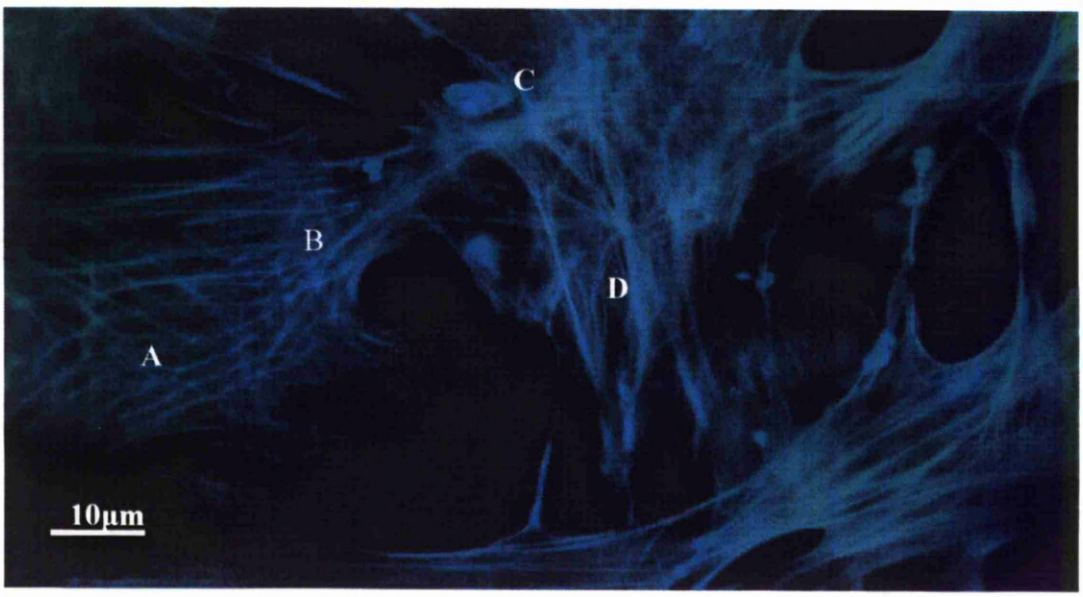

Different CLAN types in 10^{-7}M dexamethasone treated, phalloidin stained bovine meshwork cells. A basket type, B geodesic, C network, D starburst.

Figure 14: Outline of Minimum Criteria for Inclusion in CLAN Counts

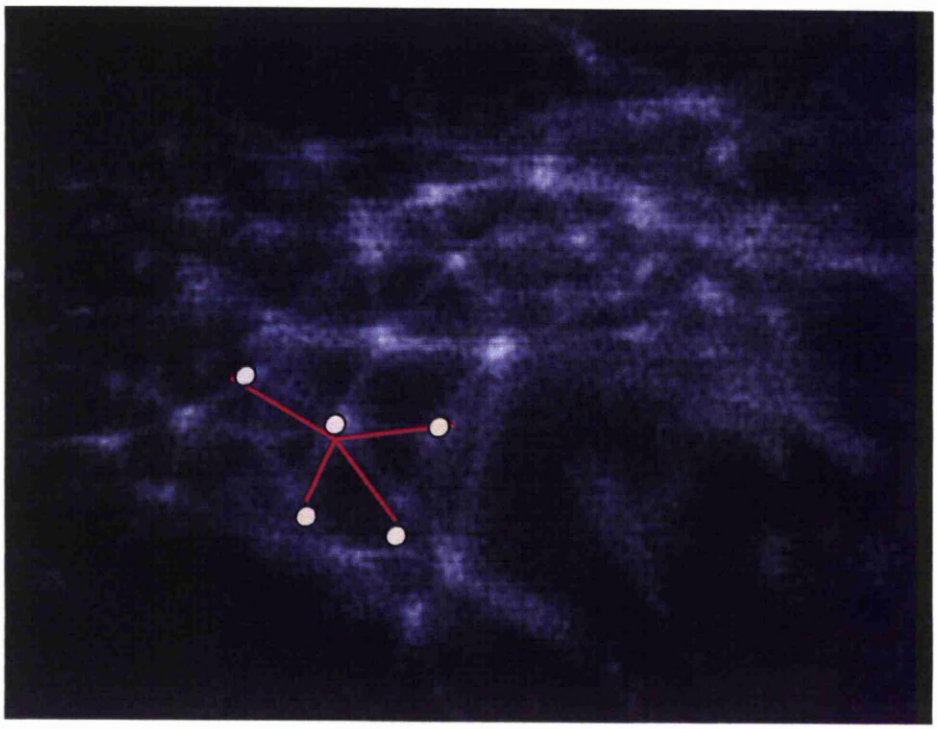

Highly magnified image of a CLAN with the minimal inclusion criteria superimposed on it. This image contains 5 hubs (yellow) and 4 spokes (red). This image shows a dexamethasone treated bovine meshwork cell which was imaged on Biorad confocal microscope using oil; a x60 lens and a digital zoom of 2.

Large and smaller CLANs formed flattened domes (as determined by z series – or sequential – imaging which could take as few as 1 or 2 sections or as many as 32). CLANs were found commonly over the nucleus, but were also found at the periphery of the cell. Domes were not the only structures observed. In sparse or pre-confluent cultures it was common to see "ring" or "basket-like" arrangements (Fig 13). Some of these arrangements could be quite large (Fig 16).

Other non geodesic arrangements of actin were frequently identified. Such structures were termed clan-like structures, and these while noted were not included in any of the counts.

3.1.2 Dexamethasone induced CLAN formation

Bovine Cells

The bovine cells were grown and harvested in media containing 10% serum. The majority of studies however where conducted in greatly reduced or absent serum.

Based on time lapse imaging, PI staining and Ki67 staining, reducing serum to 0.5% after confluence was reached had no observable adverse effect on viability over a 7 day period.

Confluent cultures of bovine cells when placed into media containing no serum media had very little or no evidence of nuclear changes or degeneration after 7 days (assessed by propidium iodide and annexin V staining).

Figure 15: CLANs in Bovine Meshwork Cells Treated With Dexamethasone

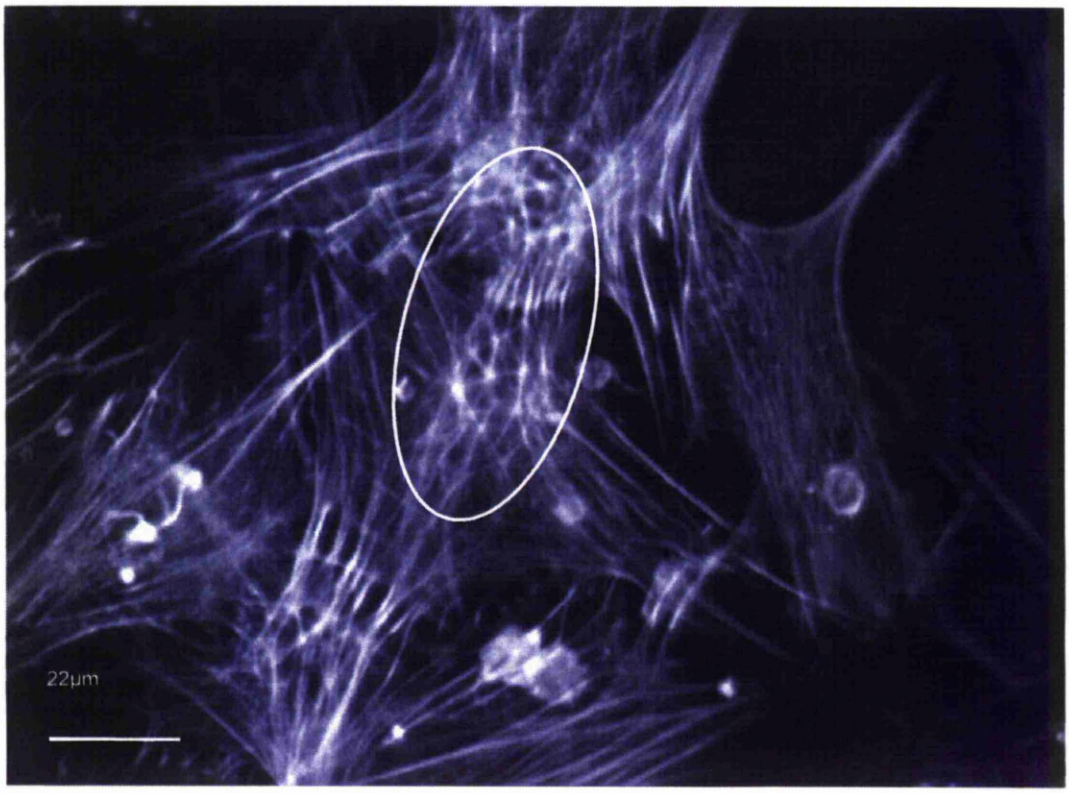

Image shows dexamethasone treated bovine meshwork cells stained with Alexa 488 phalloidin. The encircled area delineates an area where the CLAN of one cell appears to be joined up with, or linked to the CLAN in an adjacent cell.

Figure 16: Non-Geodesic CLAN Arrangement in Dexamethasone Treated Bovine Meshwork Cells

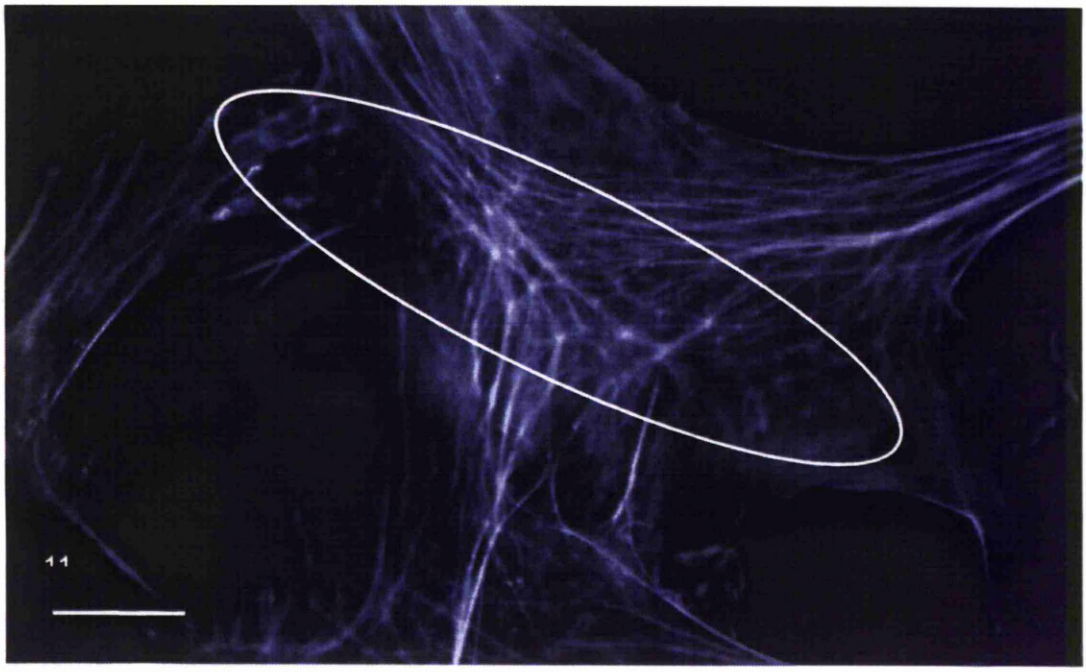

A confocal image of Alexa-488 Phalloidin (green) and Propidium Iodide (red) stained bovine meshwork cells. Area outlined shows an alternative CLAN-like structure that shows a hub and spoke arrangement that is non geodesic.

The effect of dexamethasone on CLAN formation was investigated in a time and dose dependant manner (Fig 17 and 18). Culturing cells with 10^{-7}M dexamethasone consistently produced the highest numbers of CLANs. Exposure to concentrations of less than this produced less CLANs and the cells cultured with 10^{-9} M dexamethasone contained no more CLANs than the control (vehicle only) cells (Fig. 18).

By extending the time course experiments to 14 days and utilising 10^{-7}M dexamethasone (with media replacement occurring every second day) the incidence of CLANs in the bovine cells usually reached 50% (Fig 17).

The incidence of CLANs in the control cells increased over time to approximately 10% after 14 days (Fig 17). This upward trend reached statistical significance (students t test $P<0.05$) in some, but not all experimental runs. Overall there was a 5-fold increase in the levels of CLAN formation in bovine cells exposed to 10^{-7}M dexamethasone for 14 days. This was a consistent finding for all the cultures that were examined.

Figure 17: CLAN Incidence over Time in Dexamethasone or Vehicle Treated Bovine Meshwork Cells

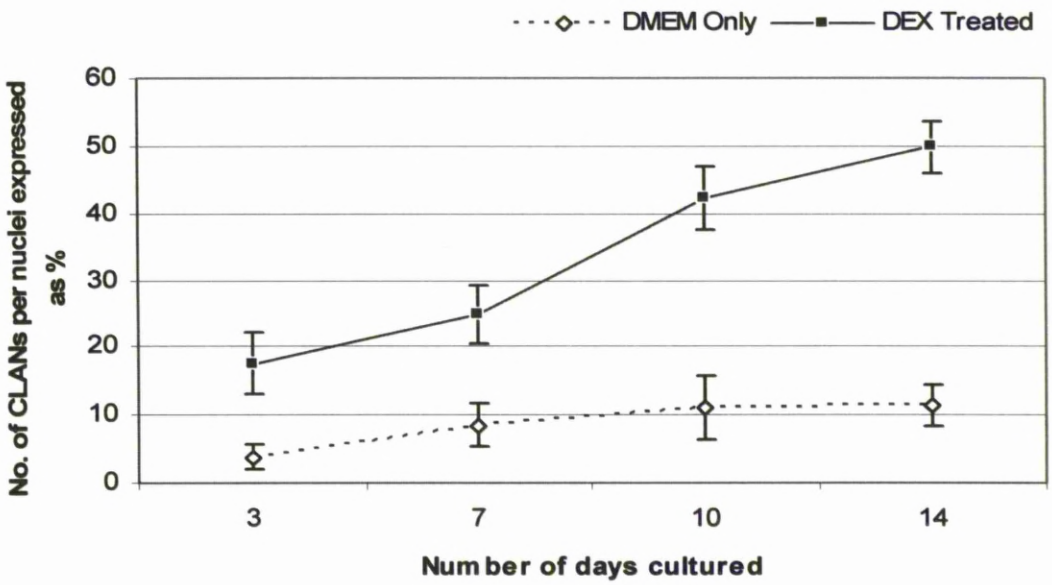

Data from experiments that shows the increase in CLAN numbers over time in bovine meshwork cells cultured with or without dexamethasone. There is a significant difference between the two data sets even by day 3 (Students t test, $P>0.005$) which continues to broaden over the experimental time period. Error bars are +/- 1 standard deviation.

Figure 18: Dexamethasone Dose Response in Bovine Meshwork Cells

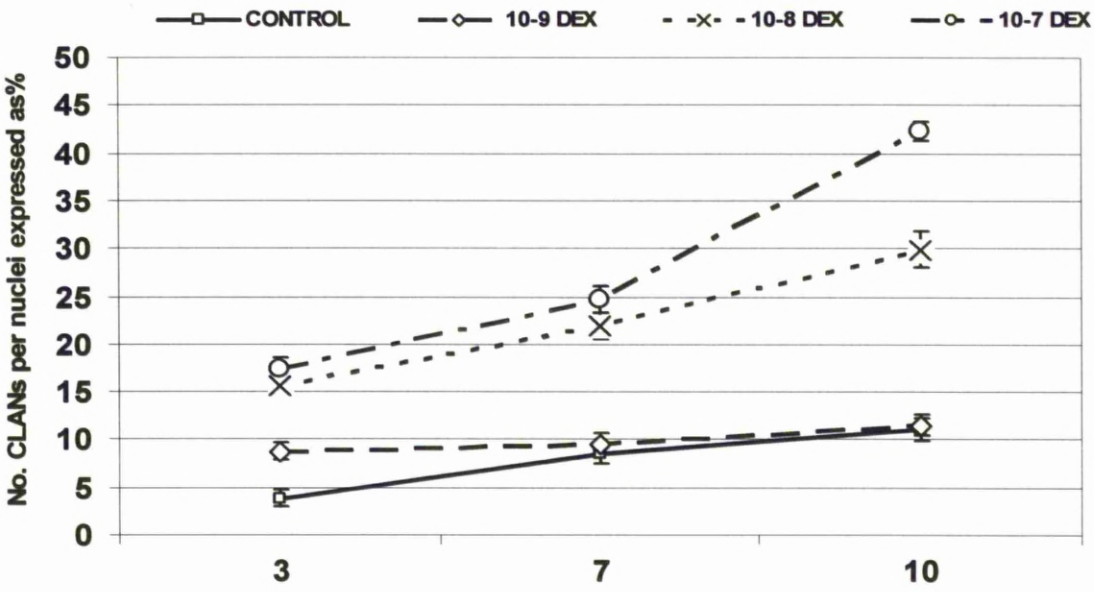

Data from experiments that show CLAN formation in bovine meshwork cells over time with differing concentrations of dexamethasone. The most concentrated solution (10^{-7}M dexamethasone) produced the greatest number of CLANs which reached statistical significance by day 10 (Students t test, $P<0.005$). Error bars are +/- 1 standard deviation.

3.1.3 Effect of Passage Number on CLAN Formation

To determine whether or not the passage number influences the incidence of CLANs an experiment was run during which regularly used passage number cells (3 to 8) were compared to high passage number cells (20 – 25). The high passage cells for this work had a slowing in the cell division rate, but there was little evidence of senescence (vacuolation, multi nucleate, enlarged cells). Cells were purposefully grown up to these high passage numbers for this work, cells of this age are not generally found in the cell bank in this laboratory.

This experiment determined that CLAN induced by dexamethasone still form in very high passage number cells, and that the level of CLANs in high passage number cells is statistically indistinguishable from those found in the low passage number cells that are used routinely (Fig 19).

Figure 19: Effect of Passage Number on Bovine Meshwork Cell CLAN Formation

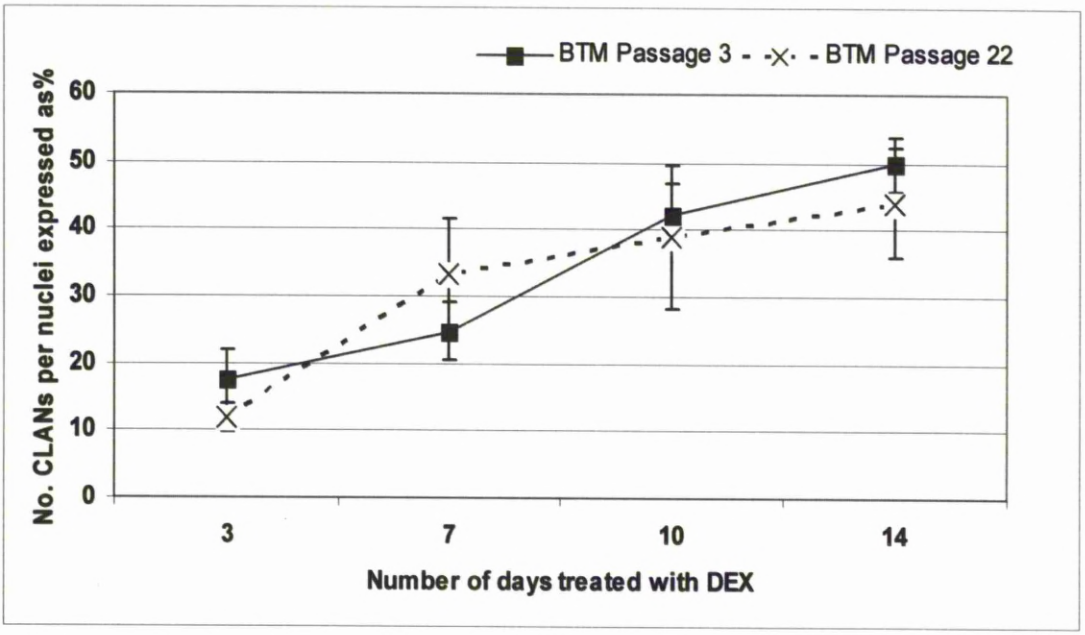

Data from experiments aimed at determining the effect of age (passage number) on CLAN formation in bovine trabecular meshwork cells. There is no statistical difference in the numbers of CLANs generated between passage 3 and passage 22 cells at any of the time points examined (students t test, P=1.000).

3.1.4 CLAN Half Life

For as long as there was a dexamethasone stimulus in the media, bovine cells were associated with high numbers of CLANs, and so CLANs appeared to be a permanent feature of steroid treated cultures. To determine if there was a wash out effect, or a lessening of CLAN numbers once the dexamethasone stimulus was withdrawn, cells were grown for 14 days in 10^{-7}M dexamethasone. After this time the dexamethasone containing media was replaced with normal media. Cells were fixed at set time points and the incidence of CLANs at each point was calculated. These experiments showed that there is a wash out effect, but in bovine cells the incidence of CLANs that were treated with dexamethasone remained statistically higher than in cells that had never been treated for 7 to 10 days after dexamethasone removal (Students t test $P<0.05$). The half life for CLANs in bovine meshwork cells following the removal of dexamethasone stimulus was determined to be 2.5 days (Fig 20).

Figure 20: CLAN Half Life in Human and Bovine Meshwork Cells

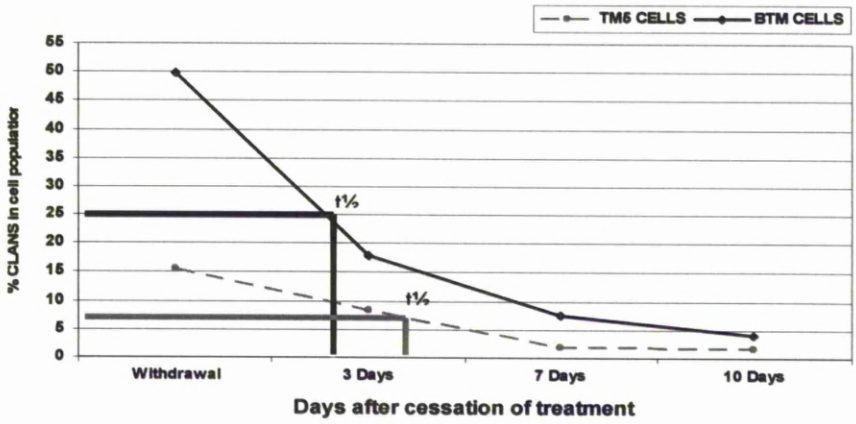

Data from a series of experiments (n = 4) aimed at discovering if there was a "wash out" effect in both human and bovine meshwork cells (a lessening of CLANs in the cell population after the removal of the dexamethasone stimulus). The half life for CLAN survival post stimulus withdrawal is approximately 2.5 days in bovine cells and approximately 3.5 days in human cell lines following the withdrawal of 10^{-7}M dexamethasone.

3.1.5 Human Trabecular Meshwork Cells

Several human trabecular meshwork cell lines were used as comparisons for the bovine cells (it was felt that this was important because the most commonly used cell type in CLAN research at the start of this work was human cells).

After 14 days in 10^{-7}M media the three human cell lines had an overall CLAN prevalence of 16% $\pm$ 4% compared to 49.8% $\pm$ 3.93 % for the bovine cells (Fig 21). The incidence of CLANs (post dexamethasone treatment) was very similar between the human and bovine meshwork cells. However there was a difference in the baseline levels of CLANs with the human cells containing 4% while the bovine cells on average had 10% CLANs in non treated cells.

CLAN induction in human cells was much more variable than in bovine cells. Different human cell lines produced different levels of CLANs. The immortalisation of human cell lines apparently had a negative effect on the CLAN forming capabilities of these cells. During this work, HTM3 and HTM5 cells have a variable, but relatively poor CLAN response when compared to non immortalised primary human cells (Fig 22).

The half life of dexamethasone induced CLANs in human cells was a little greater than in the bovine cells at 3.5 days (Fig 20).

Figure 21: CLAN Formation in Dexamethasone Treated Human Cell Lines Compared to Bovine Meshwork Cells

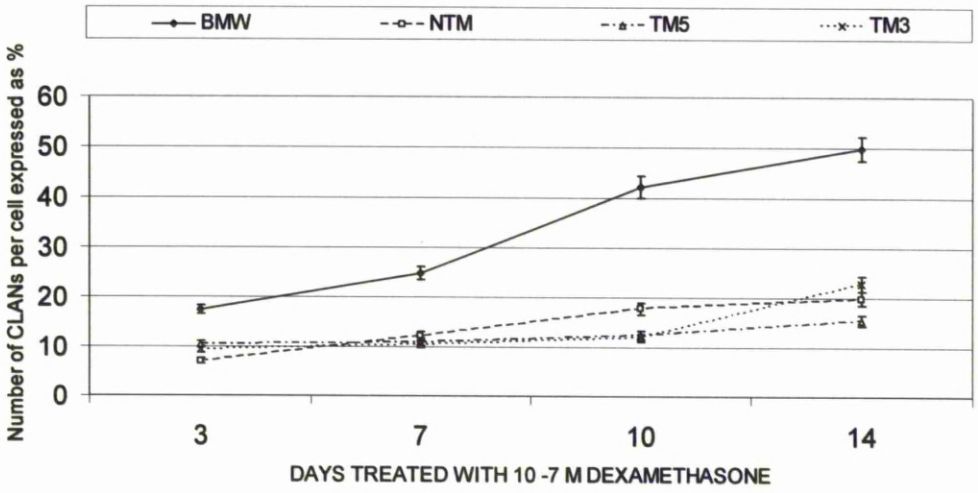

Graph depicting the outcome of several experiments performed to determine how well CLAN formation in bovine meshwork cells compares to that in human cell lines after treatment with 10^{-7}M dexamethasone. It was found that the bovine cells formed far more CLANs than any of the transformed human cells tested, all of which had a similar, if somewhat variable CLAN forming ability.

Figure 22: CLAN Formation in Human Cell Lines, Primary Human Cells and Bovine Meshwork Cells

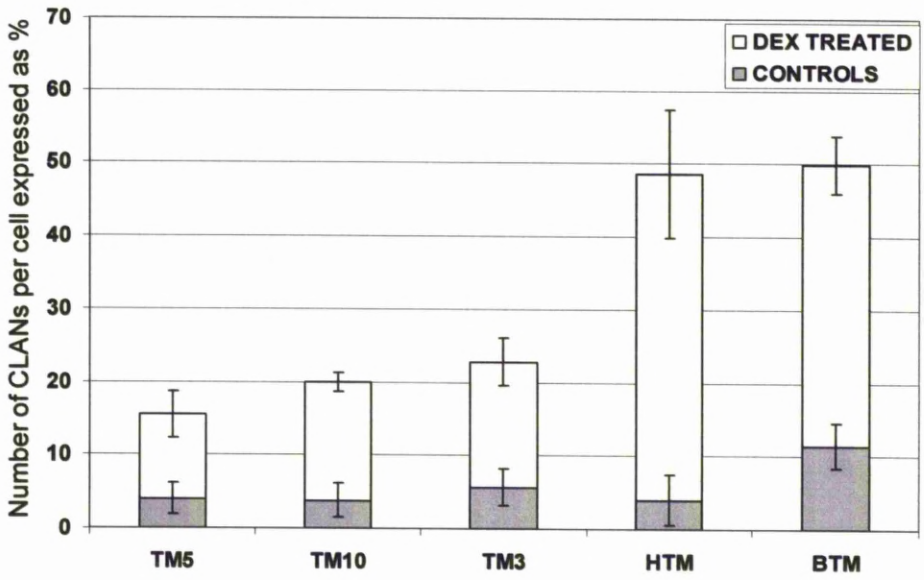

Graph depicting the outcome of several experiments (n = 5) performed to determine how well bovine trabecular meshwork cells compare to transformed human cell lines and non transformed human cells after exposure to 10-7M dexamethasone for 14 days. Transformed cell lines behaved similarly with a somewhat variable CLAN formation rate, while non transformed human cells produced many more CLANs per cell which equalled that found in the bovine cells.

3.1.6 CLANs in Organ Cultured Bovine Meshwork

As previously mentioned, the bovine meshwork is not as well organised as the human trabecular meshwork. Orientation and localisation were somewhat difficult during confocal examination because of this lack of obvious landmarks. In addition to this, the bovine meshwork had a very pronounced autofluorescence which made identification of the actin fluorescence difficult.

There was however a graduation of intracellular pigment between the different zones. The cells in the trabecular zone were relatively sparse and heavily pigmented. The cells of the reticular zone had some pigment and the cells in the area analogous to the juxta-cannilicular region were comparatively pigment free.

The dominant cytoskeletal actin organisation in the bovine meshwork tissue was a very prominent stress fibre arrangement than run parallel with the long axis of the cells (Fig 23). They were usually 0.25 to 0.5μm in diameter although they could be as thick as 1μm. They were usually between 5 to 30μm long but could run the entire long axis of the cell. These stress fibres were seen in all areas of the bovine meshwork tissue, however the smallest most numerous stress fibres were found in the cells of the innermost bovine meshwork ("JCT" region). The size decrease in the actin stress fibres was the only actin associated difference that distinguished cells in this region from those elsewhere in the meshwork. There was also a diffuse actin staining pattern that occurred sporadically throughout the meshwork.

Following exposure to dexamethasone for three days in our tissue culture system, elongated stress fibres were far less common. The actin in the tissue became far less organised with speckles, bundles, knots and tangles of relatively small actin fibrillar fragments that appeared to have no particular orientation. Even in masked quantitative

studies it was relatively easy to distinguish treated from non treated tissue because of the vast difference in the actin arrangement (Fig 24).

Polygonal actin arrangements that we considered to be CLANS were identified in the bovine meshwork tissue both with and without dexamethasone treatment (Fig 25). CLANs were difficult to find in the tissue, as compared to in the cell cultures. The difficulties in the tissue involved the autofluorescence and the complex three dimensional arrangements of the cells which were orientated in many different planes. It was possible to identify CLANs in the meshwork tissues we examined, however it was more difficult in tissue that had been treated with dexamethasone because of the above mentioned changes in the actin patterns.

Nevertheless, qualitative studies suggested that CLANs were more numerous in dexamethasone treated tissue than in non treated control tissue however there were no changes in CLAN complexity or size associated with 72 hours dexamethasone exposure, CLANs rarely involved more than 15 hubs (and associated spokes). Throughout the tissue there were areas where clusters of CLANs were found. There seemed to be no distinguishing features in these areas (other than the presence of more CLANs than average).

Figure 23: Bovine Meshwork Tissue Fixed Without Dexamethasone Treatment

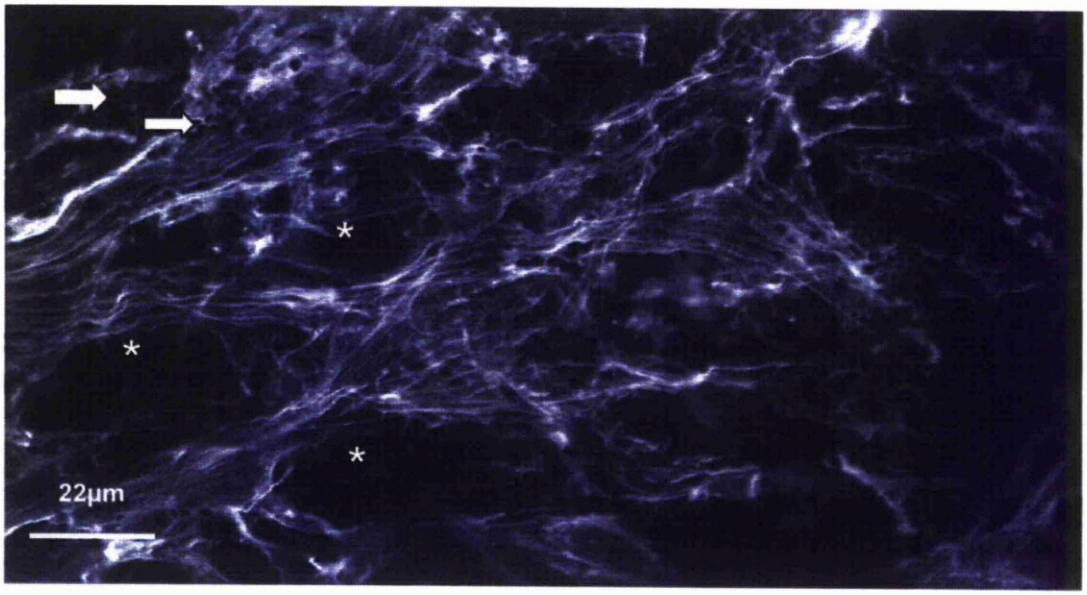

Confocal microscopic views of bovine meshwork tissue (without dexamethasone treatment) stained with phalloidin to demonstrate F actin distribution. Inter trabecular spaces (*) can be clearly seen and many stress fibres are clearly stained and visible. There are many melanin granules present within this freshly dissected tissue (arrows).

Figure 24: Bovine Meshwork Tissue after Treatment with Dexamethasone for 24 Hours

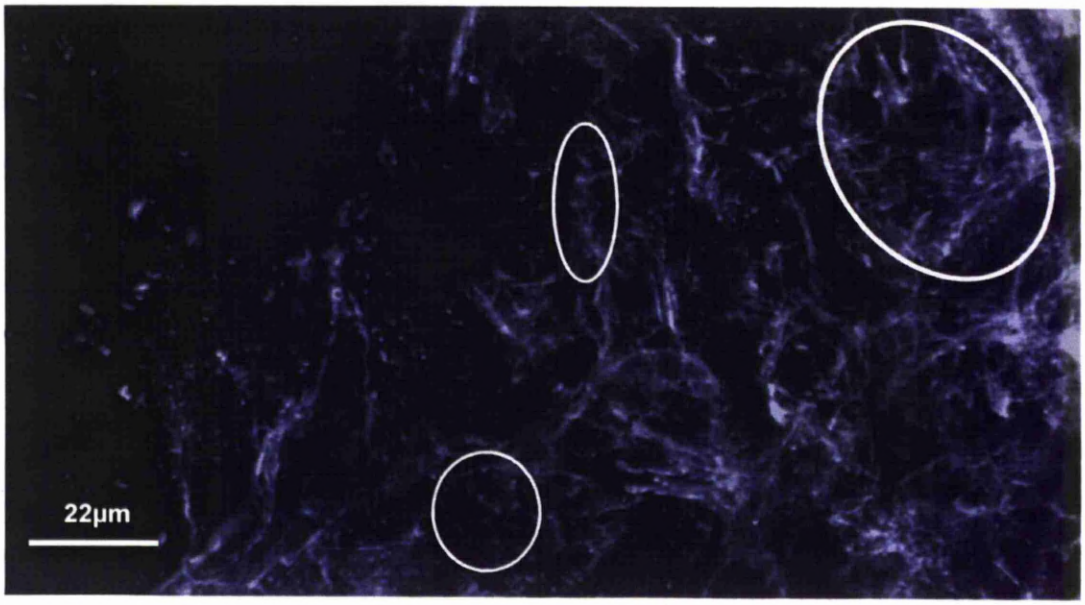

A confocal microscopic view of a highly cellular area of bovine meshwork tissue after exposure to dexamethasone for 24 hours. Brightly stained areas that are geodesically arranged, and therefore likely to be "hub" components of CLANs can be seen (circled) however the associated "spokes" are not so clearly identifiable.

Figure 25: Bovine Meshwork Tissue after Dexamethasone Treatment for 72 Hours

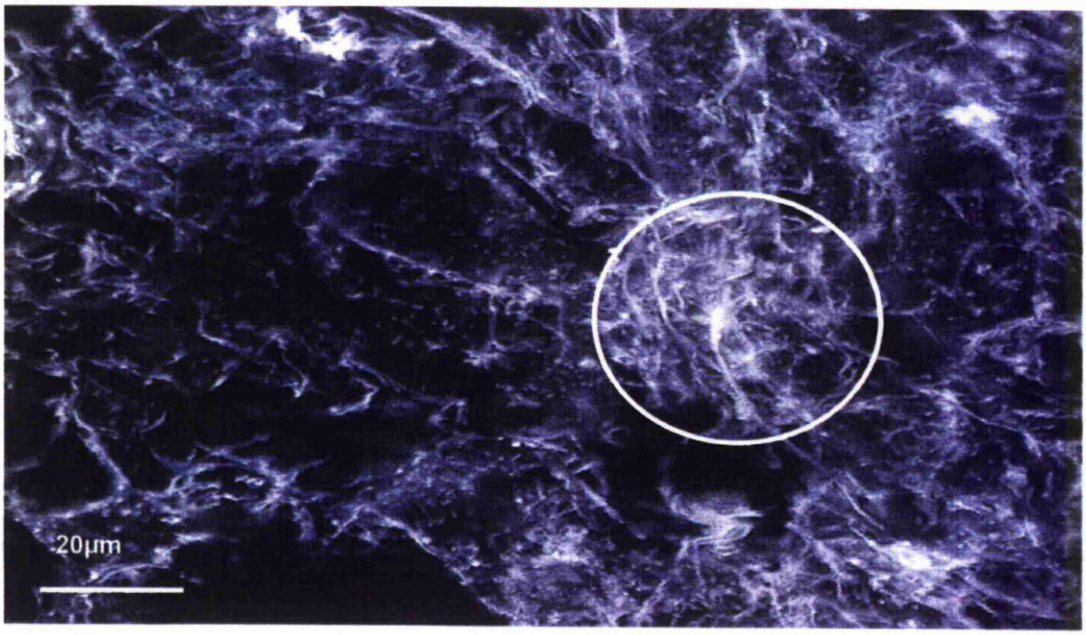

Bovine meshwork tissue stained with phalloidin following exposure to dexamethasone (10^{-7}M) for 72 hours. The normal actin distribution pattern has been severely disrupted, and the stress fibre pattern seen clearly in Figure 23 is no longer discernable. Numerous actin tangles and some polygonal actin arrangements were visible (circled). Inter trabecular spaces are also no longer as clear in other images.

3.1.7 Experiments to Identify Apoptosis in dexamethasone Treated Cells

Bovine meshwork cells (with or without serum) exposed to 10^{-7} M dexamethasone for 7 days showed a very low level of apoptosis. The propidium iodide applied before the cells were fixed was able to enter the nuclei of apoptotic cells because their nuclear envelopes had become porous (while the healthy cells were able to exclude it). It was extremely rare for any cells to show apoptotic features. Occasional cells showed senescent features, such as being multi nucleate (Fig 26 and 27).

The actin images showed that CLANs were not present in the cells that were undergoing apoptosis. In contrast, some of the cells that appeared to have CLANs (or CLAN-like structures) had no propidium iodide present in their nuclei (Fig 27).

Because no nuclear stain was used post fixation it was not possible to determine the exact number of cells present per image. However this issue was resolved by taking a large number of images (n = 200) and calculating a number of apoptosis positive images. Of all the randomly taken images only 3 showed any propidium iodide staining. If we accept that there is (minimally) 3 cells in any given image, then the level of apoptosis in these dexamethasone treated cells would be less than 1%. This was no different from the control cells that were grown identically but with vehicle in place of dexamethasone.

Figure 26: Investigations into Apoptosis in CLAN Containing Bovine Meshwork Cells

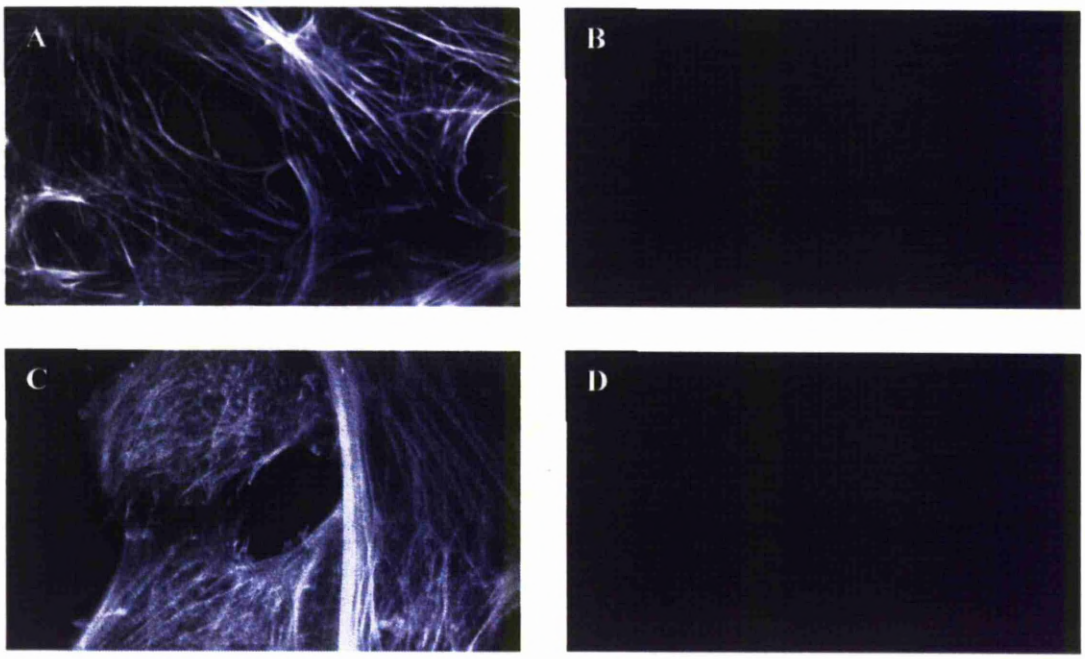

A: bovine meshwork cells stained with phalloidin after culture with 10^{-7} M dexamethasone for 7 days. Prominent stress fibres are the predominant actin pattern in this image.

B: image of the same cells using 536mm wavelength light which makes propidium iodide visible. There has clearly been no uptake of propidium iodide; therefore the cells in this image are viable.

C: another area similarly treated cells. This image has captured some altered actin patterns, but the cells appear other wise healthy.

D: the lack of anything visible in this image (which was again taken using a wavelength of light that would excite propidium iodide) shows that there are no apoptotic (or necrotic / senescent) cells in this image.

Figure 27: Nuclear Changes in Dexamethasone Treated Bovine Meshwork Cells

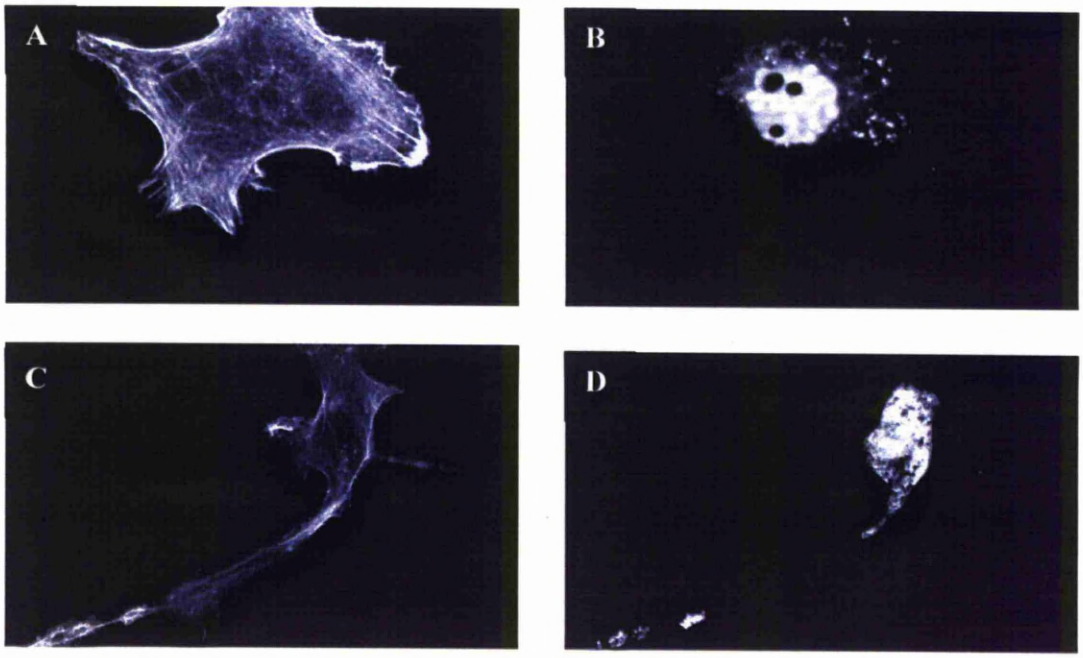

Propidium iodide stained cells after treatment with dexamethasone. (A) Does not appear to be apoptotic from the phalloidin image (B) The enlarged size of this cell and the nuclear vacuolation would suggest that this cell is probably senescent, not apoptotic. The cell in (C) was imaged toward the edge of the lab-tek. There are no CLANs or CLAN-like structures in this image. The propidium iodide image (D) shows no defined nucleus. This cell may or may not be apoptotic it is hard to be certain with this image.

3.2 Experiments to Identify in vivo CLAN Inducing Agents

3.2.1 Effect of bovine aqueous humor on morphology

Bovine meshwork cells exposed to 10, 50 and 100% aqueous humor (diluted with DMEM without serum) for 3 or 7 days had no obvious degenerative effects on the morphology of cells (observed by phase microscopy) or the nuclei (observed via propidium iodide staining), There was no cytoplasmic vacuolation or nuclear enlargement and very little apoptosis. Occasional binucleate and large cells were occasionally seen, but these were also seen in early cultures maintained in standard medium.

Confluent bovine cells became more epithelioid and rounded after exposure to undiluted aqueous, but they remained well spread at 7 days. After this time more cells were larger than usual when they were maintained in undiluted (100%) or in aqueous diluted with DMEM (50%), but no change was seen at lower concentrations or at higher concentrations at 3 days.

3.2.2 Effect of Aqueous on F-Actin Distribution and CLANs

Cultures of bovine meshwork cells were exposed to DMEM, DMEM diluted with 50% by volume aqueous humor or undiluted (100%) aqueous for up to 7 days. These were then examined qualitatively (using Alexa 488 phalloidin staining) and were compared to controls grown in standard DMEM plus serum.

The predominant F-actin pattern was strong stress fibres. No discernable differences between the stress fibres in all the samples were observed.

Polygonal networks made up of hub and spoke arrangements of F-actin were found in cells exposed to 50% aqueous or higher. The number of CLAN positive cells was

limited, but the range and sizes of the CLANs were similar in design to those induced by dexamethasone in both bovine and human cells. CLANs and CLAN-like structures were present in all samples examined, but were only common in the cells treated with undiluted aqueous (Fig 28).

3.2.3 Qualitative Analysis and Aqueous Manipulation Experiments

Quantitative analysis of CLAN numbers after exposure to aqueous for 3 days showed a significant increase over control levels (Students t test $P<0.05$) in all experimental conditions. This increase was more marked in cells grown in 100% aqueous where the CLAN incidence was over 2 times that of the control cells (Fig 28) 9% of the cells having CLANs ($P <0.01$). Further positive control cells treated with dexamethasone for the same amount of time had a CLAN incidence of approximately 17%.

Boiling aliquots aqueous for 10 minutes completely destroys the CLAN forming potential of aqueous humour (Fig 29). Treating aqueous with acid (pH 3) as described in the methods appeared to destroy the CLAN forming potential it possessed, whereas exposure of the aqueous to alkali (pH 11) reduced the CLAN incidence by approximately 50% (Students t test $p<0.05$) (Fig 30). Passing bovine aqueous through a centrifugal ultra filter with a 30,000 kDa cut off had no discernable effect on CLAN formation, but passing the aqueous through an ultra filter with a 5,000 kDa reduced CLAN formation down to background levels. These experiments were repeated four times with the same result (Fig 31).

Figure 28: CLAN Formation in Bovine Meshwork Cells Treated with Different Concentrations of Bovine Aqueous Humor

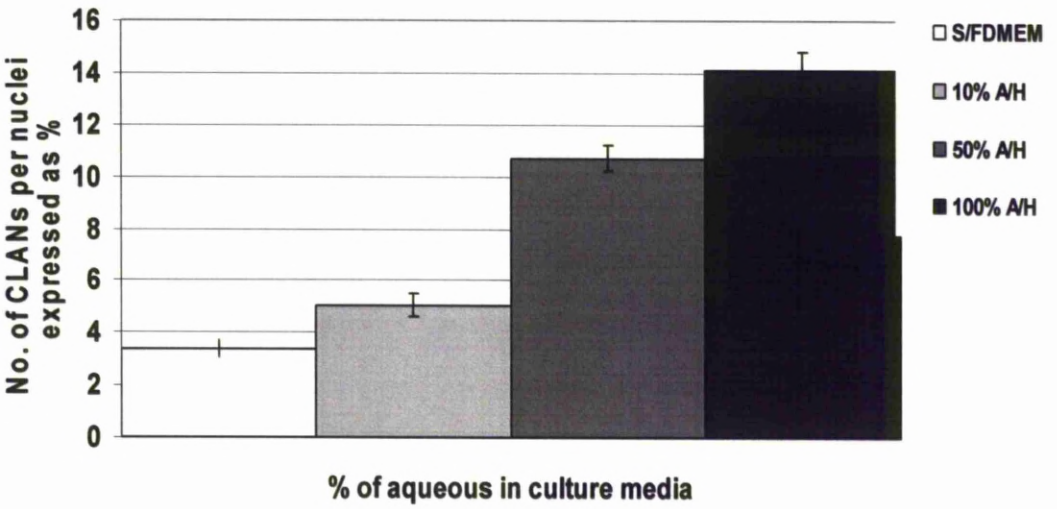

Histogram showing the abundance of CLANs in bovine meshwork cells cultured with aqueous humor or dilutions of aqueous humor and cell culture media (minus additives) For 72 hours. The less diluted the aqueous, the higher the incidence of CLANs that were observed. Error bars are $\pm$ 1 standard deviation.

Figure 29: The Effect of Heat Treatment on the CLAN Forming Capabilities of Bovine Aqueous Humor

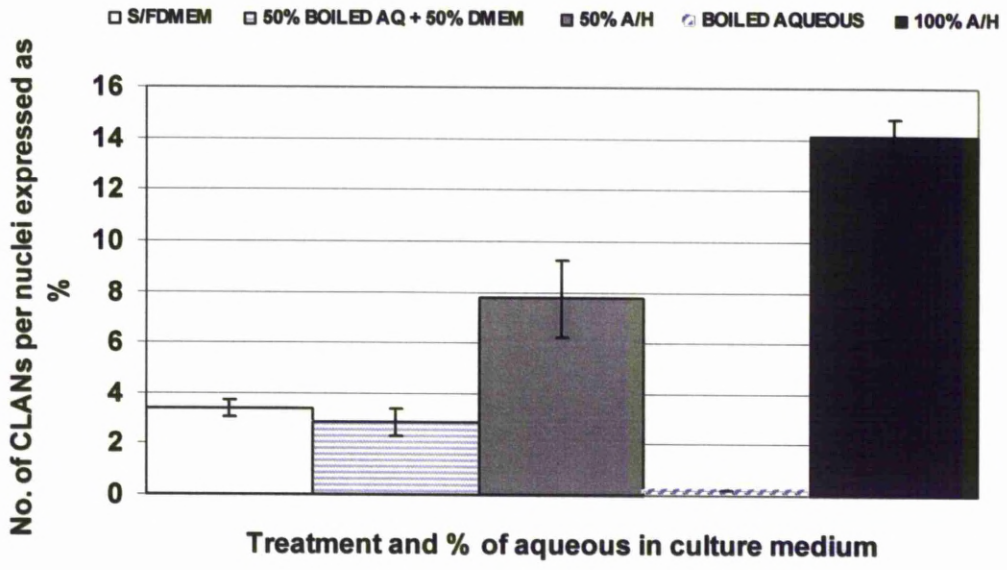

Histogram showing how the heat treatment (boiling) of bovine aqueous humor affects its ability to form CLANs. Boiling the aqueous clearly destroys any CLAN inducing agent within the aqueous which would lead to the assumption that the CLAN inducing agent is denaturable (a protein). Error bars are $\pm$ 1 standard deviation.

Figure 30: The Effect of Acid / Alkali Treatment on the CLAN Forming Capabilities of Bovine Aqueous Humor

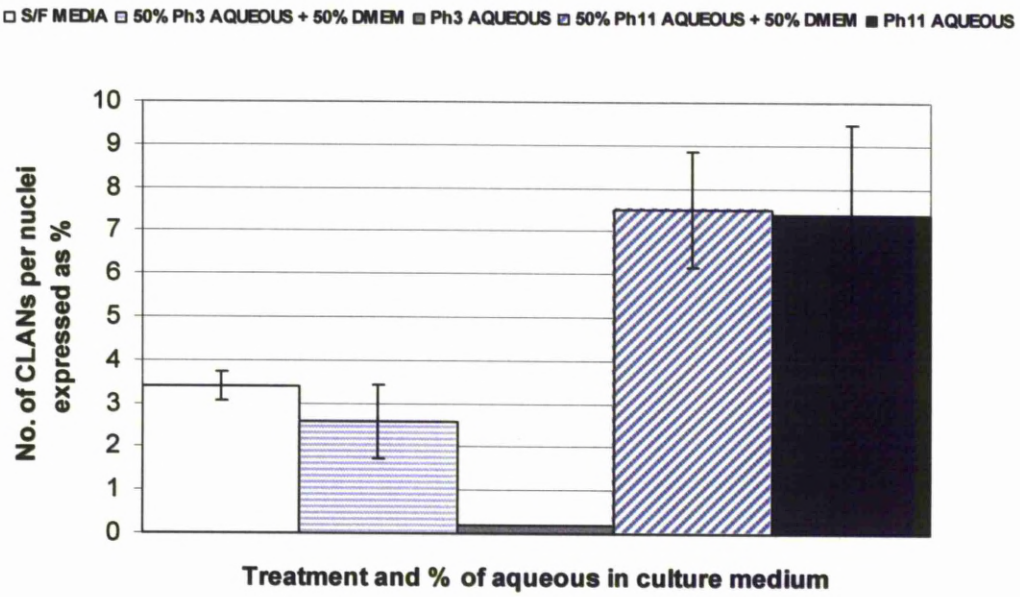

Histogram depicting the effects of altering aqueous humor pH on its CLAN inducing capabilities. The effect of strong alkali treatment appears to be no injurious to CLAN induction, however treatment with strong acid destroys any CLAN forming abilities, which would again suggest that the CLAN inducing agent is a protein. All error bars are $\pm$ 1 standard deviation.

Figure 31: Effect of Micro-filtering on the CLAN Forming Capabilities of Bovine Aqueous Humor

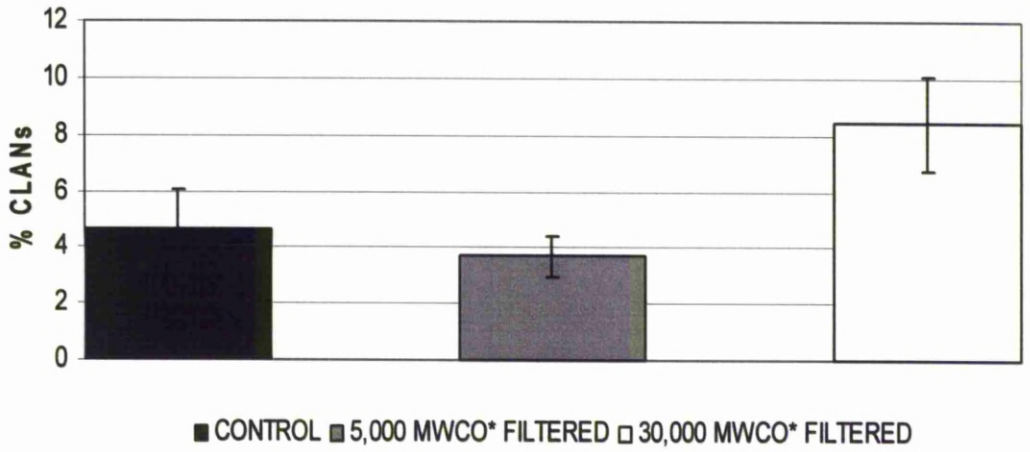

Histogram depicting the effect of filtering aqueous humor with two different centrifugal micro filters. These results indicate that the CLAN inducing agent within the aqueous is removed when the aqueous is passed through the smaller (5,000 molecular weight cut off) filter, but not when it is passed through the larger filter. This could (if the other results are considered) be taken to mean that the CLAN inducing agent in bovine aqueous humor is a small heat / acid denaturable protein. All error bars are $\pm$ 1 standard deviation.

3.2.4 Effect of TGFβ2 on Bovine Meshwork Cells

Given that aqueous humor has an effect on meshwork cells that includes CLAN induction that is greater than that seen in the controls; and given that it is also elevated in the aqueous humor of people with POAG it was decided that the effect of TGFβ2 on bovine cells should be explored. TGFβ2 was also not excluded by the preliminary investigations into the CLAN inducing agent(s) in aqueous humor.

Preliminary studies examined the effect of 1, 5 and 10ng/ml be determined as there was no previous data that had identified the optimum concentration for CLAN provocation.

It was clear very quickly that TGFβ2 had the ability to induce CLANs at a high rate, a higher rate than had been achieved with dexamethasone. There was little difference in CLAN prevalence after 3 days exposure to 1, 5 and 10ng/ml (45, 40 and 42% respectively) (Fig 32). There was however markedly more apoptosis in the cells exposed to 10ng/ml as assessed by propidium iodide staining and microscopy. Subsequent runs were undertaken at 5ng/ml and were extended to 14 days.

The CLANs observed after 14 days were striking and many were large with far more than 20 hubs each, they were mostly geodesic in arrangement but basket-like CLANs were also present, and these could be very large, comprising more than 50 hubs in some cases (Fig 33). Looking down the microscope it was difficult to find a group of cells that did not contain CLANs. The CLANs induced by TGFβ2 were very well formed and the spokes were clear in addition to the hubs.

The level of CLAN induction was surprising. After just 3 days the prevalence of CLAN containing cells in the population had reached 22%, with this increasing to 46% after 5 days, 57% after 7 days and finally reaching 68% by day 14 (Fig 33).

which compared favourably to a dexamethasone control that was run concurrently which produced 15, 22, 43 and 52% CLANs at 3, 7, 10 and 14 days respectively (also shown on fig 33. These experiments were repeated 5 times with the same result.

Figure 32: TGFβ2 Dose Response Data in Bovine Meshwork Cells

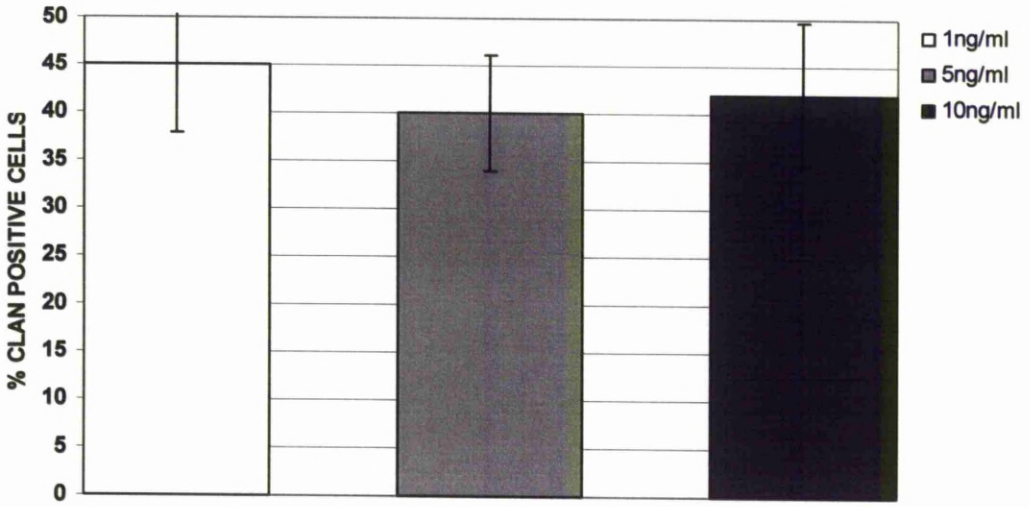

Results for experiments that aimed to determine whether or not TGFbeta2 was able to induce CLANs in bovine meshwork cells. There appeared to be a saturation level with regard to TGFbeta2, as there is no statistical difference between any of the concentrations tested (P = 0.8937). There was considerably more apoptosis in the cells treated with 10ng/ml group when compared to the 1 or 5ng/ml.

Figure 33: large CLAN in TGFβ2 Treated Bovine Meshwork Cell

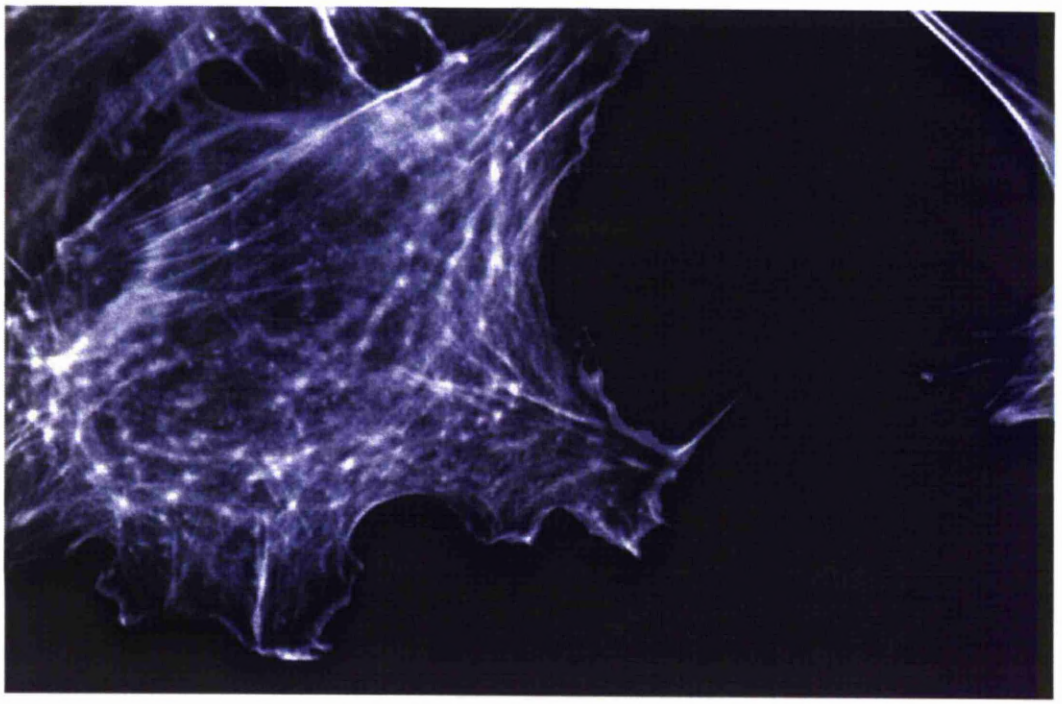

Bovine meshwork cell(s) treated with 5ng/ml TGFbeta2 for 14 days. After this time the cells were well spread but healthy, and they contained very numerous and very large CLANs of different types but predominantly geodesic or basket like. This Cell had at least 64 hub sites. When viewed down the microscope the spokes were more visible but they did not image very well.

Figure 34: Comparison of the CLAN Forming Abilities of TGFβ2 and Dexamethasone

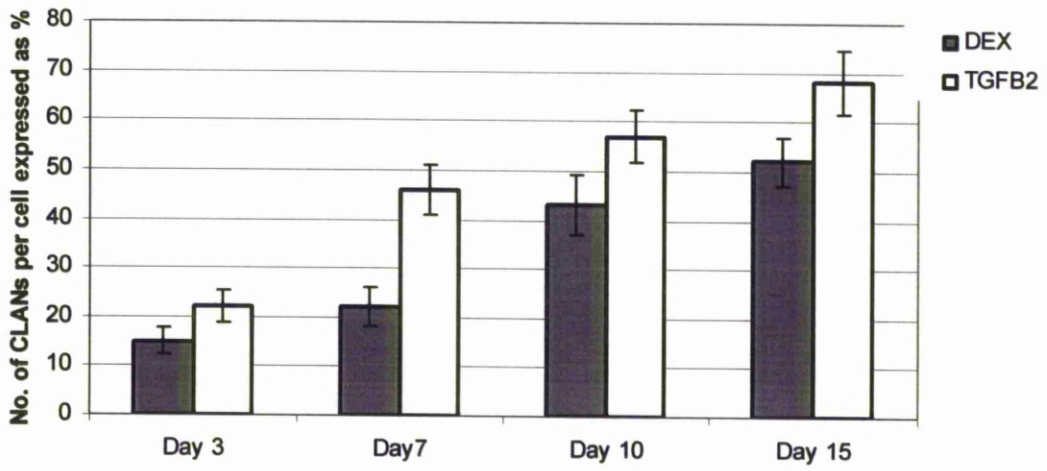

Averaged data from experiments (n = 5) comparing the ability of dexamethasone and TGFbeta2 to produce CLANs in bovine meshwork cells. The TGFbeta2 produced more CLANs than the dexamethasone did, however this difference was not found to be significant overall (P= 0.3007).

3.3 Investigations into CLAN Formation in Live Cells

3.3.1 Initial transfection experiments

Bovine Meshwork Cells

The standard fugene optimisation protocol was followed but after 24 hours there was no visible transfection in the cells. This procedure was repeated many times (n = 8) with the same result, even after 40 – 72 hours there was no visible sign that any of the cells had taken up the plasmid (Figure 39 & 42) The gene sequences were matched, and according to the manufacturer fugene was compatible with bovine cells, and so we could not determine why this might be. To check whether or not there was some problem with the plasmid it was decided that it would be transfected into Hela cells which grow fast and would be a good indicator of any problems with the plasmid.

Hela Cells

Trials of transfection were carried out using an established HeLa cell line with a known doubling time. The Fugene-6 transfection optimisation protocol showed that transfection with this plasmid could result in successful transfection.

The best result was achieved with a cDNA to fugene ratio of 1:6 (fig 41). Above this level and the plasmid was greatly over expressed to the extent that the entire cell was bright green, and visualisation of individual actin patterns was impossible (fig 40).

Figure 35: Non-Transfected bovine Meshwork Cells

Low power (x20) image of bovine meshwork cells pre-treated with dexamethasone for 3 days and transfected with human beta actin eGFP plasmid using fugene 6. This image was taken at low power to capture the maximum number of cells possible. Positively transfected cells would show up as being bright green, but positively transfected cells are absent from this image.

Figure 36: Over Expressed Plasmid in Transfected Hela Cells

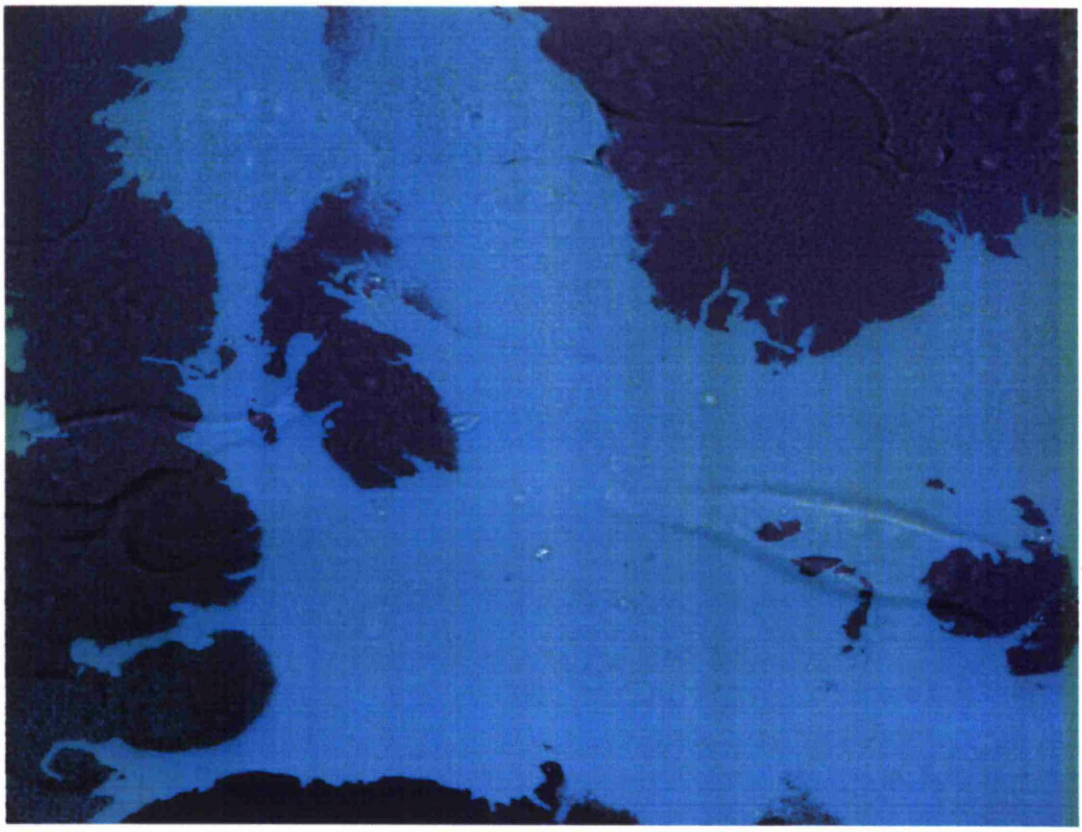

Hela cells transfected with human beta actin eGFP plasmid using a ratio of 1:3 cDNA to transfection reagent (Fugene 6). The plasmid is clearly over expressed with this quantity of transfection reagent (Image taken with oil on the Zeiss axiovert confocal microscope using a x100 objective with oil).

Figure 37: Diffuse Actin Arrangements in Transfected Hela Cells

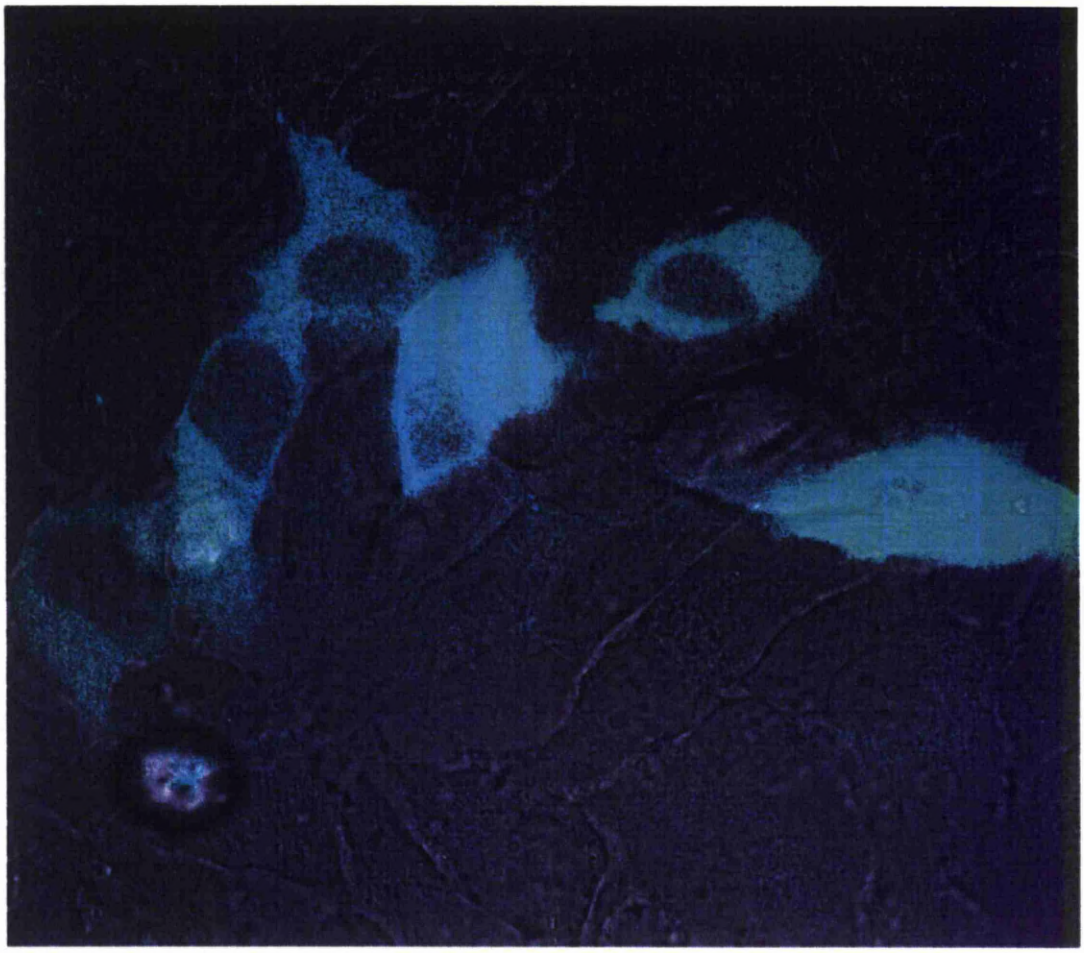

Hela cells transfected with a 1:6 cDNA to transfection reagent (Fugene 6). While a reasonable level of transfection was achieved in this particular trial; the visualisation of actin in these cells was very diffuse, no actin features (stress fibres or similar) were discernable (Image taken with oil on the Zeiss Axiovert confocal microscope using a x60 objective).

Figure 38: Collection of Images from Transfected Cells

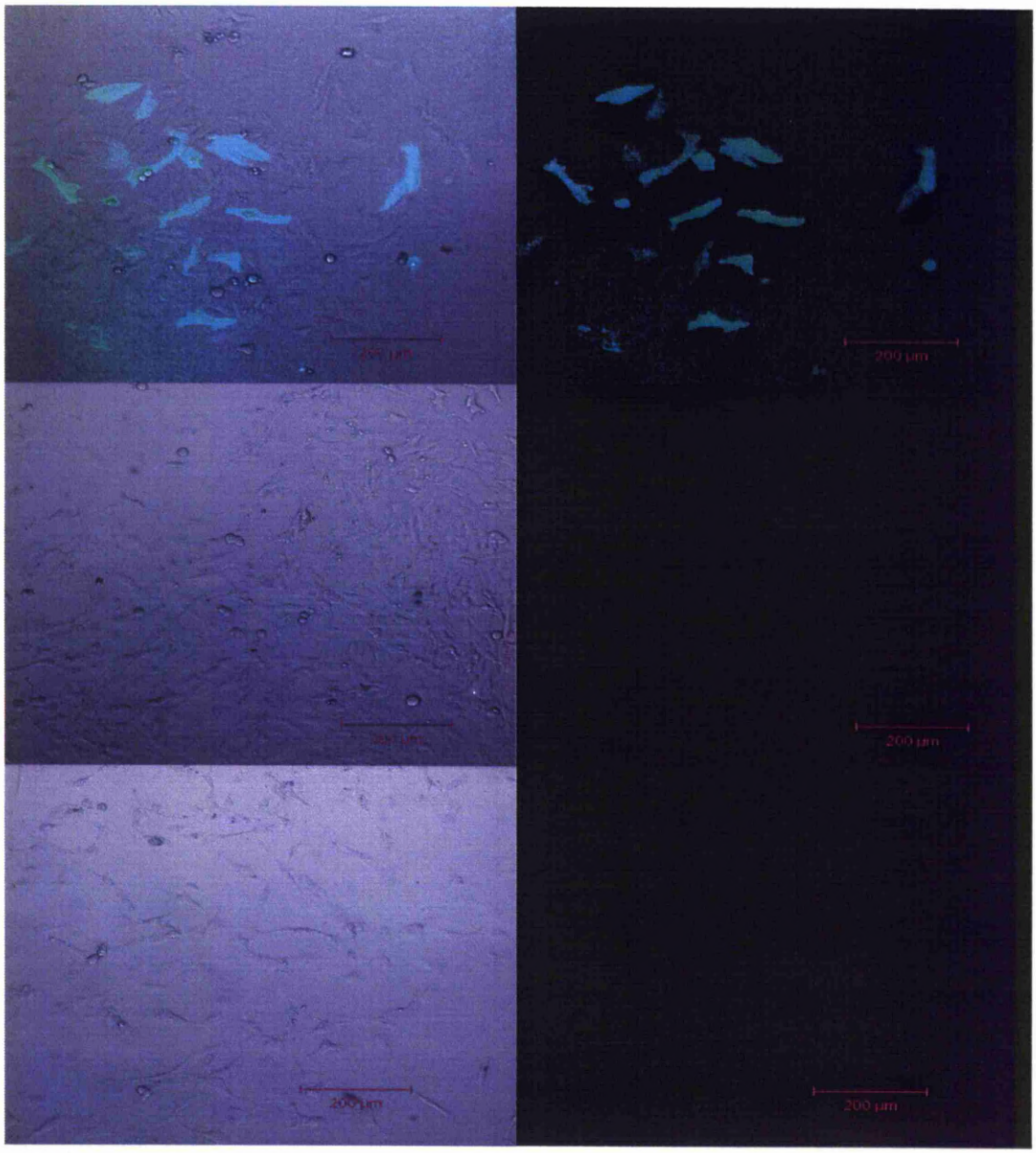

Top left and right; Hela cells transfected with 1:6 cDNA: Fugene 6.

Middle left and right; Bovine meshwork cells transfected with 1:3 cDNA: Fugene 6.

Bottom left and right; Bovine meshwork cells transfected with 2:3 cDNA: Fugene 6.

Human Trabecular Meshwork Cells

CLANs only form in meshwork cells as far as is known currently, at the time of writing this thesis. Because it was not possible to transfect bovine cells the decision was taken to transfect human cells. Both human cell lines commonly used (TM3 and TM5) were found to be transfectable, and both had good actin (stress fibre) visualisation by 24 hours post transfection.

Human TM5 cells were found to be transfectable to approximately 10%, while human TM3 cells were found to reach approximately 15% transfection efficiency both with a 1:3 cDNA to fugene ratio.

When full scale experiments were run, and cells were pre-treated with 10^{-7}M of Dexamethasone all transfection ceased. This happened at any level of cDNA to transfection reagent ratio, despite numerous repetitions.

It was therefore necessary to modify the CLAN induction technique so that cells were not pre-treated. Cells were plated out a day prior to transfection; the media was replaced with dexamethasone DMEM 24 – 36 hours post transfection immediately prior to the imaging run – which would run between 12 and 24 hours.

Figure 39: Transfected Human TM5 Cell

Human TM5 cell transfected with human beta actin eGFP; note the striking stress fibre pattern. Other cells in this image had not taken up the plasmid and so were not visible although this image was taken prior to confluence during one of the initial trials of transfection. (Image taken on Zeiss Axiovert confocal microscope, with oil and a x100 objective).

3.3.2 Experiments to improve transfection efficiency

Although the transfection in human cells was successful, the transfection rate was quite low 10 – 15%. Given the small percentage of human cells that produce CLANs; (approximately 10%) there was concern that finding a cell that had both taken up and expressed the plasmid and formed a CLAN would prove difficult.

Several methods of trying to improve transfection efficiency were tried. The method had to have several qualities; it had to be reliably reproducible and it had to not add another chemical dimension to the experiment.

Serum starvation

Cells were seeded at a number that was sufficient to give approximately 50% confluence into Iwaki plates with normal cell culture media containing 10% serum. Cells were allowed to settle for 12 hours (over night). The following day the media was replaced with serum negative media which was left on the cells for 24 hours.

One hour prior to transfection, the media was changed to normal 10% serum media. The sudden presence of serum appeared to encourage the cells to enter into the G1 phase of the cell cycle, and the by doing this more cells took up plasmid and were successfully transfected, a transfection efficiency of approximately 30 to 40% was reliably achieved in this manner.

Mechanical disruption

This method proved to be a very successful method of inducing the cells to divide and grow – thereby taking up plasmid. The media was changed immediately after mechanical disruption to remove the disrupted cells and or the enzymes that would be released. Cells were maintained in normal 10% serum over night following this

technique, and cultures treated in this manner reached approximately 50 to 60% transfection efficiency. The only problem with this technique was that the amount of disruption would likely differ slightly for each plate which would introduce another Variable, but potentially this need not be a variable that would be problematic, if a finite number of cells were chosen randomly from each plate examined. Other wise this was found to be a useful technique.

3.3.3 Time lapse experiments

Human TM5 Cells

Overview of Experiments and Results

- 3 Separate experiments were completed (a further 2 failed due to problems with the imaging system).
- 7 to 12 fields of view per experiment
- 5 of the best fields of view were selected per experiment – some fields were not productive due to cells moving out of the field of view, or dying.
- Total number of cells examined over these experiments was 171
- Total number of GFP positive cells 69 (40.5% of all cells examined)
- On average 4% of cells contained CLANs or CLAN-like structures

Human TM3 Cells

Overview of Experiments and Results

- 5 separate experiments
- 7 to 12 fields of view per experiment

- 5 fields of view per experiment were selected – again many fields were non productive
- Total number of cells examined during this experiment was 641
- Total number of GFP positive cells was 182 (32% of all cells examined)
- On average, 3.5% of cells contained CLANs or CLAN-like structures

For both experiments the imaging software was set to move between chosen fields of view at set intervals which created a movie file. Most of the experiments were run for different time lengths and so set time points were chosen for each experiment to equalise the information so that it might be subjected to statistical analysis. Time points chosen were 0, 6 and 12 hours from start of imaging / addition of dexamethasone.

Figure 40: Data from Live Human TM5 Cell Experiments

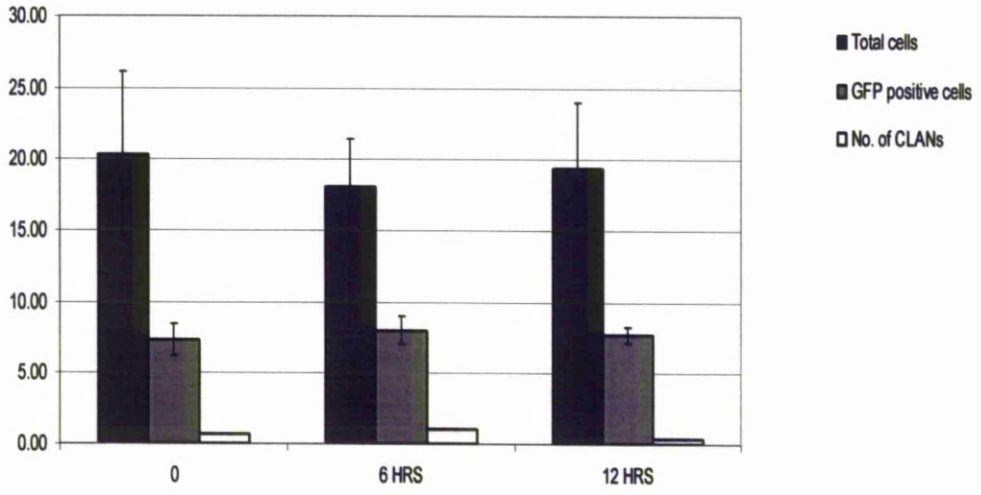

Histogram including error bars of 1 standard deviation of data from the human TM5 GFP experiments: combined data from 5 data sets per experiment and 3 experiments for each condition.

There was no significant difference between:

The total number of cells between 0 and 12 hours (Students t test P = 0.8278)

The number of eGFP positive cells between 0 and 12 hours (P = 0.8740)

The number of CLANs present in cells between 0 and 12 hours (P = 0.6779)

The percentage CLANs present in cells between 0 and 12 hours (P = 0.7567)

Figure 41: Data from Live Human TM3 Experiments

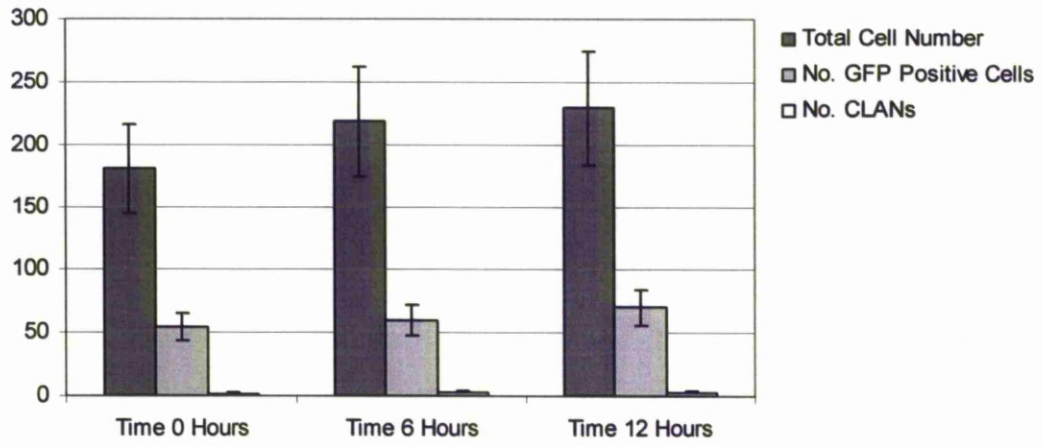

Histogram and error bars of 1 standard deviation of data from the human TM5 GFP experiments: combined data from 5 data points per experiment and 3 experiments for each condition.

There was no significant statistical difference between:

The total number of cells between 0 and 12 hours (Students t test P = 0.2660)

The number of eGFP positive cells between 0 and 12 hours (P = 0.4740)

The number of CLANs present in cells between 0 and 12 hours (P = 0.6811)

The percentage CLANs present in cells between 0 and 12 hours (P = 0.8433).

3.3.4 CLAN formation in living human trabecular meshwork cells

CLANs formed on a few occasions (n = 11) and some preliminary conclusions can be drawn based upon this work.

When CLANs form, the "hubs" appear first. CLANs can form at any time during the culture period, indeed they form without any known CLAN inducer being present, but they appear to increase in number over time, as was shown during the initial dexamethasone time course experiments. Once they form (within 8 minutes was observed here) they are followed by the spokes which appear to form even quicker than the hub points as in the series of images shown in Fig 43, they are not present in one image (Fig 43d) – but them present in the next image (Fig 43e) which was taken a mere 4 minutes later. The spokes connect the dots of the hubs to form recognisable CLANs. As stated, the spokes appear quite quickly following the appearance of the hubs, the whole structure appeared within 20 minutes on one time lapse film. CLANs can form in the same cell as stress fibres and other actin arrangements. Clans can also destabilise and dissipate within a short time of forming.

Figure 42: CLANs in Living Human TM Cells – Single Image

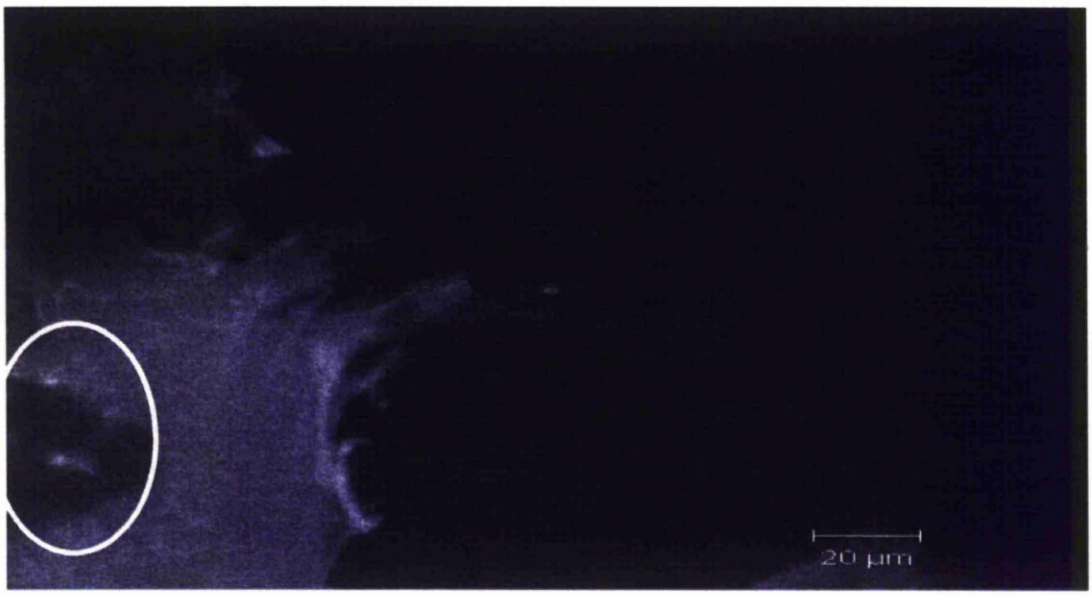

A CLAN-like area over the nucleus of a living TM5 cell transfected with human beta actin eGFP. The area is some what unfocussed unfortunately because the cells move, bulge up and put some areas out of focus. The pin points of bright staining however would be strongly indicative of this being part of a CLAN.

Figure 43a: CLAN Forming in Human TM5 Cell – Image 1 of 8

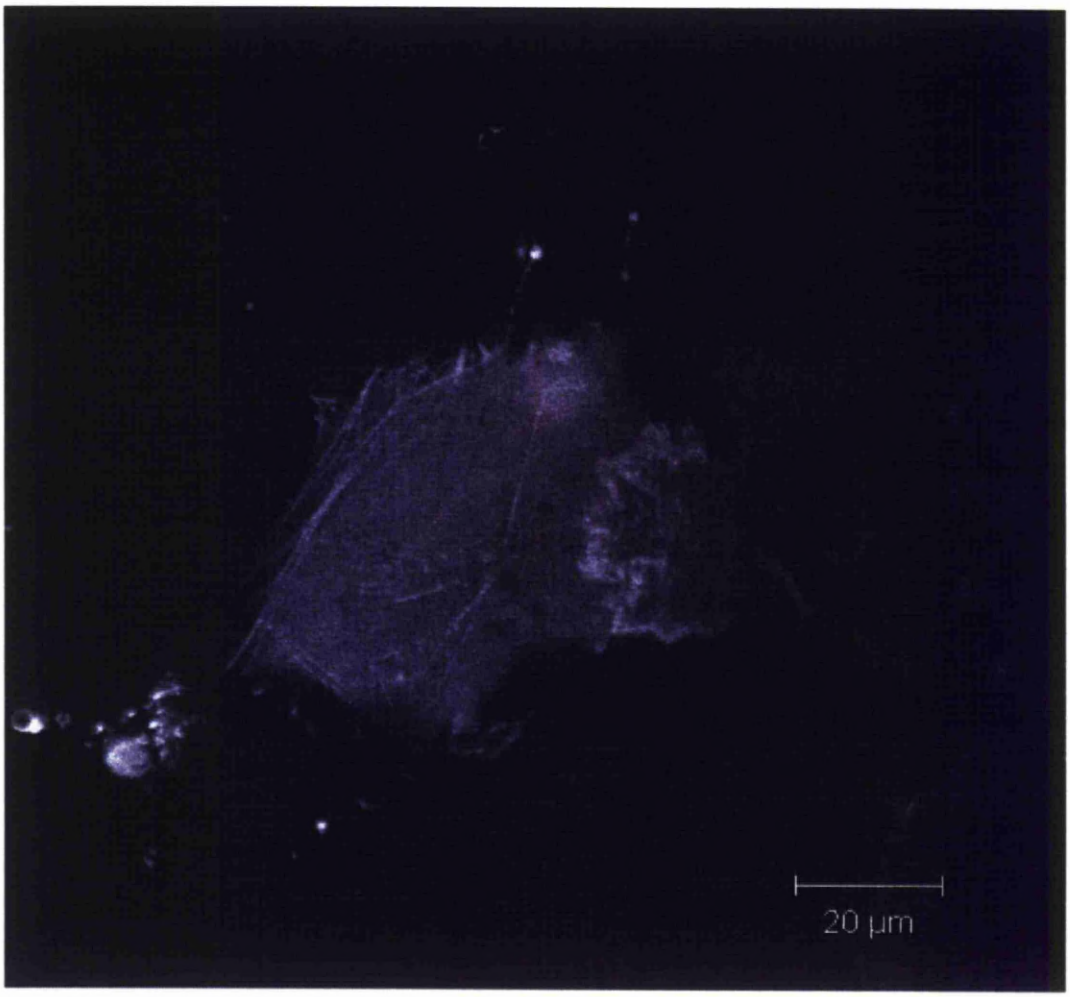

A human TM5 cell transfected with human beta actin eGFP this cell was selected for imaging because it was well spread, CLANs often form in cells that are well flattened and adherent.

Figure 43b: CLAN Forming in Human TM5 Cell – Image 2 of 8

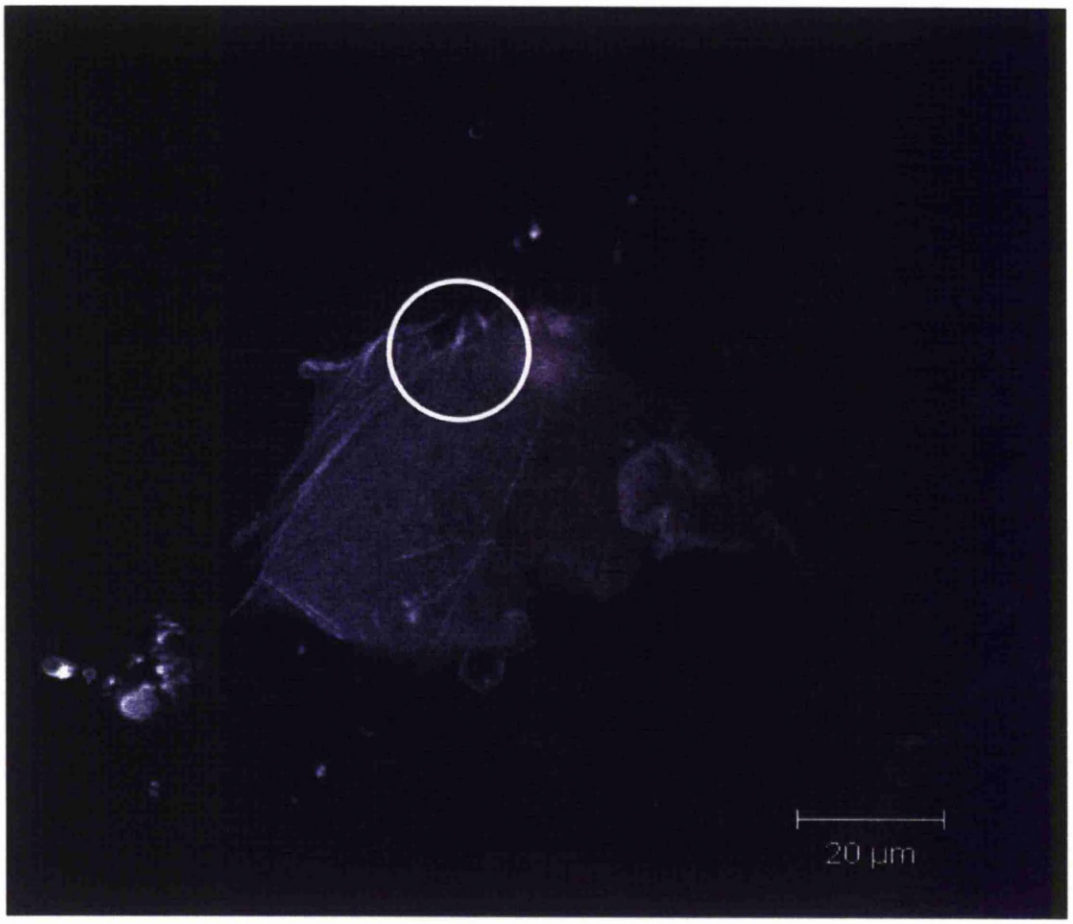

The same cell now showing pinpoint areas of increased staining that does not have any defined pattern as yet. Some stress fibres are forming on the left hand edge of the cell. Time elapsed since last image is 4 minutes.

Figure 43c: CLAN Forming in Human TM5 Cell – Image 3 of 8

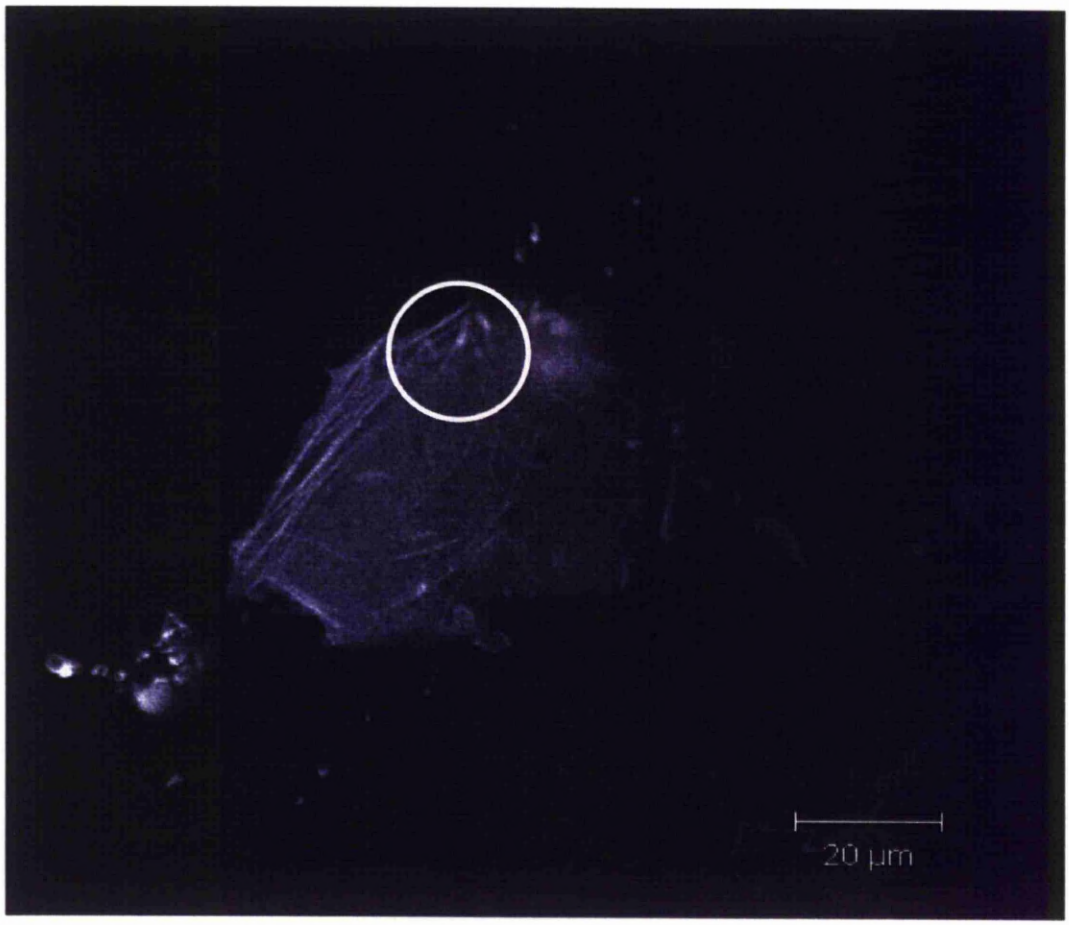

The focal area has become more organised and is taking on a recognisable CLAN shape with 5 "hubs" and 2 or 3 "spokes". The stress fibres are elongated and more pronounced and seem to have extended toward the top of the cell where the focal area is. Time elapsed since last image is 4 minutes. This is the first image of a CLAN forming in a live cell, there is no other such work of this type present in the past or current literature, this is a entirely new, unique experiment and result.

Figure 43d: CLAN Forming in Human TM5 Cell – Image 4 of 8

The focal area has become yet more defined and is now a definite CLAN although the spokes are clearly visible, as yet the hubs are not yet clear. The stress fibres appear to terminate where the CLAN has formed. There is also now a second focal region toward the bottom of the image, that may or may not be hubs forming for another CLAN. Time elapsed since last image is 4 minutes.

Figure 43e: CLAN Forming in Human TM5 Cell – Image 5 of 8

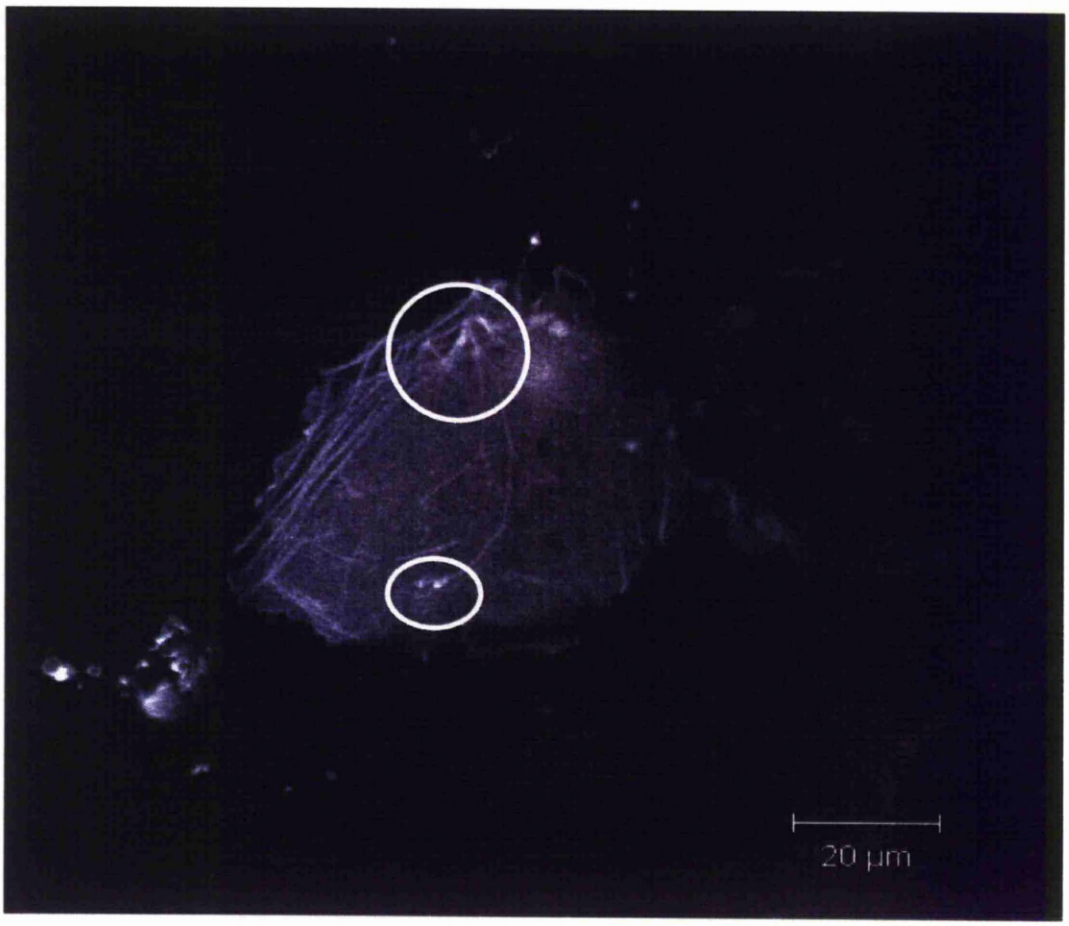

The CLAN is now very pronounced and the spokes are clearly visible. Also, a second CLAN appears to be forming (lower circle). Time elapsed since the previous image is 4 minutes.

Figure 43f: CLAN Forming in Human TM5 Cell – Image 6 of 8

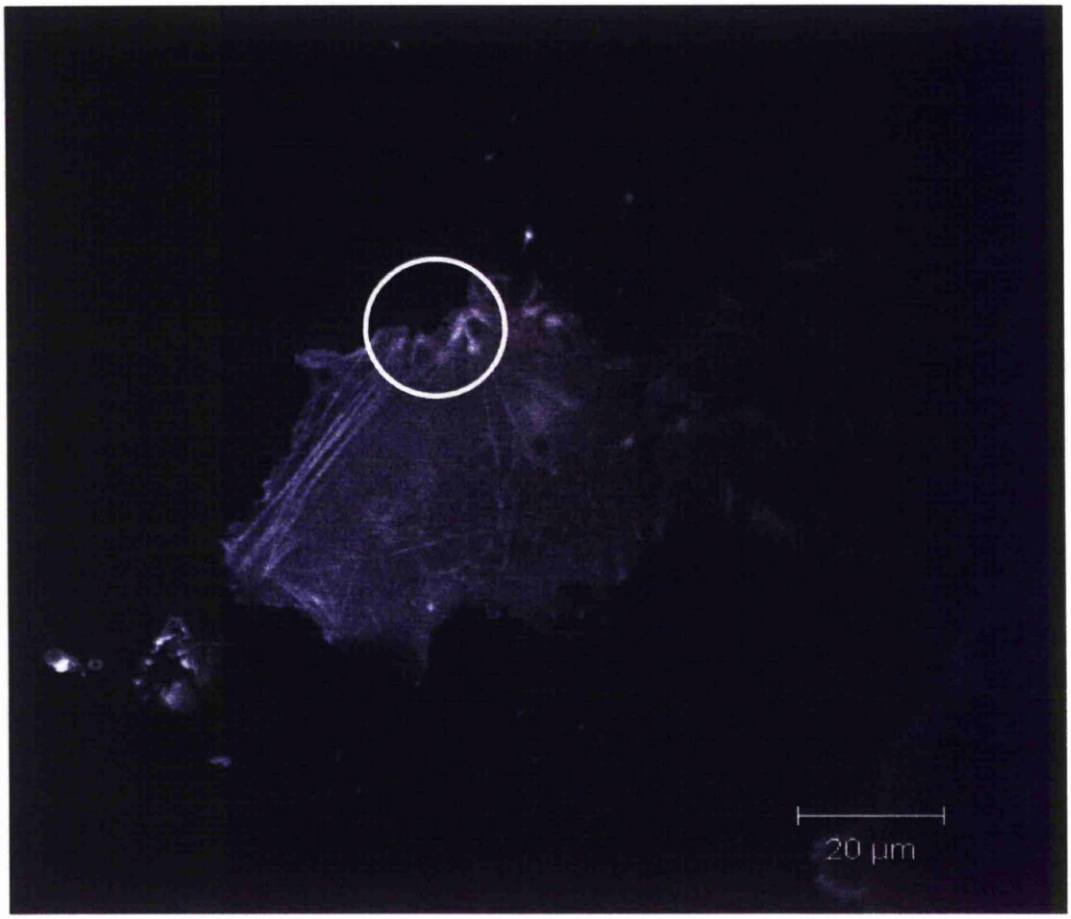

The CLAN now consists of 5 hubs and 4 spokes and is very geodesic. Time elapsed since previous image is again a further 4 minutes after the previous image.

Figure 43g: CLAN Forming in Human TM5 Cell – Image 7 of 8

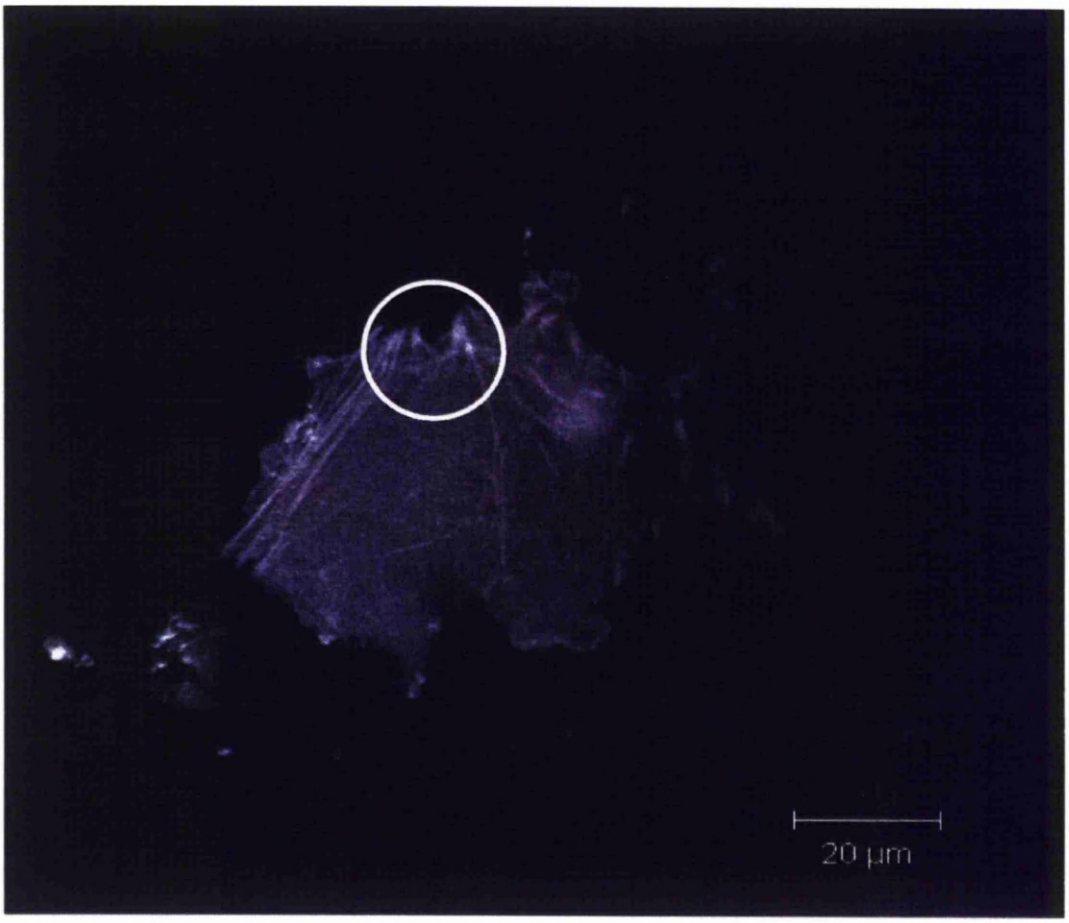

In this image the spokes are less pronounced, as are the hub sites and it appears as though the CLAN is disintegrating. Time elapsed since last image is 4 minutes.

Figure 43h: CLAN Forming in Human TM5 Cell – Image 8 of 8

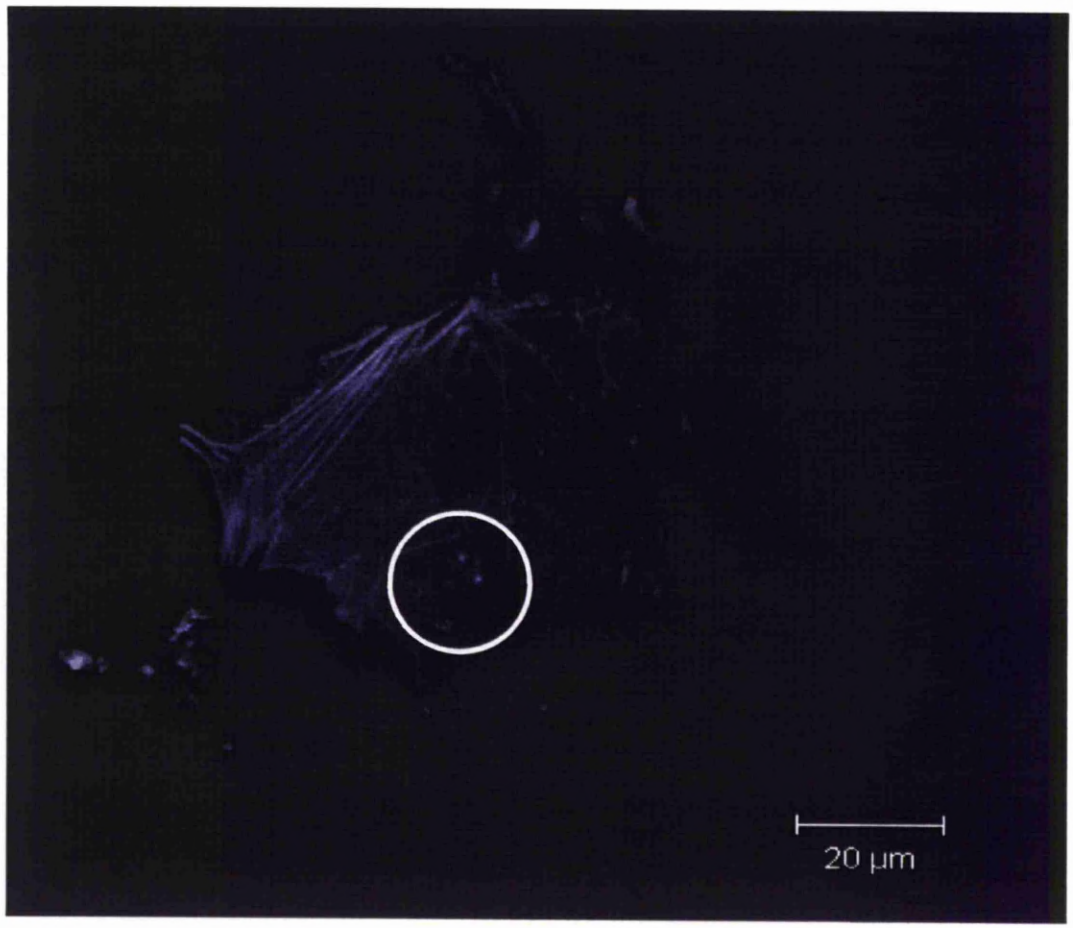

The CLAN from the previous image has now completely dissipated. There are stress fibres now extending to the top of the cell, and the smaller focal area is again visible toward the bottom of the image where more hub points appear to be forming.

4.0 Discussion

4.1 Initial Investigations into the CLAN forming potential of Bovine Meshwork Cells

4.1.1 CLANs in Bovine and Human (Trabecular) Meshwork Cells and Tissues

CLANs and CLAN-like structures have been previously described in detail by numerous groups; but all the work prior to this was undertaken in human trabecular meshwork cells and tissues. The difficulty with relying solely on human tissues and cells is that the availability of human tissue is limited and there is much variability between different patients / donors with regard to CLAN induction (Wade et al, 2009). Bovine cells and tissues are readily available at any time. The bovine trabecular meshwork is very large compared to the human and it is so easier to dissect. Additionally the cells in culture are robust and can be maintained in low serum conditions with little difficulty something problematic, particularly with human primary cultures.

The anatomy of the bovine outflow system is different from the human equivalent, having a "reticular" rather than the primate-styled "trabecular" organization (Flugel et al, 1991) and some of the bovine meshwork contractile responses differ from the human (Thieme et al, 1999). However, on the whole, the human trabecular meshwork cells and the bovine meshwork cells have many features and physiological responses in common.

It should be expected then, that the actions of glucocorticoid on the (trabecular) meshwork of human and bovine have many similarities. As discussed, corticosteroids can cause IOP elevation and corticosteroid glaucoma in vulnerable human patients (Wordinger and Clark 1999; Tripathi et al., 1999), and IOP elevation is a consistent

finding following corticosteroid application to cattle (Gerometta et al., 2004). Glucocorticoids have a widespread pleiotropic effect (Wordinger and Clark, 1999) and many of their actions in human cells (Hernandez et al., 1985; Yun et al., 1989; Lepple-Wienhues et al, 1991) also occur in bovine cells (Wiederholt et al, 1995; Zhou et al., 1998).

In addition, mRNA and total protein encoded by the glaucoma gene MYOC is up regulated by dexamethasone in human trabecular meshwork cells (Nguyen et al., 1998; Tamm, 2002; Fan et al., 2008) and the expression of MYOC-mRNA is increased in the bovine meshwork by dexamethasone (Taniguchi et al.,2000). Dexamethasone and other glucocorticoids, have been shown to modify the F-actin cytoskeleton of confluent human trabecular meshwork cells in culture by inducing CLAN formation (Clark et al, 1994).

The induction process is not exclusive to cultured trabecular meshwork cells because it can be reproduced in ex vivo "intact" trabecular meshwork tissue that has been perfused with dexamethasone as shown in our laboratory in earlier studies (Clark et al, 2005, Hoare et al, 2009). The dexamethasone induction of CLANs is so far as is known, apparently exclusive to trabecular meshwork cells (Clark et al, 1994), but now we know from the work done in this thesis that it is not exclusively to human trabecular meshwork cells.

This study details for the first time that dexamethasone-induced CLAN formation is also a feature of bovine meshwork cells in culture and in bovine tissue ex vivo.

The CLANs induced in bovine meshwork cell cultures were identical to those seen in human cell cultures both in size and in their organization. Bovine and human meshwork cells both responded well to 10^{-7}M dexamethasone, which is equivalent to the aqueous humor concentration of the steroid following topical administration of

dexamethasone drops to the eye, as reported by (Watson et al., 1988). The percentage of confluent bovine meshwork cells exhibiting CLANs within their cytoplasm was around 50% after 14 days dexamethasone exposure, and this was reasonably consistent from culture to culture. Such a response compared favourably to non-transformed primary human trabecular meshwork cells and better than the transformed human cell lines commonly used in the current investigation. It remains to be established whether or not the transformation process has a CLAN inhibiting action, but it seems likely that this is so.

By way of contrast, there did seem to be a consistency in the bovine meshwork cell CLAN response to dexamethasone such that (within limits) passage number was not a confounding factor; and also cultures derived from different eyes all responded in a remarkably similar manner. The bovine meshwork cells, once established in culture and at confluence were sufficiently robust to withstand long periods in minimal serum or serum free conditions and even in these situations dexamethasone induced consistent percentage of cells to form CLANs. There is some evidence to suggest that the IOP elevation provoked in cattle by topical corticosteroids is far more uniform (Gerometta et al, 2004) than in humans with their populations of IOP responders and non-responders (Tripathi et al, 1999). It is interesting to speculate that the steroid induced high incidence of CLANs in the human and bovine meshwork cell populations is in some way contributing to the IOP elevation associated with dexamethasone treatment. As yet, there is no direct evidence that this is the case. However establishing the possible relationship between CLAN incidence and steroid induced IOP elevation is a sensible future research direction that ought to be followed up. The question also arose as to the reason why there were relatively small, but consistent numbers of CLANs in confluent cultures that had no dexamethasone or

another steroid added to the tissue culture medium. A reasonable assumption was that Cortisol within the serum in the cell culture media was responsible for provoking baseline levels of CLANs (Clark et al, 1994).

It is now less likely that this assumption is correct, because the Cortisol content of batches of FCS used in this work was measured by HPLC, and this found that the corticosteroid content of the batches tested to be not more than a mere 7nM (courtesy of L. Bailey and B. Taylor, Clinical Chemistry Department, University of Liverpool). Additionally, the baseline levels of CLANs in bovine meshwork cells when exposed to reduced serum or serum free conditions was low but not absent. With human trabecular meshwork cell cultures, a few CLANs were found in controls exposed to vehicle but not dexamethasone (Clark et al, 1994), and this was also the case in this bovine meshwork cell study where a few cells had CLANs (between 1 and 5%). In addition, the basal levels of CLANS in these bovine meshwork cells cultured without dexamethasone modestly increased with passing time in culture, so that around 10% of the cell population had CLANs after two weeks in culture. There is no reason to assume that corticosteroids are the only CLAN inducing agent, but at the outset of this thesis there were no known alternatives, other than possibly mechanical stretch (Tumminia et al, 1998).

The current findings suggest that cultured bovine meshwork cells are valuable for the investigation of the F-actin cytoskeleton in general, and of CLANs in particular.

Glucocorticoid induced CLANs may be restricted in terms of the cell type in which they can form (Clark et al, 1994), but this work has shown that they are not species exclusive. In addition, the list of agents that may be used for the induction of CLANs in trabecular meshwork cells is increasing from just corticosteroids (Clark et al, 1994; Clark et al, 2005), to mechanical stretching (Tumminia et al, 1998), and now by this

thesis it has grown to include aqueous humor and TGFB2. It is likely that further stimulants (and perhaps even CLAN inhibiting chemicals) will be found in the near future that will help determine whether or not these structures have a crucial role in normal and abnormal trabecular meshwork cell and tissue function.

4.1.2 CLAN Type and Variation

The types of CLANs observed in the bovine cells were the same as those that had previously been identified in human cells. There are a range of non geodesic CLAN arrangements that seem to be ubiquitous as they appeared in both species (Read et al, 2007, Wade et al, 2009). These different structures may have different functions, or they all may serve one purpose, but as yet it is not possible to say with any certainty what this function(s) might be. The different CLAN types seemed to not have a specific location within the cell, any cell CLAN type could be found any where in the cell (peripherally, over the main body of the cytoplasm, peri-nuclear or nuclear).

4.1.3 Effect of Passage Number on CLAN Formation

Although at the outset of this study work was limited to the investigation of CLANs in early passage cells, it was of interest that dexamethasone induction of CLANs remained high in bovine cells whether they were from low or high passage cultures (up to 25 passages). In vivo, the trabecular cells would undergo numerous mitotic divisions, and so this information was felt pertinent as if CLAN formation dropped off at higher passages then the likihood of these structures being involved in a disease that occurs commonly in aging eyes must be doubtful. However, the CLAN prevalence in late passage cells is as high as it is in low passage cells. There is no loss of CLAN forming ability with advancing age. It is interesting that the ability to form CLANs is maintained to such a high passage when at this age many other functions

may have been lost. This requires further investigation for a complete answer as to why this might be, however the fact that this ability is preserved so highly could potentially mean that CLAN formation is important in some ways in these cells.

A feature of the dexamethasone-induced CLAN formation process in human cells as shown in this work and in other studies (Clark et al, 1994) is the high degree of variation in response between different cultures. Clark reported one human cell line that did not form CLANs (Clark et al, 1994), and in this study the cell line (NTM5) that produces steroid induced CLANs in only 15% of cells, whereas other human cells can reach around 60%, albeit after 14 days of dexamethasone exposure. The variability in steroid induced CLAN formation in human trabecular meshwork cells may relate to the known variability of response of meshwork cells to steroid in general. The variable response could be a part of the whole spectrum of responders and non responders that characterises the human eye in vivo and ex vivo (Clark, 1995; Wordinger and Clark 1999).

4.1.4 CLAN Half Life

The survival time of CLANs after dexamethasone withdrawal from human trabecular meshwork cultures was first reported by (Clark et al, 1994) and was comparable to that observed here. The research detailed here has shown that CLANs were reasonably persistent whether they were in human or in bovine cells. After the removal of dexamethasone in this work, CLAN incidence fell back down to baseline levels, but only after a week or so. The half life of bovine meshwork CLANs was marginally shorter at about 2.5 days compared to the various human cells where the half life was always over 3 days. It is not clear why the CLANs are lost more quickly in bovine cells when they are so much larger and in most cases more numerous than

they are in human cells. It may just come down to a species difference, but it could be something to do with the actin isoforms in these cells. It is possible that the isoforms predominance is different in human and bovine cells but this research did not attempt to answer this question.

4.1.5 CLANs in Bovine Meshwork Tissue

The cells in the dexamethasone exposed ex vivo strips of meshwork did exhibit CLANs and CLAN like structures as did the control specimens. Although they were numerous, the CLANs were small and difficult to identify compared to those found in the human equivalent tissue (Clark et al, 2005). As yet we cannot determine if this was a species difference since the bovine meshwork strips were soaked in dexamethasone for 3 days or less while the ex vivo human trabecular meshwork was intact and perfused with dexamethasone, as part of an anterior segment organ culture system (Clark et al, 1995b), for up to 15 days (Clark et al, 2005).

Bathing bovine meshwork strips in various media containing dexamethasone is a simple technique, but it is not as useful as having the meshwork appropriately connected within the scleral sulcus – the dramatic change in stress fibre orientation and shape seen in dexamethasone soaked bovine meshwork strips might merely be due to a lack of tissue cohesion or because of a loss of pressure or perhaps cells deep within the tissue do not receive as much nutrient replenishment and gas exchange as they might normally. Such a view is supported by the fact that meshwork cells in tissue culture, as observed in this work and in previous investigations (Clark et al, 1994), mostly maintained straight stress fibres in the presence of dexamethasone (possibly because the trabecular meshwork cells are strongly adherent to the rigid base of the culture flask and possibly because the flow in this system puts the cell

under "stress" through its motion or flow, thereby maintaining structural integrity whereas as stagnant or non flowing system would reduce stress on the cells and possibly cause them to lose stress fibres). Anterior segment organ culture perfusion chambers suitable for the bovine may well help resolve these issues relating to dexamethasone associated CLANs and also to stress fibres in this tissue. Of direct relevance to this work are the findings in a new study undertaken by Tektas et al (2010) who found that bovine eyes treated with prednisolone for 4 weeks exhibited many of the same changes that have previously been observed in the human eyes with POAG or after steroid treatment, namely extra-cellular matrix plaques under the endothelium of the inner wall in the outflow loops. The conclusion was that this made the bovine eye a good model for glaucoma research, a finding further supported by the work in this thesis.

4.2 Effect of Bovine Aqueous Humor on Morphology

4.2.1 Aqueous Manipulation Experiments and CLAN Induction

Others have shown that growing human trabecular meshwork cells in medium containing human aqueous markedly affected the morphology and functional activities of the human meshwork cells, apparently due to proteins in the aqueous (Fautsch et al., 2005). In addition, CLAN-like structures have been reported in the trabecular meshwork of normal and glaucomatous subjects not exposed to steroid (Hoare et al, 2009).

It seemed reasonable to speculate that aqueous humor may have cytoskeletal modifying components within it that might affect trabecular meshwork cell actin structure. Therefore, we exploited the abundance of bovine aqueous and the hardiness

of the cultures to show that these cells had a significantly elevated number of CLANs when incubated in either 100% bovine aqueous or 50% bovine aqueous in DMEM, when compared to DMEM alone. The induction was greatest in 100% bovine aqueous and was only slightly less than that produced by 10^{-7}M DEX in the same experimental runs. It is still unknown exactly what the CLAN-inducer(s) are in bovine aqueous humor, but it does not appear to be corticosteroid related for several reasons. HPLC analysis indicated that the total corticosteroid content in a pooled sample of aqueous was less than 1nM. In addition, our rudimentary analysis of aqueous humor indicated that the CLAN inducing action is probably associated with something that can be denatured and is reasonably small (between 5,000 and 50,000 Daltons). The unknown component of aqueous humor is a fairly potent CLAN producer in bovine trabecular meshwork cells and may be as good if not better than dexamethasone, given that it may not be at its optimum CLAN provoking concentration in aqueous.

These results justify a careful examination of aqueous CLAN induction to identify the causative agents, as well as to extend our investigations to human samples.

4.2.2 Effect of TGFβ2 on Bovine Meshwork Cells

Because cells grown in aqueous humor exhibited a pronounced CLAN prevalence, and because preliminary experiments did not exclude it as a possibility, and because some patients with primary open angle glaucoma have increased concentrations of TGFβ2 (Tripathi et al, 1994) it was felt prudent to examine the effect of direct application to bovine cells.

As there was no bench mark for concentrations of this compound with regard to CLAN formation, a trial with arbitrary concentrations (1, 5 and 10ng/ml) were selected. The normal concentration in adult aqueous humor has been reported to be

around 2ng/ml. By selecting these concentrations for the optimisation / trial it was hoped that a "normal" response might be provoked (1ng/ml) and the other concentrations would give some indication of what an exaggerated response might look like.

Cells treated with TGFβ2 at any concentration appeared healthy throughout the culture period. These cells had healthy looking nuclei on the whole and were well spread. There were no obvious signs of harm to most of the cells but there was a significant amount of apoptosis in the cultures treated with 10ng/ml, compared to the 1 and 5ng/ml cultures. As 2ng/ml was physiological, and 1 was less than this, it was decided that 5ng/ml would be the concentration used for subsequent work.

There were many CLANs in cultures treated with TGFβ2, not only were they very numerous, but they were also very large compared to the average CLAN observed with dexamethasone treatment. They also had the feature of appearing to extend across cell borders and one CLAN appeared to merge with a CLAN in the adjacent cell. This phenomenon was also observed in bovine cells treated with dexamethasone, (but not in human cells) and the presumed linking process may have consequences with regard to aqueous outflow resistance in vivo, the "linking together" of many cells could conceivably lead to increased resistance to outflow through the normally somewhat elastic meshwork tissue and could be causal factor in the increased IOP seen in POAG. The linking together of cells might also have other consequences for the cell and could possibly impede the normal cytoskeletal functioning of these cells, preventing endo / exocytosis or phagocytosis, all important functions of these cells (Grierson and Hogg 1995).

4.3 Investigations into CLAN Formation in Transfected Live Cells

4.3.1 Initial Transfection Experiments

Bovine Meshwork Cells

The bovine cells for this work were taken from primary cultures that were on the fourth passage. They were healthy cells; they no longer contained any melanin granules and were growing robustly.

Despite these facts and the best practice being followed these cells would not transfect – not at any concentration of Fugene 6 or cDNA and not if given extended time periods in which to start showing some sign of having taken up the plasmid.

Prior to commencing this work the sequences in the plasmid were matched carefully with the bovine sequences and it was at that time reassuring to see that they matched so well. The first trial of bovine cells used were not pre-treated with dexamethasone, the conditions were as prescribed by the transfection reagent manufacturer, and so it cannot be said with any certainty exactly why these cells would not transfect.

At first it was thought that there was perhaps some problem with the plasmid and so the decision was taken to trial transfection in Hela cells.

Hela Cells

Hela cells were successfully transfected with the human beta actin eGFP plasmid. In fact, in most cases the plasmid was highly over expressed, and the entire cell was seen to be bright green – with no actin definition. Although actin definition in these cells may not be clear generally.

The lowest concentration of cDNA to Fugene 6 (1:6) proved to be the most useful and good visibility of the cells was achieved with this ratio, however, there was no clear actin definition even with this best transfection run.

Human Trabecular Meshwork Cells

Given the inability to transfect bovine cells and the necessity to see CLANs using this plasmid – the logical next step was to attempt to transfect human trabecular meshwork cells.

TM5 cells were trialled first purely because those cells were already at confluence at this time and were ready to use. Optimisation tests showed that these cells were transfectable and also that the optimum transfection ratio gave excellent visualisation of the actin within these calls.

Later experiments showed that the human TM3 cells were equally transfectable and also gave very good actin visualisation (as determined by the ability to see stress fibres initially).

4.3.2 Experiments to Improve Transfection Efficiency

Although the human trabecular meshwork cells were transfectable – the transfection efficiency was low (approximately 10%) even if 48 hours were allowed post transfection. The cells did not have the fastest growth rate and were certainly far slower to grow than the Hela cells.

A method was sought therefore to improve the transfection efficiency in the human trabecular meshwork cells. The method could not be chemical as to add another chemical might provoke more complicated results – and the desired outcome was for the human cells to produce CLANs identical to the ones that had been previously observed and it was not certain whether or not the addition of a new chemical might alter these in some way.

Serum Starvation

Serum starvation causes a cell population to enter into G_0 (quiescence) or arrest in G_1 phase of the cell cycle. Having all cells in the same cell cycle phase is desirable because it is then possible to kick them into the cell cycle again in a synchronous manner, so that most of the cells will divide at the same time, hopefully taking up the plasmid as they do.

Cells were seeded to give approximately a 50% confluence level in Iwaki plates. This was to ensure there would be sufficient room for the cells to multiply in once the serum was reintroduced. The following day the media was changed to normal 10% DMEM while the transfection procedure was carried out. The cells were then left for 36 to 48 hours before they were re-examined. By this technique a transfection efficiency of approximately 30% was achieved – a 3 fold increase from that achieved without cell synchronisation / serum starvation.

Cells transfected with this plasmid and the serum starvation looked no different to non transfected cells when viewed with phase contrast. They continued to grow and were still expressing the eGFP protein a week after initial transfection.

There was no discernable effect on cellular morphology or any observable nuclear changes. The cells were motile when views with the axiovert confocal microscope and gave no indication that they were anything other than normal.

Mechanical Disruption

I will preface this discussion by stating that this is not a recognised technique and it is not, as of the date of writing, mentioned in the literature, to the best of the writer's knowledge.

Serum starvation was thought to be a good technique because it did not introduce any new chemical into the chemical cocktail to which these cells were exposed. However, the effect of forced cell quiescence may in itself have some biochemical effect on the cells that was non observable, but potentially important in the formation of CLANs.

Given that the goal of serum starvation was only to provoke the cells to divide, another method of doing this was designed, just so it could be used as a control for the serum starved cells.

Cells at confluence will stop dividing due to contact inhibition. If such cells are then disrupted the theory under test was that the remaining cells would begin to divide to "fill in the gaps" and regain confluence.

Although the method of disruption was crude – using a pipette tip to physically dislodge cells from the plate by dragging the tip through them – this was, nonetheless a very effective method of inducing cell division. The amount of cell growth was dependant on the level of disruption to a point, but too much disruption to the cell layer had the opposite effect.

The swift replacement of the media was important because of leaking enzymes from damaged cells.

Once transfected, the new cell growth could clearly be seen in "lines" or "zigzags" where the pipette tip had been dragged through them.

The cells remaining after this technique were identical to those observed after serum starvation which meant that the serum starvation and the mechanical disruption methods were equally useful in producing a higher level of transfected human trabecular meshwork cells.

4.3.3 Time Lapse Experiments

The cells used for this work where the "normal" trabecular meshwork cells taken from a 19 year old donor with no history of eye disease. At best they had produced only (approximately) 15% CLANs after 2 weeks of treatment with dexamethasone. Using the serum starvation method of cellular synchronisation, 30% of the total numbers of cells were seen to be eGFP positive. This meant that of all the cells available only approximately 4% were both eGFP positive and CLAN producing.

Of course, there was no way to tell from the outset which cells would form CLANs or not. There was also a balance to be had between choosing many cells to follow and the time elapsed between images of the same cell; too long and important information could be missed, too few fields of view and the chances of seeing a CLAN form would be less. The issue was further confounded by the fact that during its repositioning, the microscopes imaging system did not always focus on the entire cell; it would stop its focus as soon as the top of the cell came into view clearly, and this must mean that some CLANs would be missed through ill focus. Additionally one final problem was that some cells moved away from their starting position, the microscope was set to return to a set coordinate, so if the cell of interest moved, it was lost.

Of the cells that showed CLANs or CLAN like structures the features that occurred most commonly in CLAN producing cells were as follows. CLAN producing cells were usually well spread and clearly visible (I.e. they had taken up and sufficient plasmid to have their features clearly defined and visible. They also had good stress fibre content and (fortunately) these cells did not appear to move out of shot as readily as some did. Despite these issues over 100 cells were successfully followed.

4.3.4 CLAN Formation in Living Human Trabecular Meshwork Cells

Fig 47 in results is a series of images which shows the formation and dissolution of a CLAN in a HTM5 cell.

Of all the CLANs imaged, this one was the most clearly defined however there were several other supportive examples observed throughout this work. A few interesting observations can be made of this series of images. The images were taken approximately 4 minutes apart. The CLAN in the top of the image is present in some form for 7 images which showed it has formed and dissolved again within 28 minutes. This cell was not newly seeded and so this CLAN was not the transient type described in many other papers in "settling" cells. This cell had been seeded 48 hours previously. It is seen to form by first the "hubs" and later the "spokes".

Each CLAN is made up of separate geodesic units – consisting of a hexagon-like arrangement of hubs – 1 central, 6 arranged as though on the points of a hexagon around the central point. In this case it appears as though the central hub appears first, and is then followed by the surrounding hubs. These are then "joined up" by the formation of spokes which run between the hubs.

It might be that the hubs; especially the first hub to form, is in some way an "organising centre" for the rest of the structure. This is at this point mere speculation, but the fact that it forms first is indicative of an organising role.

As these images were taken 4 minutes apart they were not able to capture the spoke formation. More work on this technique, and fewer cells with far less time between images might show how the spokes appear. If they originate from the central hub then its role as an organising centre for each geodesic unit would be further supported.

If it were possible, the isolation and investigation of these hubs would prove highly valuable, the spokes are likely to be only scaffold as far as can be reasonably

postulated, clearly there are numerous areas of this original work that could be expanded upon. However, the findings of this work would suggest that CLAN formation and loss are far faster processes than was originally suspected (prior to this work, the literature suggested that once formed, these structures were relatively stable) the findings in this thesis suggests that CLANs can form in a matter of minutes and can be lost again in a similar time frame, whereas the work done with fixed (static) cells suggests that the time scale is days. It may be that a rapid turnover in some places in some cells gives the illusion of longevity, but this as yet is speculation.

4.4 Further Work and Miscellaneous Theories

There still are a number of questions and unresolved issues associated with TM cell CLANs; such as how they form and what is their effect on meshwork cell biomechanics? Do they play a direct pathogenic role in outflow resistance and glaucoma or are they as a consequence of some other as yet unknown pathogenic event, i.e. are they a cause or a consequence of glaucomatous change or entirely unrelated?

Some CLAN associated proteins such as alpha-actinin and syndecan-4 have been identified (Clark et al, 2005; Filla et al, 2006), but their role in CLAN formation remains speculative.

Polygonal networks of F-actin have structural "tensegrity" but exactly how this architectural feature (Ingber, 1998) might translate into trabecular meshwork cell / tissue function or pathology is unclear.

Experimental stretching of human trabecular meshwork cells in vitro induces cytoskeletal changes including the formation of geodesic CLAN–like structures (Tumminia et al, 1998). The contribution and consequences of CLANs or CLAN-like

structures therefore warrants further investigation, especially as the cells of the trabecular meshwork are subjected to stretch in vivo.

We observed an alteration in the actin cytoskeleton of bovine meshwork cells treated with dexamethasone. This alteration ranged from a reduction in the number of stress fibres to the formation of actin tangles and CLANs. It is possible that the dissolution of the normal actin cytoskeleton following exposure to dexamethasone results in the cell becoming unstable (or unsupported). In cells that are usually subjected to flow over the surface of the cell, while their basal aspects remain firmly attached, this dissolution of the normal cellular support could conceivably lead to a certain amount of stress or torque across the top of the cell. If the presence of dexamethasone is in some way preventing the formation of stress fibres which would presumably act as a kind of brace against such forces, then the formation of CLANs may be the next default cytoskeletal response. There is some evidence that points towards this theory being at least partly true. Ingber (1999) showed that low fluid shear across cell membranes bought about through microgravity (earth based systems) caused increased basal adhesion and cytoskeletal rearrangements mediated via mechanosensitive channels in the plasma membrane (Nickerson et al, 2004). Other work in bacteria has shown that cells are able to regulate their turgor (or their "fullness" and deformation) through various gated channels and their cytoskeleton by sensing perturbations across the cell surface (Blount et al, 1996; Blount et al, 1999a; Blount and Moe, 1999b).

Many cells form geodesic cytoskeletal arrangements temporarily – for example when they are in suspension – or while becoming established in a culture flask. It would seem that such cells, which are normally adherent cells, could form these physically strong structures for a number of reasons, including maintenance of sub-cellular

organisation, resistance of compression (Ingber, 1999) and protection (from outside forces) and also possibly so that they remain stable (presuming these sub membranous structures might act almost as an exoskeleton would) allowing for the proper organisation of organelles (etc) within the cell.

If this theory holds true, then the smaller CLANs that form may be as a result of small scale membrane disturbances, under which these structures form to support the area (almost as a cellular sticking plaster or brace). The long term exposure of trabecular meshwork cells to CLAN inducing chemicals could cause the formation of larger CLANs through the initiation of large scale actin disruption and subsequent membrane instability caused by the constant flow of aqueous over these cells (in vivo). Because in vivo the CLAN inducing chemical is present constantly (in the case of TGFβ2 or long term dexamethasone treatment for ophthalmologic disease) there is no opportunity for these structures to dissipate and for normal structure to be restored, which in an elastic tissue could be limiting and disease initiating.

Although CLANs form similarly in response to dexamethasone and to TGFβ2, two seemingly unrelated compounds, there is a common mechanism by which both compounds could result in the same outcome.

Both dexamethasone and TGFβ2 cause an increase in the amount of TGFβ1 present in the cell. An increase in TGFβ2 causes an increase in TGFβ1 by a complicated positive feedback mechanism whereby the presence of TGFβ2 triggers the activation of SMAD (via the activation of a number of kinases, including AP1, fos and C-jun) which results in the direct production of more TGFβ2 (which subsequently causes an increase in the production of TGFβ1) (Fu et al, 2002). Dexamethasone acts by binding to the glucocorticoid receptor and translocating to the nucleus where it binds to a GRE or glucocorticoid response element within the TGFβ1 suppressor gene

where it acts to down regulate suppression, thereby allowing transcription of the TGFβ1 gene proper which results in a rise of cellular TGFβ1 and TGFβ2 (Boland et al. 1996, Staršíchová et al, 2009).

TGFβ1 has several effects on the cell including, cell spreading, increases in cell adhesion and major cytoskeletal changes (Staršíchová et al, 2009) including an increase in the number of basal stress fibres (Boland et al, 1996) an increase in the G to F actin polymerisation and actin tangles (Moustakas and Stournaras 1999) and also a decrease in alpha smooth muscle actin (Robertson et al, 2010). Some of these features were present in CLAN containing cells although none of the references undertook work in trabecular meshwork cells. It could be a useful avenue of research to pursue a similar study to that undertaken by Boland et al, but using trabecular meshwork cells in place of tracheal epithelial cells.

It is possible that limiting the amount of TGFβ2 (which would in turn reduce the concentration of TGFβ1) would reduce the incidence of CLANs. Such experiments were not conducted during this present study, but this could clearly be an area in that might prove productive in regard to CLAN research. If knocking out TGFβ2/ TGFβ1 was able to reduce CLAN incidence then doing so pharmacologically might be a viable future treatment option.

TGFβ2 might also be a useful tool for any further work that might look at live cell imaging of CLANs. Dexamethasone pre-treatment completely removed the ability to transfect the cells, but as it is already present within the cells, it could be that TGFβ2 would not. The difficulties with trying to capture CLAN formation are as previously discussed quite large. The non transfectability of the bovine cells, and the inability to pre-treat the human cells with dexamethasone meant that the cultures would contain only very few CLAN containing cells. Add to this the fact that only 30% (at best) of

cells were eGFP positive and it is clear that this area needs further work to be productive. The fact that CLANs were imaged forming at all in this relatively small scale study was extremely fortunate, given the likelihood of doing so. If the pre-treatment issue could be over come (possibly with TGFβ2) then the ability to follow more CLANs would be easily achievable as many cells would contain CLANs at the start of the imaging run, and such cells could be purposefully chosen. Much other information could be gained using the live cell imaging techniques outlined in this work (or through a variation of it). The CLANs caught forming in this study was at the time of writing the only such CLANs to have been observed doing so. The data obtained from this work, albeit limited due to time constraints will provide valuable clues to many researchers to move CLAN formation research along. Such work could examine now the hubs, which we now know form in advance of the spokes and subsequent geodesic arrangements. How exactly these hubs or organising centres are able to distribute them selves so precisely is another area that would make interesting research.

Further research should also be aimed at trying to identify exactly what component of aqueous humour is causing CLANs. It is possible that TGFβ2 is responsible, and this possibility was not ruled out by the preliminary experiments carried out during this research.

5.0 Summary of Novel Findings

Cells and tissues from another species do form CLANs both with and without dexamethasone stimulation.

CLAN formation in bovine cells at least equals that in human cells and tissues and may be greater in some cases especially when compared to transformed human cell lines.

CLAN formation in bovine cells is remarkably robust and reliable, with numerous cultures tested producing very similar responses. This compares favourably with human cells which have a highly varied response to CLAN inducing stimulus.

CLANs form regardless of passage number – even up to extremely high passages (25)

The array of CLAN types displayed in bovine cells are identical to those displayed in human cells – geodesic, "basket" like, "star burst" like etc.

CLANs can form domes or be more flattened.

CLAN formation in bovine cells and tissues is both time and dose dependent.

The half life of CLANs in bovine cells after dexamethasone was removed from the cell culture media was 2.5 days compared to 3.7 days for human cells.

CLANs in bovine tissue are present but are difficult to identify due to the presence of numerous actin tangles – at least in the "organ bath" method used in this work.

CLANs do not appear to be associated with apoptosis or other cell damage.

Bovine aqueous humor induces CLANs in bovine cells, this effect is diminished by acid treating the aqueous and by passing it though a 5,000 kDa molecular weight cut off filter, but not reduced by alkali treatment or by passage through a 30,000 kDa molecular weight cut off filter.

CLANs are induced in human and bovine cells by TGFβ2. The pathway for this must be in some way saturable as treatment with 1, 5 or 10ng per ml results in very similar levels of CLAN induction, although cell death and apoptosis is markedly higher in the cells given the highest dose.

It is possible to visualise CLANs forming in live human cells using a human beta actin eGFP plasmid, however this is not an easy technique to undertake and needs more work to make it productive.

Bovine meshwork cells are not transfectable with the plasmid used in this work, despite the fact that the gene sequences matched.

Pre treatment of human cells with dexamethasone prevents subsequent transfection by an as yet unknown mechanism.

From this work it is possible to say that when CLANs form, hubs appear first and are followed shortly after by the spokes, Hubs may be organising centres for CLAN formation.

CLANs and stress fibres can co-exist in the same cell at the same time.

CLANs and CLAN like structures can form and dissipate quite quickly (one was observed during time lapse work here forming and dissipating within a 28 minutes). This would suggest that while CLANS must be at least semi permanent, somewhat stable structures (because there is an increase over time) that they are also a short term feature in trabecular meshwork cells. There may in fact be two sub sets of CLANs – one that is short term and others that persist as long as a CLAN inducing stimulus exists. This again needs further investigation.

Some of the work (The data and information relating to CLAN formation in bovine meshwork cells, and that relating to the capabilities of aqueous humor to induce CLANs and the experiments to elucidate the causal agent) was published last year. The work with TGFβ2 is being continued by another student, and the live cell CLAN work will be written up for publication shortly.

Wade, N.C., Grierson, I., O'Reilly, S., Hoare, M.J., Cracknell, K., Paraoan, L.I., Brotchie, D., Clark, A.F. (2009) *Cross-Linked Actin Networks (CLANS) in Bovine Trabecular Meshwork cells,* Experimental Eye Research; 89(5) 648-659.

6.0 References

References for Chapter 1.1

Anderson, P.J., Wang, J., Epstein, D.L. (1980) Metabolism of Calf Trabecular (Reticular) Meshwork, Investigative Ophthalmology & Visual Science; 19: 13-20.

Arey, L.B., (1965) A Text Book and Laboratory Manual of Embryology, 7th Edition, WB Saunders Company, London 529-541.

Barany, E.H., Scotchbrook, S. (1954) Influence of Testicular Hyaluronidase on the Resistance to Flow through the Angle of the Anterior Chamber, Acta Physiologica Scandinavica; 30: 240-248.

Bron, A.J., Tripathi, R.C., Tripathi, B.J. (1997) Wolff's Anatomy of the Eye and Orbit, 8th Edition, ISBN-13: 978-0412410109.

Budras, K.D. and Habel, R.E. (2004) Bovine Anatomy: An illustrated text, Schlutersche Publishers, ISBN 10: 3899930002.

Crean, E.V., Sherwood, M.E., Casey, R., Miller, M.W., Richardson, T.M. (1986) Establishment of Calf Trabecular Meshwork Cell-Cultures, Experimental Eye Research; 43: 503-517.

Dellmann, H., Brown, E.M. (1976) Eye and Ear: In: Textbook of Veterinary Histology, Lea & Febiger, Philadelphia, 423-456.

Dyce, K.M., Sack, W.O. and Wensing, C.J.G. (1987) The Sense Organs In: Textbook Of Veterinary Anatomy, WB Saunders Company, London.

Flugel, C., Tamm, E., Lutjendrecoll, E. (1991) Different Cell-Populations in Bovine Trabecular Meshwork - An Ultrastructural and Immunocytochemical Study, Experimental Eye Research, 52, 681-690.

Garner, A. and Klintworth, G.K. (2008) Pathobiology of Ocular Disease, 3rd Edition, Informa Healthcare, ISBN-13: 978-0849398162.

Gerometta, R., Podos, S.M., Candia, O.A., Wu, B., Malgor, L.A., Mittag, T., Danias, J. (2004) Steroid-induced ocular hypertension in normal cattle, Archives of Ophthalmology; 122: 1492-1497.

Grierson, I., Kissun, R., Ayad, S., Phylactos, A., Ahmed, S., Unger, W.G., Day, J.E. (1985) The morphological features of bovine meshwork cells in vitro and their synthetic activities, Graefes Archive for Clinical and Experimental Ophthalmology; 223: 225-236.

Grierson, I., Millar, L., Deyong, J., Day, J., Mckechnie, N.M., Hitchins, C., Boulton, M., (1986) Investigations of Cytoskeletal Elements in Cultured Bovine Meshwork Cells, Investigative Ophthalmology and Visual Science; 27: 1318-1330.

Grierson, I., Hogg, P. (1995) The proliferative and migratory activities of trabecular meshwork cell, Progress in Retinal and eye research; 15: 33-67.

Hogan, M.J., Alvarado, J.A., Weddell, J.E. (1971) Histology of the Human Eye, Philadelphia: W.B. Saunders publishers.

Leeson, T. and Leeson, R. (1970) Histology, 2nd Edition, WB Saunders Company, London.

Ollivier, F.J., Samuelson, D.A., Brooks, D.E., Lewis, P.A., Kallberg, M.E., Komáromy, A.M. (2004) Comparative morphology of the tapetum lucidium (in selected species), Vetrinary Ophthalmology; 7: 11-22.

Prince, J.H., Diesem, C.D., Eglitis, I., Ruskell, G.I. (1960) Anatomy and histology of the eye and orbit in domestic animals, Charles C. Thomas Publishers, Springfield, Illinois, U.S.A.

Rosenthal, R., Choritz, L., Schlott, S., Bechrakis, N.E, Jaroszewski, J., Wiederholt, M., Thieme, H., (2005) Effects of ML-7 and Y-27632 on carbachol- and endothelin-1-induced contraction of bovine trabecular meshwork, Experimental Eye Research; 80: 837-845.

Slatter, D. (2001a) Development and Congenital Abnormalities In: Fundamentals of Vetrinary Ophthalmology, 3rd Edition, WB Saunders Company, London.

Slatter, D. (2001b) Structure and function of the eye In: Fundamentals of veterinary ophthalmolog, 3rd edition, W.B. Saunders Company, Philadelphia, London.

Thieme, H., Nass, J.U., Nuskovski, M., Bechrakis, N.E., Stumpff, F., Strauss, O., Wiederholt, M. (1999) The effects of protein kinase C on trabecular meshwork and ciliary muscle contractility, Investigative Ophthalmology and Visual Science; 40: 3254-3261.

Tian, B.H., Geiger, B., Epstein, D.L., Kaufman, P.L., (2000) Cytoskeletal involvement in the regulation of aqueous humor outflow, Investigative Ophthalmology and Visual Science; 41: 619-623.

Wiederholt, M., Bielka, S., Schweig, F., Lutjendrecoll, E., Lepplewienhues, A. (1995) Regulation of Outflow Rate and Resistance in the Perfused Anterior Segment of the Bovine Eye, Experimental Eye Research; 61: 223-234.

References for Chapter 1.2

Barishak, Y.R. (1992) in Straub, W. (editor) Embryology of the eye and its adnexae, Developments in Ophthalmology; 24: Karger.

Berman, E.R. and Voaden, M., in: Graymore CN (1970) Biochemistry of The Eye, Academic Press, London.

Bill, A. and Svedbergh, B. (1972) Scanning electron microscopic studies of the trabecular meshwork and the canal of Schlemm, Acta Ophthalmologica 50:295.

Bill, A. (1977) Basic physiology of the drainage of aqueous humor, Experimental Eye Research; 25: 291-304.

Boldea, R.C., Roy, S., Mermoud, A. (2001) Aging of Schlemm's canal in non-glaucomatous eyes, International Ophthalmology; 244: 67-77.

Brilakis, H.S., Johnson, D.H. (2001) Giant vacuole survival time and implications for aqueous humor outflow, Journal of Glaucoma; 10: 277-283.

Bron, A.J., Tripathi, R.C., Tripathi, B.J. (1997) Wolff's Anatomy of the Eye and Orbit, 8th Edition, ISBN-13: 978-0412410109.

Clark, A.F. and Wordinger, R.J. (2009) The role of steroids in outflow resistance, Experimental Eye Research; 88: 752–759.

Ehrich, D., Tripathi, B., Tripathi, R., Duncker, G. (2005) Effects of interleukin-1beta and dexamethasone on the expression of matrix metalloprotease mRNA by trabecular cells exposed to elevated hydrostatic pressure, Acta Ophthalmologica Scandinavica; 83: 104–108.

Ethier, C.R., Coloma, F.M., Sit, A.J., Johnson, M. (1998) Two pore types in the inner-wall endothelium of Schlemm's canal, Investigative Ophthalmology and Visual Science; 39: 2041–2048.

Fautsch, M.P., Howell, K.G., Vrabel, A.M., Charlesworth, M.C., Muddiman, D.C. and Johnson, D.H. (2005) Primary Trabecular Meshwork Cells Incubated in Human Aqueous Humor Differ from Cells Incubated in Serum Supplements, Investigative Ophthalmology and Visual Science; 46: 2848-2856.

Fuchshofer, R. and Tamm, E.R., (2009) Modulation of extracellular matrix turnover in the trabecular meshwork, Experimental Eye Research; 88: 683–688.

Gasiorowski, J.Z., Russell, P. (2009) Biological properties of trabecular meshwork cells, Experimental Eye Research; 88: 671-675.

Grierson, I. and Lee, W.R. (1975) Pressure-induced changes in the ultrastructure of the endothelium lining Schlemm's canal, American Journal of Ophthalmology, 80, 863-884.

Grierson, I. and Lee, W.R. (1977) Light microscopic quantitation of the endothelial vacuoles in Schlemm's canal, American Journal of Ophthalmology, 84(2):234–246

Grierson, I., Hogg, P. (1995) The proliferative and migratory activities of trabecular meshwork cells, Progress in Retinal and eye research; 15: 33-67.

Hogan, M.J., Alvarado, J.A., Weddell, J.E. (1971) Histology of the Human Eye, Philadelphia: W.B. Saunders publishers.

Johnstone, M.A. and Grunt, W.G. (1973) Pressure-dependent changes in structures of the aqueous outflow system of human and monkey eyes, American Journal of Ophthalmology; 75: 365–383.

Kelley, M.J., Rose, A.Y., Keller, K.E., Hessle, H., Samples, J.R., Acott, T.S. (2009) Stem cells in the trabecular meshwork: present and future promises, Experimental Eye Research; 88: 747–751.

Llobert, A., Gasull, X., Gual, A. (2003) Understanding trabecular meshwork physiology: A key to the control of intraocular pressure?, News in Physiological Science; 18: 205-209.

Marshall, G.E., Konstas, A.G., Lee, W.R. (1991) Immuno-gold ultrastructural localization of collagens in the aged human outflow system, Ophthalmology; 98: 692–700.

Parc, C.E., Johnson, D.H., Brilakis, H.S. (2000) Giant vacuoles are found preferentially near collector channels, Investigative Ophthalmology and Visual Science; 41: 2984-2990.

Polansky, J.R., Weinreb, R.N., Baxter, J.D. and Alvarado, J. (1979) Human trabecular cells. I. Establishment in tissue culture and growth characteristics, Investigative Ophthalmology and Visual Science;18:1043–1049.

Polansky, J.R., Fauss, D.J., Zimmerman, C.C. (2000) Regulation of TIGR/MYOC gene expression in human trabecular meshwork cells, Eye; 14: 503–514.

Raviola, G. (1982) Schwalbe line's cells: a new cell type in the trabecular meshwork of Macaca mulatta, Investigative Ophthalmology and Visual Science; 22: 45–56.

Rohen, J.W., Futa, R., Lutjen-Drecoll, E. (1981) The fine structure of the cribriform meshwork in normal and glaucomatous eyes as seen in tangential sections, Investigative Ophthalmology and Visual Science; 21: 574–585.

Snell, R. and Lemp, M. (1998) Clinical Anatomy of the Eye, 2nd Edition, Blackwell Science, ISBN-13: 978-0632043446

Tamm, E.R. (2008) The functional role of myocilin in glaucoma. In: Shields MB, Tombrun-Tink J, Barnstable CJ (Eds.) Ophthalmology Research: Mechanisms of the Glaucomas. Humana Press, 219–231.

Tamm, E.R. (2009) The trabecular meshwork outflow pathways: structural and functional aspects, Experimental Eye Research. 88: 648-655.

Tektas, O. and Lutjen-Drecoll. E, (2008) Structural changes of the trabecular meshwork in different kinds of glaucoma, Experimental Eye Research; 88: 769-75.

Tektas, O.Y., Hammer, C.M., Danias, J., Gerometta, C.R., Podos, S.M., Lutjen-Drecoll, E. (2010) Morphologic changes in the outflow pathways of bovine eyes treated with corticosteroids, Investigative Ophthalmology and Vision Science; 51:4060-4066.

Tortora, G.J. and Derrickson, D.H. (2009) Principles of anatomy and physiology, 12th Edition, ISBN 978-0-470-08471-7 Willey Science.

Tschumper, R.C., Johnson, D.H. (1990) Trabecular meshwork cellularity. Differences between fellow eyes, Investigative Ophthalmology and Visual Science; 31: 1327–1331.

Wordinger, R.J. and Clark, A.F., (1999) Effects of glucocorticoids on the trabecular meshwork: towards a better understanding of glaucoma, Progress in Retinal Eye Research; 18: 629–667.

Yue, B. (1996) The extracellular matrix and its modulation in the trabecular meshwork, Survey of Ophthalmology; 40: 379–390.

References for Chapter 1.3

Alm, A. and Nilsson, S.F.E. (2009) Uveoscleral outflow, a review, Experimental Eye Research; 88: 760-768.

Asejczyk Widlieka, M. and Pierscionek, B.K. (2007) Fluctuations in intraocular pressure and the potential effect on aberrations of the eye, British Journal of Ophthalmology; 1054-1058.

Bill, A. (1965) The aqueous humor drainage mechanism in the cynomolgus monkey (Macaca irus) with evidence for unconventional routes, Investigative Ophthalmology and Visual Science; 4: 911–919.

Bill, A. (1971) Aqueous humour dynamics in monkeys (Macaca irus and Cercopithecus ethiops, Experimental Eye Research; 11: 195–206.

Bron, A.J., Tripathi, R.C., Tripathi, B.J. (1997) Wolff's Anatomy of the Eye and Orbit, 8th Edition, ISBN-13: 978-0412410109.

Do, C.W., Kong, C.W., Chan, C.Y., Lam, C., To, C.H. (2006) Aqueous humor formation and its regulation by nitric oxide; a mini review, Neuroembryology and Aging; 4: 8-12.

Grierson, I. and Lee, W.R. (1975) Pressure induced changes in the ultrastructure of the endothelium lining of Schlemm's Canal, American journal of Ophthalmology. 80;863.

Hogan, M.J., Alvarado, J.A., Weddell, J.E. (1971) Histology of the Human Eye, Philadelphia: W.B. Saunders publishers.

Ismail, R.M., Edelbi, A.H., Rosinger, N. (1977) Chemical composition of the aqueous of bovine eyes dependant on predetermined time upon removal, Albrecht Von Graefes 29;202(1):55-62.

Kanski, J.J. and McAllister, J.A. (1989) Glaucoma, a colour manual of diagnosis and treatment, Butterworths. ISBN: 0-407-01644-9.

Krupin, T. and Civan, M.M. (1996) The physiologic basis of aqueous humor formation, In: Ritch R, Shields MB, Krupin T, editors. The Glaucomas. 2. MO, USA: Mosby, St Louis; 250–281.

Liu, J.H.K. (1998) Circadian Rythym of intraocular pressure, Journal of Glaucoma; 7: 141-147.

Lütjen-Drecoll, E., Rohen, J.W. (1984) Morphological basis for drug action on aqueous outflow, In: Drunce SM, editor. Applied Pharmacology in the Medical Treatment of Glaucomas. Grune and Stratton; New York: 459–475.

Morton Grunt, W. (1951) Clinical Measurements of Aqueous Outflow, AMA Archives of Ophthalmology. 1951; 46(2):113-131.

Nelson, M.T., Josovic, P.M., Su, P., Kang, H.W., Van Deusen, A., Baumgart, J.P., David, T.P., Snutch, T.P., Barrat, P.Q., Lee, J.H., Zorumski, C.F., Perez-Reyes, E. (2007) Molecular mechanisms of subtype-specific neuronal T type calcium channels by ascorbate, Journal of Neuroscience; 27: 12577-12583.

Pederson, J.E., Toris, C.B. (1987) Uveoscleral outflow: diffusion or flow? Investigative Ophthalmology and Visual Science; 28: 1022–1024.

Rice, M.E. (2000) Ascorbate regulation and its neuroprotective role in the brain, Trends in Neuroscience; 23: 209-216.

Shahidullah, M., Wilson, W.S., Yap, M., To, C.H. (2005) Effects of ion trunsport and channel blocking drugs on aqueous humor formation in isolated bovine eyes, Investigative Ophthalmology and Visual Science; 44: 1185-1191.

Tamm, S., Tamm, E., Rohen, J.W. (1992) Age-related changes in the human ciliary muscle. A quantitative morphologic study, Mechanisms of Ageing and Development; 62: 209–221.

Tam, E.R. (2009) The trabecular meshwork outflow pathways: structural and functional aspects, Experimental Eye Research; 88: 648-655.

To, C.H., Kong, C.W., Chan, C.Y., Shahidullah, M., Do, C.W. (2002) The mechanism of aqueous humor formation, Clinical and Experimental Optometry; 85: 335-349.

References for Chapter 1.4

Abedin, S., Simmons, R.J., Grunt, W.M. (1982) Progressive low-tension glaucoma: treatment to stop glaucomatous cupping and field loss when these progress despite normal intraocular pressure, Ophthalmology; 89(1):1-6.

Allingham, R.R., Liu, Y., Rhee, D.J. (2009) The genetics of primary open-angle glaucoma: a review, Experimental Eye Research; 88: 837-44.

Armaly, M.F. and Becker, B. (1965) Intraocular pressure response to topical corticosteroids, The Federation of American Societies for Experimental Biology Journal; 24: 1274-1278.

Becker, B. (1965) Intraocular Pressure Response to Topical Corticosteroids, Investigative Ophthalmology and Visual Science; 4: 198-205.

Bito, L.Z. (1997) Prostaglandins: a new approach to glaucoma management with a new intriguing side effect, Survey of Ophthalmology; 41: S1-14.

Boger, W.P. 3rd (1983) Short-term "escape" and long-term "drift". The dissipation effects of the beta adrenergic blocking agents, Survey of Ophthalmology; 28: 235-42.

Bonomi, L., Babighian, S., Bonadimani, M., Perfetti, S., Brusini, P., Bernardi, P., Coser, S., De Concini, M., Cumer, P., Pedrotti, M., Totolo, G., Carli, M. (2000) Correlation between glaucoma and vascular factors, and circumstances leading to the diagnosis of glaucoma,. Acta Ophthalmologica Scandinavica Supplement; 232: 34-5.

Brundt, J.D., Beiser, J.A., Kass, M.A., Gordon, M.O., and the Ocular Hypertension Treatment Study (OHTS) Group (2001) Central corneal thickness in the ocular hypertension treatment study, Ophthalmology; 108:1779-1788.

Brubaker, R.F. (2001) Measurement of uveoscleral outflow in humans, J Glaucoma; 10(5):45-48.

Caproli, J., Sears, M., Bausher, L. (1984) Forskolin lowers IOP by reducing aqueous outflow, Investigative Ophthalmology and Visual Science; 98: 73-78.

Clark, A.F., Wilson, K., Mccartney, M.D., Miggans, S.T., Kunkle, M., Howe, W., (1994) Glucocorticoid-Induced Formation of Cross-Linked Actin Networks in Cultured Human Trabecular Meshwork Cells, Investigative Ophthalmology & VisualScience; 35: 281-294.

Clark, A.F., Wilson, K., Dekater, A.W., Allingham, R.R., Mccartney, M.D., (1995) Dexamethasone-Induced Ocular Hypertension in Perfusion-Cultured Human Eyes, Investigative Ophthalmology & Visual Science; 36:478-489.

Clark, A.F. and Wordinger, R.J. (2009) The role of steroids in outflow resistance, Experimental eye research 88:752-9.

Clark, A.F., Steely, H.T., Dickerson, J.E., English-Wright, S., Stropki, K., McCartney, M.D., Jacobson, N., Shepard, A.R., Clark, J.I., Matsushima, H., Peskind, E.R., Leverenz, J.B., Wilkinson, C.W., Swiderski, R.E., Fingert, J.H., Sheffield, V.C. and Stone, E.M. (2001) Glucocorticoid Induction of the Glaucoma Gene MYOC in Human and Monkey Trabecular Meshwork Cells and Tissues, Investigative Ophthalmology and Visual Science; 42: 1769-1780.

Croxtall, J. D., Choudhury, Q. and Flower, R. J. (2000), Glucocorticoids act within minutes to inhibit recruitment of signalling factors to activated EGF receptors through a receptor-dependent, trunscription-independent mechanism. British Journal of Pharmacology, 130: 289–298.

Dielemans, I., Vingerling, J.R., Algra, D., Hofman, A., Grobbee, D.E., de Jong. P.T. (1995) Primary open-angle glaucoma, intraocular pressure, and systemic blood pressure in the general elderly population. The Rotterdam Study, Ophthalmology; 102: 1126.

Dimasi, D.P., Burdon, K.P., Craig, J.E. (2010) The genetics of central corneal thickness. British Journal Ophthalmology; 94:971-976

Doughty, M.J. (2001) Ocular pharmacology and therapeutics, BH Opticians. ISBN 0-7506-4520-2.

Edward, D.P., Fajarunanant, T.S. (2008) A comprehensive update on congenital glaucoma, Current Pediatric Reviews; 4:19-30.

Ellis, J.D., Evans, J.M., Ruta, D.A., Baines, P.S., Leese, G., MacDonald, T.M., Morris, A.D. (2000) Glaucoma incidence in an unselected cohort of diabetic patients: is diabetes mellitus a risk factor for glaucoma? DARTS/MEMO collaboration. Diabetes Audit and Research in Tayside Study. Medicines Monitoring Unit. British Journal Ophthalmology; 84:1218-24.

Epstein, D.L., Allingham, R.R., Schuman, J.S. (1997) Chandler and Grunt's Glaucoma, 4th edition.

Fingert, J.H., Clark, A.F., Craig, J.E., Alward, W.L., Snibson, G.R., McLaughlin, M., Tuttle, L., Mackey, D.A., Sheffield, V.C., Stone, E.M. (2001) Evaluation of the myocilin (MYOC) glaucoma gene in monkey and human steroid-induced ocular hypertension, Investigative Ophthalmology and Visual Science; 42: 145-152.

Forsius, H. (1979) Prevalence of pseudoexfoliation of the lens in Finns, Lapps, Icelanders, Eskimos, and Russians, Trunsactions of the Ophthalmological Societies of the U K. 99: 296-8.

Foster, A. and Resnikoff, S. (2005) The impact of Vision 2020 on global blindness, Eye; 19: 1133-1135.

Foster, P., Buhrmann, R., Quigley, H.A., Johnson, G.J. (2002) The definition and classification of glaucoma in prevalence surveys, British Journal of Ophthalmology; 86(2):238-42.

Funk, J. (2009) Glaucoma, Ther Umsch; 66(3):173-81.

Gaul, G.R., Will, N.J., Brubaker, R.F. (1983) Comparison of a non-cardioselective beta-adrenoreceptor blacker and a cardio-selective blocker in reducing aqueous flow in humans, Archives of Ophthalmology; 90: 1369-1372

Gupta, V., Jha, R., Srinivasan, G., Dada, T., Sihota, R. (2007) Ultrasound biomicroscopic characteristics of the anterior segment in primary congenital glaucoma, Journal of the American Association for Paediatric Ophthalmology and Strabismus; 11: 546-50.

Irving, L.H., Kroman, H.S. (1960) Methyl and fluoro substituted prednisolones in theblood and aqueous humor of the rabbit, Archives of Ophthalmology; 63: 943-7.

Johnson, D., Gottanka, J., Flügel, C., Hoffmann, F., Futa, R., Lütjen-Drecoll, E. (1997) Ultrastructural changes in the trabecular meshwork of human eyes treated with corticosteroids, Archives of Ophthalmology; 115: 375-383.

Kanski, J.J. and McAllister, J.A. (1989) Glaucoma, a colour manual of diagnosis and treatment, Butterworths. ISBN: 0-407-01644-9.

Kersey, J.P., Broadway, D.C. (2006) Corticosteroid induced glaucoma: a review of the literature, Eye; 20: 407–416.

Klein, B.E., Klein, R. (1981) Intraocular pressure and cardiovascular risk variables, Arch Ophthalmol; 99: 837-839.

Lee, Y.A., Shih, Y.F., Lin, L.L., Huang, J.Y., Wang, T.H. (2008) Association Between High Myopia and Progression of Visual Field Loss in Primary Open-angle Glaucoma, J Formos Med Assoc; 107: 952-7.

Leske, M.C. and Podgor, M.J. (1983) Intraocular pressure, cardiovascular risk variables, and visual field defects, American Journal of Epidemiology; 118: 280-287

Leske, M.C., Heijl, A., Hyman, L., Bengtsson, B., Komaroff, E. (2004) Factors for progression and glaucoma treatment: the Early Manifest Glaucoma Trial, Current Opinion in Ophthalmology; 15: 102-106.

Liapi, C. and Chrousos, G.P. (1992) Glucocorticoids In: Jaffe SJ, Arunda JV (eds) Paediatric Pharmacology, 2nd Edition, WB Saunders Co, Philadelphia; 466-475

Linden, C. and Alm, A. (1999) Prostaglandin analogues in the treatment of glaucoma, Drugs Aging; 14(5):387-98.

Lo, W.R., Rowlette, L.L., Caballero, M., Yang, P., Hernandez, M.R., Borrás, T. (2003) Tissue differential microarray analysis of dexamethasone induction reveals poyential

mechanisms of steroid glaucoma, Investigative Ophthalmology and Visual Science; 44: 473-85.

Mapstone, R., (1977) Partial angle closure, British Journal of Ophthalmology; 61: 525-530.

Melamed, S. and Ashkenazi, I. (1994) Juvenile-onset open angle glaucoma. In: Albert D, Jakobiec F, (Ed) Principles and Practice of Ophthalmology; 1345-9.

Mitchell, P., Smith, W., Chey, T., Healey, P.R. (1997) Open-angle glaucoma and diabetes the Blue Mountains eye study, Australia, Ophthalmology; 104: 712-8.

Mitchell, P., Hourihan, F., Sandbach, J. (1999) The relationship between glaucoma and myopia: the Blue Mountains Eye Study, Ophthalmology; 106: 2010–15.

Neufeld. A.H., Bartels, S.P., Liu, J.H. (1983) Laboratory and clinical studies on the mechanism of action of Timolol, Survey of Ophthalmology; 28: 286-292.

Okamoto, N., Hatsukawa, Y., Shiraishi, J., Harada, N., Matsumoto, N. (2005) Chromosome 1q deletion and congenital glaucoma, Pediatrics International; 47: 447-9.

Perkins, E.S. and Phelps, C.D. (1982) Open angle glaucoma, ocular hypertension, low-tension glaucoma, and refraction, Archives of Ophthalmology; 100: 1464-7

Polansky, J.R., Cherksey, B.D., Alvarado, J.A. (1992) Update on adrenergic drug therapy, In: Drunce SM, Van Buskirk EM, Neufeld AH (eds), Pharmacology of glaucoma, Williams and Wilkins: 301-321.

Quigley, H.A., Tielsch, J.M., Katz, J., Sommer, A. (1996) Rate of progression in open-angle glaucoma estimated from cross-sectional prevalence of visual field damage, Am J Ophthalmol; 122: 355-63.

Resnikoff, S., Pascolini, D., Etya'ale, D., Kocur, I., Pararajasegaram, R., Pokharel, G.P., Mariotti, S.P. (2004) Global data on visual impairment in the year 2002, Bulletin of the World Health Organisation; 82: 844-851.

Rhee, D.J., Ramos-Esteban, J.C., Nipper, K.S. (2006) Rapid resolution of topiramate-induced angle-closure glaucoma with methylprednisolone and mannitol, Am J Ophthalmol; 141: 1133-4.

Ritch, R. (1984) Exfoliation syndrome: the most common identifiable cause of open angle glaucoma, J Glaucoma; 3: 176-8.

Ritch, R. (1994) Exfoliation syndrome and occludable angles, Truns Am Ophthalmol Soc; 92: 845-944.

Roth, M. and Epstein, D.L. (1980) Exfoliation syndrome, American Journal of Ophthalmology; 89: 447-481.

Schachtschabel, U., Lindsey, J.D., Weinreb, R.N. (2000) The mechanism of action of prostaglandins on uveoscleral outflow, Current Opinion in Ophthalmology; 11: 112-5.

Schmitt, C., Lotti, V.J., DeDouarec, J.C. (1981) Beta-adrenergic blockers: lack of relationship between antagonism of iso-proterenol and lowering of IOP in rabbits: In Sears ML (ed) New directions in ophthalmic research, Yale University Press; 147-162.

Shields, M.B. (1998) Textbook of Glaucoma. 4th Edition, 269-86.

Sihota, R., Sood, A., Gupta, V. (2004) A prospective longterm study of primary chronic angle closure glaucoma, Acta Ophthalmol Scand; 82: 209-13

Stone, E.M., Fingert, J.H., Alward, W.L., Nguyen, T.D., Polansky, J.R., Sunden, S.L. (1997) Identification of a gene that causes primary open angle glaucoma, Science; 275: 668-70.

Stryer, L. (1995) Biochemisty (4th Edition), Freeman Publishers.
ISBN 0-7167-2009-1.

Tektas, O. and Lutjen-Drecoll, E. (2008) Structural changes of the trabecular meshwork in different kinds of glaucoma, Experimental Eye Research; 88: 769-75.

The AGIS Investigators (2001) The Advanced Glaucoma Intervention Study (AGIS): 9. Comparison of glaucoma outcomes in black and white patients within treatment groups, American Journal of Ophthalmology 132: 311-320.

Thompson, S.K., Hayman, A.V., Ludlam, W.H., Deveney, C.W., Loriaux, D.L., Sheppard, B.C. (2007) Improved quality of life after bilateral laparoscopic adrenalectomy for Cushing's disease: a 10-year experience, Annals of Surgery; 245: 790-4.

Tielsch, J.M., Katz, J., Sommer, A., Quigley, H.A., Javitt, J.C. (1994) Family History and Risk of Primary Open Angle Glaucoma: The Baltimore Eye Survey, Archives of Ophthalmology; 112:69-73.

Tripathi, R.C., Li, J., Tripathi, B.J., Chalam, K.V., Adamis, A.P. (1998) Increased level of vascular endothelial growth factor in aqueous humor of patients with neovascular glaucoma, Ophthalmology; 105: 232-7.

Wang, B.S., Narayanaswamy, A., Amerasinghe, N., Zheng, C., Me, M., Chan, Y.H., Nongpiur, M.E., Friedman, D.S., Aung, T. (2010) Increased iris thickness and association with primary angle closure glaucoma, British Journal of Ophhalmology: 2010 Jun 7. [Epub ahead of print]

Watson, D., Noble, M.J., Dutton, G.N., Midgley. J.M., Healey, T.M. (2008) Penetration of Topically Applied Dexamethasone Alcohol Into Human Aqueous Humor; Archives of Ophthalmology; 106: 686-687.

Werner, E. (1996) Progressive normal tension-glaucoma. I. Analysis, Glaucoma; 5: 422-446.

Wiggs, J.L., Del Bono, E.A., Schuman, J.S., Hutchinson, B.T., Walton, D.S. (1995) Clinical features of five pedigrees genetically linked to the juvenile glaucoma locus on chromosome1q21q31, Ophthalmology; 102: 1782-1789.

Wilson, M.R., Hertzmark, E., Walker, A.M., Childs-Shaw, K., Epstein, D.L. (1987) A case-control study of risk factors in open angle glaucoma, Archives of Ophthalmology; 5: 1066-1071.

Wolfs, R.C.W., Klaver, C.C.W., Ramrattan, R.S., Van Duijn, C.M., Hofman, A., De Jong, P.T.V. (1998) Genetic Risk of Primary Open-angle Glaucoma: Population-Based Familial Aggregation Study, Archives of Ophthalmology.116:1640-1645.

Yablonski, M.E., Zimmerman, T.J., Waltman, S.R., Becker, B. (1978) A fluorophotometric study of the effect of topical Timolol on aqueous humor dynamics, Experimental Eye Research; 27: 135-142.

Ziai, N., Dolan, J.W., Kacere, R.D., Brubaker, R.F. (1993) The effects on aqueous dynamics of PhXA41, a new prostaglandin F2 alpha analogue, after topical application in normal and ocular hypertensive human eyes, Arch Ophthalmology 111(10):1351-1358.

Zimmerman, K.S. and Kooner, T.J. (2001) Clinical pathways in Glaucoma, Thieme Medical Publishers. ISBN 0865779198.

Zurier, R.B., Weissman, G. (1973) Anti-immunologic and anti inflammatory effects of steroid therapy, Medical Clinics of North America; 57: 1295-1307.

References for Chapter 1.5

Adams, J.C. (1995) Formation of stable micro-spikes containing actin and the 55 kDa actin bundling protein, fascin, is a consequence of cell adhesion to thrombospondin-1: implications for the anti-adhesive activities of thrombospondin-1, Journal of cell Science; 108: 1997-1990.

Allen, R.D. (1987) The microtubule as an intracellular engine, Scientific American; 256: 42-49.

Bañuelos S, Saraste, M, Djinović-Caruga K (1998) Structural comparisons of calponin homology domains: implications for actin binding. Structure 6:1419-1431

Becker, W.M. and Deamer, D.W. (1991) The world of the cell, California, The Benjamin Cummings Publishing Company Inc. ISBN 0-8053-0870-9.

Bershadsky, A., Chausovsky, A., Becker, E., Lyubimova, A., Geiger, B. (1996) Involvement of microtubules in the control of adhesion-dependent signal trunsduction, Current Biology; 6: 1279-1289.

Brakebusch C, Fässler R (2003) The integrin-actin connection, an eternal love affair. Journal of the European Molecular Biology Organisation 22:2324-2333

Brinkley, B.R. (1985) Microtubule organising centres, Annual Reviews in Cell Biology; 1: 145-172.

Chien S (2007) Mechanotransduction and endothelial cell homeostasis: the wisdom of the cell. American Journal of Physiology – Heart and Circulatory Physiology 292:H1209-H1224

Chen, J., Shen, Y., Jiao, R., Zhai, Z. (1999) Composition and structure of nucleolar skeleton (nucleolar matrix): Actin and fibrillarin are two main protein components of nucleolar skeleton, Science in China, series C – Life Sciences; 42: 34-42.

Chretien, D., Fuller, S.D., Karsenti, E. (1995) Structure of growing microtubule ends: two-dimensional sheets close into tubes at variable rates, Journal of Cell Biology; 129: 1311-28.

Clark, A.F., Wilson, K., Mccartney, M.D., Miggans, S.T., Kunkle, M., Howe, W. (1994) Glucocorticoid-Induced Formation of Cross-Linked Actin Networks in Cultured Human Trabecular Meshwork Cells, Investigative Ophthalmology and Visual Science. 35, 281-294.

Clark, A.F., Miggans, S.T., Wilson, K., Browder, S., McCatney, M.D., (1995a) Cytoskeletal changes in cultured human glaucoma trabecular meshwork cells, Journal of Glaucoma; 4: 183-188.

Clark, A.F., Wilson, K., Dekater, A.W., Allingham, R.R., Mccartney, M.D. (1995b) Dexamethasone-Induced Ocular Hypertension in Perfusion-Cultured Human Eyes, Investigative Ophthalmology & Visual Science; 36: 478-489.

Clark, A.F., Brotchie, D., Read, A.T., Hellberg, P., English-Wright, S., Pang, I.H., Ethier, C.R., Grierson, I. (2005) Dexamethasone alters F-actin architecture and promotes cross-linked actin network formation in human trabecular meshwork tissue, Cell Motility and the Cytoskeleton; 60: 83-95.

Clark, A.F., Wordinger, R.J. (2009) The role of steroids in outflow resistance, Experimental Eye Research; 88(4): 752-759.

Cramer, L.P., Siebert, M., Mitchison, T.J. (1997) Identification of novel graded polarity actin filament bundles in locomoting heart fibroblasts: Implications for the generation of motile force, Journal of Cell Biology; 136: 1287-1305.

Downing, K.H. and Nogales. E. (1998) Tubulin and microtubule structure, Current Opinion in Cell Biology 10: 16-22.

Entcheva E and Bien H (2009) Mechanical and spatial determinants of cytoskeletal geodesic dome formation in cardiac fibroblasts. Integrative Biology 1:212-219

Epstein, D.L., Rowlette, L.L., Roberts, B.C. (1999) Acto-myosin drug effects and aqueous outflow function, Investigative Ophthalmology and Visual Science; 40: 74-81.

Fettiplace R, Hackney CM (2006) The sensory and motor roles of auditory hair cells. National Review of Neuroscience 7:19-29.

Filla, M.S., Woods, A., Kaufman, P.L., Peters, D.M. (2006) beta 1 and beta 3 integrins cooperate to induce syndecan-4-containing cross-linked actin networks in human trabecular meshwork cells, Investigative Ophthalmology & Visual Science; 47: 1956-1967.

Forgacs G (1995) On the possible role of cytoskeletal filamentous networks in intracellular signaling: an approach based on percolation. Journal of Cell Science 108:2131-2143

Geiger B, Spatz JP, Bershadsky AD (2009) Environmental sensing through focal adhesions. National Reviews in Molecular Cell Biology 10:21-33.

Geiger B, Yehuda-Levenberg S, Bershadsky AD (1995) Molecular interactions in the submembrane plaque of cell-cell and cell-matrix adhesions, Acta Anatomica (Basel); 154: 46-42.

Giannone G, Sheetz MP (2006) Substrate rigidity and force define form through tyrosine phosphatase and kinase pathways. Trends in Cell Biology 16:213-223.

Girard KD, Chaney C, Delannoy M, Kuo SC, Robinson DN (2004) Dynacortin contributes to cortical viscoelasticity and helps define the shape changes of cytokinesis. Journal of the European Molecular Biology Organisation 23:1536-1546.

Goldmann, H. (1962) Cortisone Glaucoma, Archives of Ophthalmology; 68: 621-626.

Gordon, W.E. and Bushnell, A. (1979) Immunofluorescent and Ultrastructural Studies of Polygonal Microfilament Networks in Respreading Non-Muscle Cells, Experimental Cell Research; 120: 335-348.

Hoare, M., Grierson, I., Brotchie, D., Pollock, N., Cracknell, K.P.B., Clark, A.F. (2009) Cross linked actin networks (CLANs) in the trabecular meshwork of the normal and glaucomatous human eye in situ, Investigative Ophthalmology & Visual Science. in press.

Holmes KC, Popp D, Gebhard W, Kabsch W (1990) Atomic model of the actin filament. Nature 347:44-49.

Honjo, M., Tanihara, H., Inatani, M., Kido, N., Sawamura, T., Yue, B.Y., Narumiya, S., Honda, Y. (2001a) Effects of rho-associated protein kinase inhibitor Y-27632 on intraocular pressure and outflow facility, Investigative Ophthalmology and Visual Science; 42: 137-144.

Honjo, M., Inatani, M., Kido, N., Sawamura, T., Yue, B.Y., Honda, Y., Tanihara, H. (2001b) Effects of protein kinase inhibitor, HA1077, on intraocular pressure and outflow facility in rabbit eyes, Archives of Opthalmology; 119: 1171-1178.

Huveneers S, Danen EH (2009) Adhesion signaling-crosstalk between integrins, Src and Rho. Journal of Cell Science 122:1059-1069

Hynes RO (2002) Integrins: bidirectional, allosteric signaling machines. Cell 110:673-687

Ingber DE (1998) The Architecture of Life. Scientific American 48-57

Ingber DE (2006) Cellular mechanotransduction: putting all the pieces together again. Journal of the Federation of American Societies for Experimental Biology 20:811-827

Ireland GW and Voon FC (1981) Polygonal networks in living chick embryonic cells, Journal of Cell Science52, 55-69.

Janmey PA, Hvidt S, Lamb J, Stossel TP (1990) Resemblance of actin-binding protein/actin gels to covalently crosslinked networks. Nature 345:89-92.

Koukouritaki, S.B., Theodoropoulos, P.A., Margioris, A.N., Gravanis, A., Stournaras, C., (1996) Dexamethasone alters rapidly actin polymerization dynamics in human endometrial cells: Evidence for non-genomic actions involving cAMP turnover, Journal of Cellular Biochemistry; 62(2): 251-261.

Kozielski, F. and De Bonis, S., Burmeister, W.P., Cohen-Addad, C. and Wade, R.H. (1999) The crystal structure of the minus-end-directed microtubule motor protein ncd reveals variable dimer conformations, Structure; 7: 1407-16.

Langanger, G., De Mey, J., Moeremans, M., Daneels, G., de Brabander, M., Small, J.V. (1984) Ultrastructural localization of alpha-actinin and filamin in cultured cells with the immunogold staining (IGS) method, Journal of Cell Biology; 99: 1324-1334.

Langanger, G., Moeremans, M., Daneels, G., Sobieszek, A., De Brabander, M., De Mey, J. (1986) The molecular organisation of stree fibres in cultures cells, Journal of Cell Biology; 102: 200-209.

Lazarides, E. and Burridge, K. (1975) Alpha Actinin: Immunofluorescent localisation of a muscle structural protein in non muscle cells, Cell; 6: 289-298.

Lazarides, E. (1976) Actin, Alpha-Actinin, and Tropomyosin Interaction in Structural Organization of Actin-Filaments in Nonmuscle Cells, Journal of Cell Biology; 68: 202-219.

Lazarides, E. and Revel, J.P. (1979) The molecular basis of cell movement, Scientific American; 240: 100-13.

Lazarides, E. (1980) Intermediate filaments as mechanical integrators of cellular space, Nature; 283: 249-256.

Meller, K., Theiss, C. (2006) Atomic force microscopy and confocal laser scanning microscopy on the cytoskeleton of permeabilised and embedded cells, Ultramicroscopy; 106: 320-325.

Mizuno D, Tardin C, Schmidt CF, MacKintosh FC (2007) Nonequilibrium mechanics of active cytoskeletal networks. Science 315:370-373

Parry, D.A. and Steinert, P.M. (1999) Intermediate filaments: molecular architecture, assembly, dynamics and polymorphism, Quarterly Reviews of Biophysics; 32: 99-187
Pollard TD (2007) Regulation of actin filament assembly by Arp2/3 complex and formins. Annual Review of Biophysics and Biomolecular Structure 36:451-477

Puklin-Faucher E, Sheetz MP (2009) The mechanical integrin cycle. Journal of Cell Science 122:179-186.

Rao, P.V., Deng, P.F., Kumar, J., Epstein, D.L. (2001) Modulation of aqueous humor outflow facility by the Rho kinase-specific inhibitor Y-27632, Investigative Ophthalmology and Visual Science; 42: 1029-1037.

Rao, P.V., Peterson, Y.K., Inoue, T., Casey, P.J. (2008) Effects of pharmacologic inhibition of protein gerunylgerunyltrunsferase type I on aqueous humor outflow through the trabecular meshwork, Investigative Ophthalmology and Visual Science; 49: 2464-2471.

Read, A.T., Chan, D.W.H., Ethier, C.R. (2006) Actin structure in the outflow tract of normal and glaucomatous eyes, Experimental Eye Research; 82: 974-985.

Renieri, G., Choritz, L., Rosenthal, R., Meissner, S., Pfeiffer, N., Thieme, H. (2008) Effects of endothelin-1 on calcium-independent contraction of bovine trabecular meshwork, Graefes Archive for Clinical and Experimental Ophthalmology; 246: 1107-1115.

Revenu C, Athman R, Robine S, Louvard D (2004) The co-workers of actin filaments: from cell structure to signals. National Reviews in Molecular Cell Biology 5:1-12.

Riveline D, Zamir E, Balaban NQ, Schwarz US, Ishizaki T, Narumiya S, Kam Z, Geiger B, Bershadsky AD (2001) Focal contacts as mechanosensors: externally applied local mechanical force induces growth of focal contacts by an mDia1-dependent and ROCK-independent mechanism. Journal of Cell Biology 153:1175-1186.

Robling AG, Castillo AB, Turner CH (2006) Biomechanical and molecular regulation of bone remodeling. Annual Reviews Biomedical Engineering 8:455-498

Sabanay, I., Gabelt, B.T., Tian, B., Kaufman, P.L., Geiger, B. (2000) H-7 effects on the structure and fluid conductance of monkey trabecular meshwork, Archives of Ophthalmology; 118: 955-962.

Sabanay, I., Tian, B., Gabelt, B.T., Geiger, B., Kaufman, P.L. (2004) Functional and structural reversibility of H-7 effects on the conventional aqueous outflow pathway in monkeys, Experimental Eye Research; 78: 137-150.

Sato N, Funayama N, Nagafuchi A, Yonemura S, Tsukita S, Tsukita S (1992) A gene family consisting of ezrin, radixin and moesin. Its specific localization at actin filament/plasma membrane association sites. Journal of Cell Science 103:131-143

Spaeth, G.L., Rodrigues, M.M., Weinreb, S. (1977) Steroid-induced glaucoma: A. Persistent elevation of intraocular pressure B. Histo-pathological aspects, Trunsactions of the American Ophthalmological Society annual meeting; 75: 353-381.
Steinert, P.M., Jones, J.C., Goldman, R.D. (1985) Intermediate filaments, Journal of Cell Biology; 99(1 Pt 2): 22-27.

Steinert, P.M., Steven, A.C., Roop, D.R. (1985) The molecular biology of intermediate filaments, Cell; 42: 411-20.

Steinert, P.M. and Roop, D.R. (1988) Molecular and cellular biology of intermediate filaments, Annual Reviews of Biochemistry; 57: 593-625.

Snyder, R.W., Stamer, W.D., Kramer, T.R., Seftor, R.E.B. (1993) Corticosteroid Treatment and Trabecular Meshwork Proteases in Cell and Organ-Culture Supernatants, Experimental Eye Research; 57: 461-468.

Tadokoro S, Shattil SJ, Eto K, Tai V, Liddington RC, de Pereda JM, Ginsberg MH, Calderwood DA (2003) Talin binding to integrin beta tails: a final common step in integrin activation. Science 302:103-106

Tamada M, Sheetz MP, Sawada Y (2004) Activation of a signaling cascade by cytoskeleton stretch. Developmental Cell 7:709-718

Tan JL, Tien J, Pirone DM, Gray DS, Bhadriraju K, Chen CS (2003) Cells lying on a bed of microneedles: an approach to isolate mechanical force. Proceedings of the National Academy of Science of the USA 100:1484-1489.

Tan, J.C.H., Peters, D.M., Kaufman, P.L. (2006) Recent developments in understanding the pathophysiology of elevated intraocular pressure, Current Opinion in Ophthalmology; 17: 168-174.

Thieme, H., Nuskovski, M., Nass, J.U., Pleyer, U., Strauss, O., Wiederholt, M. (2000) Mediation of calcium-independent contraction in trabecular meshwork through protein kinase C and rho-A, Investigative Ophthalmology and Visual Science; 41: 4240-4246.

Tian, B., Millar, C., Kaufman, P.L., Bershadsky, A., Becker, E., Geiger, B. (1998) Effects of H-7 on the iris and ciliary muscle in monkeys, Archives of Ophthalmology; 116: 1070-1077.

Tian, B., Wang, R.F., Podos, S.M., Kaufman, P.L. (2004) Effects of topical H-7 on outflow facility, intraocular pressure, and corneal thickness in monkeys, Archives of Ophthalmology; 112: 1171-1177.

Tseng Y, Kole TP, Lee JS, Fedorov E, Almo SC, Schafer BW, Wirtz D (2005) How actin crosslinking and bundling proteins cooperate to generate an enhanced cell mechanical response. Biochemical and Biophysical Research Communications 334:183-192.

Vogel V, Sheetz M (2006) Local force and geometry sensing regulate cell functions. National Reviews of Molecular Cell Biology 7:265-275

Wade, R.H. and Hyman, A.A. (1997) Microtubule structure and dynamics, Current Opinion in Cell Biology; 9: 12-7.

Wang CJ, Levchenko A (2009) Microfluidics technology for systems biology research. Methods Mol Biol 500:203-219

Wilhelm C (2008) Out-of-equilibrium microrheology inside living cells. Journal of the American Physics Society 101:028101-028104

Wilson, K., Mccartney, M.D., Miggans, S.T., Clark, A.F. (1993) Dexamethasone-Induced Ultrastructural-Changes in Cultured Human Trabecular Meshwork Cells, Current Eye Research; 12: 783-793.

Wordinger, R.J., Clark, A.F. (1999) Effects of glucocorticoids on the trabecular meshwork: Towards a better understanding of glaucoma, Progress in Retinal and eye research; 18: 629-667.

Zamir E, Geiger B (2001) Components of cell-matrix adhesions. Journal of Cell Science 114:3577-3579.

References for chapter 2.0

Barden, J.A., Miki, M., Hambly, B.D., Dos Remidios, CG. (1987) Localisation of the phalloidin and nucleotide-binding sites on actin, European Journal of Biochemistry; 162: 583-588.

Clark, A.F., Wilson, K., McCartney, M.D., Miggans, S.T., Kunkle, M., Howe, W., (1994) Glucocorticoid-Induced Formation of Cross-Linked Actin Networks in Cultured Human Trabecular Meshwork Cells, Investigative Ophthalmology & VisualScience; 35: 281-294.

Grierson, I., Kissun, R., Ayad, S., Phylactos, A., Ahmed, S., Unger, W.G., Day, J.E. (1985) The morphological features of bovine meshwork cells in vitro and their synthetic activities, Graefes Archive for Clinical and Experimental Ophthalmology; 223: 225-236.

Hogg, P., Calthorpe, M., Ward, S., Grierson, I. (1995) Migration of cultured bovine trabecular meshwork cells to aqueous humor and constituents, Investigative Ophthalmology and Visual Science; 36, 2449-2460.

Joseph, J.P., Grierson, I., Hitchings, R.A. (1989) Partial characterisation of the fibroblast chemotactic constituents of aqueous humor, International Ophthalmology. 13, 125-130.

Pang, I.H., Shade, D.L., Clark, A.F., Steely, H.T., Desantis, L. (1984) Preliminary characterisation of a transformed cell strain derived from human trabecular meshwork, Current Eye Research; 13, 51-63.

Wulfe, E., Deboben, A., Faulstich, F.A., Weiland, T.H. (1979) Fluorescent phallotoxin, a tool for the visualisation of cellular actin, Proceedings of the National Academy of Science; 76, 4498-4502.

References for chapter 4.0

Blount, P,, Sukharev, S.I., Moe, P.C., Schroeder, M.J., Guy, H.R., Kung, C. (1996) Membrane topology and multimeric structure of a mechanosensitive channel protein of Escherichia coli, Journal of Embryology. 15:4798-4805.

Blount P, Sukharev SI, Moe PC, Martinac B, Kung C. (1999a) Mechanosensitive channels of bacteria, Methods in Enzymology. 294:458-482.

Blount, P., and Moe, P.C. (1999b) Bacterial mechanosensitive channels: integrating physiology, structure and function, Trends in Microbiology.7:420-424

Boland, S., Boisvieux-Ulrich, E., Houcine, O., Baeza-Squiban, A., Pouchelet, M., Schoevaert, D. and Maruno, F. (1996) TGF beta 1 promotes actin cytoskeleton reorganization and migratory phenotype in epithelial tracheal cells in primary culture, Journal of Cell Science; 109(9):2207-2219.

Clark, A.F. (1995) Basic Sciences in Clinical Glaucoma: Steroids, Ocular Hypertension, and Glaucoma, Journal of Glaucoma; 4(5): 303-375.

Clark, A.F., Wilson, K., De Kater, A.W., Allingham, R.R., McCartney, M.D. (1995) Dexamethasone-induced ocular hypertension in perfusion-cultured human eyes, Investigative Ophthalmology and Visual Science; 36: 478-489.

Filla, M.S., Woods, A., Kaufman, P.L., Peters, D.M. (2006) Beta 1 and beta 3 integrins cooperate to induce syndecan-4-containing cross-linked actin networks in human trabecular meshwork cells, Investigative Ophthalmology and Visual Science; 47:1956–1967

Grierson, I., Hogg, P. (1995) The Proliferative and migratory activities of trabecular meshwork cells, Progress in Retinal Eye Research; 15:33–67.

Hoare, M.J., Grierson, I., Brotchie, D., Pollock, N., Cracknell, K. and Clark, A.F. (2009) Cross-Linked Actin Networks (CLANs) in the Trabecular Meshwork of the Normal and Glaucomatous Human Eye In Situ, Investigative Ophthalmology and Visual Science. 50: 1255-1263.

Ingber, D. (1999) How cells (might) sense microgravity, The Federation of American Societies for Experimental Biology.13:3-15

Nickerson, C.A., Ott, C.M., Wilson, J.W., Ramamurthy, R., Pierson, D.L. (2004) Microbial Responses to Microgravity and Other Low-Shear Environments, Microbiology and Molecular Biology Reviews; 68(2): 345–361

Moustakas, A. and Stournaras, C. (1999) Regulation of actin organisation by TGF-beta in H-ras-transformed fibroblasts, Journal of Cell Science; 112(8):1169-1179

Read, A.T., Darren, W., Chan, W.H., Ethier, C.R. (2007) Actin structure in the outflow tract of normal and glaucomatous eyes, Experimental Eye Research; 84(1):214-226.

Robertson, J.V., Golesic, E., Gauldie, J., West-Mays, J.A. (2010) Ocular Gene Trunsfer of Active TGF-β Induces Changes in Anterior Segment Morphology and Elevated IOP in Rats, Investigative Ophthalmology and Visual Science.51:308-318

Staršíchová, A., Kubala, L., Lincová, E., Pernicová, Z., Kozubík, A., Souček, K. (2009) Dynamic Monitoring of Cellular Remodeling Induced by the Trunsforming Growth Factor-beta1, Biological Procedures Online (Epublished ahead of print).

Tektas, O.Y., Hammer, C.M., Danias, J., Gerometta, C.R., Podos, S.M., Lutjen-Drecoll, E. (2010) Morphologic changes in the outflow pathways of bovine eyes treated with corticosteroids, Investigative Ophthalmology and Vision Science; 51:4060-4066.

Tripathi, R.C., Li, J., Chan, W.F., Tripathi, B.J. (1994) Aqueous humor in glaumatous eyes contains an increased level of TGF-β_2, Experimental Eye Research.19:723–728.

Tumminia, S.J., Mitton, K.P., Arora, J., Zelenka, J.P., Epstein, D.L., Russell, P. (1998) Mechanical stretch alters the actin cytoskeletal network and signal trunsduction in human trabecular meshwork cells, Investigative Ophthalmology & Visual Science; 39: 1361-1371.

Wade, N.C., Grierson, I., O'Reilly, S., Hoare, M.J., Cracknell, K., Paraoan, L.I., Brotchie, D., Clark, A.F. (2009) Cross-Linked Actin Networks (CLANS) in Bovine Trabecular Meshwork cells, Experimental Eye Research; 89(5) 648-659.

Wordinger, R.J. and Clark, A.F. (1999) Effects of glucocorticoids on the trabecular meshwork: towards a better understanding of glaucoma, Progress in Retinal and Eye Research; 18(5); 629-667.

An electronic version of this thesis may be requested from the author via;

nikki_wade@hotmail.co.uk